UILU-ENG-95-2020

CIVIL ENGINEERING STUDIES
Hydraulic Engineering Series No. 48

ISSN: 0442-1744

VIDEO-BASED PARTICLE TRACKING VELOCIMETRY TECHNIQUE FOR MEASURING FLOW VELOCITY IN POROUS MEDIA

By

Anthony J. Dill

Marcelo H. García

and

Albert J. Valocchi

Sponsored by:

Illinois Water Resources Center (WRC-S-125)

HYDROSYSTEMS LABORATORY
DEPARTMENT OF CIVIL ENGINEERING
UNIVERSITY OF ILLINOIS AT URBANA-CHAMPAIGN
URBANA, ILLINOIS

December 1995

ACKNOWLEDGMENTS

This report is based on the thesis submitted by Anthony J. Dill in partial fulfillment of the requirements for the degree of Master of Science in Environmental Engineering in Civil Engineering in the Graduate College of the University of Illinois at Urbana-Champaign in 1994.

This research was supported by a grant from the Illinois Water Resources Center. This support is gratefully acknowledged.

We also thank Yarko Niño for his technical advice and authorship of the original particle tracking computer code which provided the basis for the algorithms developed under this project.

Table of Contents

1. Introduction

The goal of this research project was to develop a video-based particle tracking velocimetry (PTV) technique for measuring velocity profiles within an idealized porous medium. This porous medium must be optically transparent and have the same refractive index as the fluid flowing through the media. Refractive index matching allows undistorted imaging of the interior pores of the column, but eliminates real soils from possible analysis. The media used in this experiment was polymethylmethacrylate (PMMA) spheres and the fluid was a mixture of silicone oils. PTV is a particular member of a family of fluid velocity measuring techniques known as particle image velocimetry (PIV). PIV techniques are powerful tools for simultaneously determining fluid velocities at many points in a flow field at the same time. All PIV techniques have similar basic requirements including the seeding of the fluid with small, neutrally buoyant tracer particles, illumination of a plane of the flow field with a laser, recording of tracer images onto some medium, and analysis of the images to yield velocity vectors. Each tracer particle must be imaged at two or more instances in time in order to yield a displacement and resulting velocity vector (Adrian 1991, Fingerson et al. 1991).

The motivation for development of this non-invasive flow velocity measurement technique was the fact that experimental measurement and analysis of pore-water velocities have been developed to a much lesser extent than theoretical modeling of groundwater flow. Furthermore, model computational support of pollutant transport is far ahead of model validation due to a lack of experimental data. This project, therefore, hopes to further the experimental side of pore-water velocity measurements in order to verify existing theories of groundwater flow and pollutant transport in porous media.

Historically, fluid velocity measurement in complex flow regimes has been performed by laser Doppler velocimetry (LDV), which gives accurate point velocities, but for only one spatial location in a flow field. Thus, it is necessary to reconstruct a flow field from individual measurements which are taken at different times. LDV, therefore, can not be used for measuring an instantaneous unsteady flow field or for capturing instantaneous turbulent flow structures. Even for steady, laminar flows, however, it is still convenient to use PIV, which allows simultaneous measurement of velocities at multiple points in a flow field. Furthermore, comparing PIV measurements for a flow field at different times can be used to determine if steady, laminar flow conditions actually exist everywhere in the flow field.

As previously mentioned, this project specifically explored the development of a video-based PIV system as opposed to the more common photographic-based systems. There are inherent advantages and disadvantages of a video system when compared to a photographic system. First, video systems have the disadvantage of much less resolution than

is available with photographic systems. This means that the density of vectors obtained for a given field of view at an instance will be less for video systems than for photographic systems. On the other hand, photographic systems demand the purchase and development of film which is more costly and time-consuming than recording images on video tape. Also, the images recorded on video tape can be monitored and played back instantly to check image quality, whereas photographic film takes time to develop. Another advantage of video systems over photographic systems for porous media analysis is the ability to analyze a series of frames in order to obtain accurate velocities for slow moving particles. Since pore-water velocity fields will have a large difference between minimum and maximum tracer velocities, it is desirable to evaluate the velocities for different tracers with different timesteps so as to minimize relative errors in displacement measurements. Relative errors in displacements are largest when actual displacements are smallest since it is assumed that absolute error in tracer displacement measurement is independent of total displacement. Because PIV systems utilizing video are simpler and have advantages in flow fields with largely varying velocity magnitudes, a video-based system was developed for this project. Furthermore, one of the goals of this project was to determine if the added simplicity of a video-based system was able to offset the lower resolution and provide a simple, useful system for PTV in porous media.

In addition to developing a technique for tracking particles and measuring point velocities, it was important to develop a reliable method for interpolating the entire velocity field from randomly spaced velocity vectors. Due to the limited resolution of video techniques and the random spacing of particles in a fluid it is useful to be able to fill in the gaps in a velocity field to obtain a more complete and useful picture. An algorithm, therefore, was chosen to interpolate a velocity field at regularly spaced grid points for the experimentally measured velocity vectors.

2. Literature Review

2.1 History of Flow Visualization

The application of PIV to porous media is a recent development in the field of fluid velocity measurements. One essential feature of an experiment using PIV with a porous medium is that the medium and seeded fluid are transparent and have matching indices of refraction to allow visualization of the tracer particles within the pores. Because of this requirement, an artificial medium and fluid must be used instead of soil and water, which is a major disadvantage of all PIV techniques. In order to isolate a portion of the flow field, a sheet of laser light is used to illuminate a plane within the porous medium (Northrup et al. 1993, Salch et al. 1992). Images of the plane can be captured using either video or photographic medium. These images can be subsequently analyzed using various PIV techniques to yield velocity vectors for the captured flow field (Fingerson et al. 1991).

One of the first uses of refractive index matching to observe the flow in a porous medium was an experiment by Wegner et al. (1971). In this experiment Plexiglass spheres were used in combination with decahydronapthalene to form an index-matched system. Dye was released from one of the interior spheres and flow patterns around the spheres were observed. The results from this experiment were largely qualitative and did not involve velocimetry.

Early use of an index-matched porous media system to obtain quantitative velocity measurements made use of LDV (Dybbs and Edwards 1982). This experiment used a mixture of silicone oils in combination with either Plexiglass spheres or Pyrex rods to achieve index matching. Velocity measurements for flow around a packed bed of spheres showed that average pore-water velocities were twice as great at the walls than at the center of the column. Furthermore, the velocity at the walls was greater than at the center of the porous medium for the entire length of the porous medium, but did vary with local geometry. Dybbs and Edwards also reported similar findings by other experimentalists where velocity measurements for a packed bed of spheres in a column showed that the effect of the wall on pore-water velocities was noticed no more than two sphere diameters from the wall. Also, peak velocities near the wall were found to range from 30% to 100% greater than at the center of the column for a column to sphere diameter ratio of 30 and approximately 100% greater than the center for a column to sphere ratio of 8. Dybbs and Edwards also observed four distinct flow regimes as the Reynolds number for the packed bed of spheres was varied. First, a Darcy flow regime was observed for Reynolds number less than 1, where flow was dominated by viscous forces and local geometry determined the exact nature of the flow. Second, a steady, laminar inertial flow regime occurred for Reynolds number between 1 and 150, where boundary layers became

pronounced and an inertial "core" began to develop. Third, an unsteady laminar flow regime developed for Reynolds number between 150 and 300. In this flow regime, the first evidence of laminar wake oscillations in the pores was observed. Fourth, a highly unsteady flow regime resembling turbulent flow was observed for a Reynolds number greater than 300. Further experiments by Dybbs and Edwards (1984) concluded that Pyrex had much better optical quality than Plexiglass and that temperature control was important for optimum index matching.

The application of PIV to porous media is more recent and apparently the first attempts to do this were made by Salch et al. (1992) and Northrup et al. (1993). Again, a major advantage of using PIV techniques over LDV is the ability to capture an entire flow field at an instant rather than measuring one point at a time as with LDV. Salch et al. used a mixture of silicone oils and broken Pyrex rods for the index-matched system. The oil mixture was seeded with 4 micron (μm) aluminum tracers and a laser was used to illuminate a plane of the porous media for imaging. Multi-exposure photographs of the flow field were taken and analyzed using Young's fringes analysis or high-image-density PIV. This involves interrogation of the photographs with another laser and subsequent analysis of the interference patterns formed by the double images of clusters of particles to obtain two-dimensional point velocity vectors.

In a similar project by Northrup et al. (1993), an index-matched system was seeded with fluorescent microspheres in what was termed fluorescent particle image velocimetry (FPIV). In this experiment the fluid used was a mixture of silicone oils and the media was spheres of polymethylmethacrylate (PMMA). Analysis of the images relied on the same basic principles as the Salch et al. experiment. The use of fluorescent particles, however, allowed for improved imaging since a narrow-bandpass filter could be used to shield out any scattered laser light and accept only fluorescent light. Furthermore, the filter blocked much of the fluorescence of the silicone oils which allowed for greater contrast between tracer particles and background. The results of the velocimetry for the column of spheres were used to compare the measured average axial pore-water velocities with the predicted value from macroscopic properties of flow rate, cross-sectional area, and porosity. The average measured pore-water velocities for the plane which was analyzed in the experiment were slightly greater than the theoretical prediction, and this was attributed to two main sources of error. First, the measurements for the particular plane were likely influenced by local variation in porosity. If all the planes in the column were analyzed it is likely that some variation in velocities would exist due to heterogeneity and that the total average axial velocity should approach the theoretical value. Also, since the PIV method employed in this experiment uses a double-exposed photograph for the velocimetry calculations, only the particles for which reasonable displacements occur are successfully analyzed. In particular, particles which are moving slowly may form an

overlapped image since there is not time for sufficient displacement. This omission of velocity values from some of the slow-moving particles was partly responsible for the overestimated average axial pore-water velocity and reveals the limitations of double-pulsed photography for measuring both fast and slow particles in the same field of view, which is desirable for studying laminar, steady, pore-water velocity profiles.

In addition to obtaining two-dimensional velocity vectors, it is a future objective of the researchers involved in this project to obtain velocity vectors in all three dimensions. One method of determining the third component of velocity involves stereoscopic techniques such as those described by Adrian (1991), which would require two cameras, although the third component of the velocity determined in this manner is somewhat less reliable than the in-plane velocity components. Arroyo and Greated (1991), however, describe a technique by which the use of mirrors can allow measurements of all three velocity components with just one camera. Besides being less expensive, this method also would eliminate errors resulting from correlating images from two different cameras. In addition to using stereoscopic techniques, the continuity equation can be solved to determine the third component of velocity. This method was employed by Rosenstein (1980) to deduce the out-of-plane component of velocity (V_z) in a porous medium consisting of interconnected Pyrex rods. In order to obtain V_z, a series of adjacent planes were analyzed and the change in V_z from plane to plane (dV_z/dZ) was determined from the continuity equation. The walls of the column and surfaces of rods inside the column were used as boundary conditions where V_z was zero. V_z was then calculated at points in each plane by stepping away from the solid boundaries and using a linearly interpolated velocity from the previous point.

Another area of concern is the media on which the images will be recorded. Photographic film has the advantage over video of having much greater resolution than is possible with a typical video camera (Fingerson et al., 1991). This allows for filming and analysis of a much larger field of view for the same resolution than is possible with video analysis. Video, however, has the advantage of being quicker, simpler, and probably less expensive than photographic techniques which require purchasing and development of film, followed by interrogation or digitization of the photographs. Also, video techniques allow the analysis of a series of frames in order to track tracer particles with a wide range of velocities within a given field of view. This is especially useful in porous media flow velocity measurements. Video techniques have successfully been used by Chen and Fan (1992) to capture the flow regime in a three-phase, index-matched fluidized bed using PIV. In these experiments, however, only the solid and liquid phases had the same refractive indices, the gas phase did not. This limited the amount of gas phase which could be present in the column since it would distort images. Glass beads were used as the solid media, sodium iodide solution as the liquid, and air as the gas.

Measurement of gas bubble and fluid velocities were performed in the column, but with limited resolution. Only naturally occurring particles in the sodium iodide solution were used as tracer particles and additional seeding of tracers could have possibly increased the observed liquid velocity field resolution. Cui and Adrian (1992) have also used video techniques with an index-matched granular suspension to calculate solids distribution in a Couette flow rheometer at varying shear rates.

2.2 Particle Tracking Velocimetry

PTV is a low-image-density operating mode of PIV in which individual tracer particles in a fluid are tracked in order to obtain point velocities (Adrian 1991). The PTV method chosen for this project involves analysis of sequential, single-exposure video images and uses a cross-correlation method for tracking binary particle images. Prior to measuring velocities in a porous medium, verification of the PTV procedure and the velocity interpolation algorithm was performed with simpler flow regimes: laminar flow between plates around washers and laminar flow in a square tube.

As previously mentioned, PTV is a low-image-density mode of PIV. This indicates that the concentration of tracer particles is low such that the exact location of each tracer particle can be monitored through time in order to calculate a velocity vector at a point. The low tracer concentration ensures that incidence of tracer overlap in the observed plane is minimal. This is different from the high-image-density mode of PIV in which the concentration of tracers is high and locations of individual tracers are not identified. In this mode a transparency of a multi-exposed photograph is typically interrogated at points which contain clusters of particle images. When a collimated light source is directed onto the clusters of images, interference patterns known as Young's fringes are created and can be analyzed to yield a velocity vector for the cluster of particles at a given point in the flow field (Adrian 1991).

PTV can be further broken down into two categories: single frame and multi-frame techniques. Single frame techniques include streak and multiple image velocimetry. Both of these techniques suffer from confusion of overlapping streaks or images since each tracer particle is imaged at more than one time on the same photograph or other recording medium. Furthermore, the direction of flow is not inherently obvious unless special pulsing techniques are used to identify the beginning or end of a streak or series of particle images (Adrian 1991). Also, since the velocity field resolution for video techniques is limited by the number of pixels available for imaging, a multi-exposure or streak image is an inefficient use of the recording medium when compared to a single-exposed image, where all tracer particles are only imaged once. For these reasons a multi-frame technique was chosen for this research project.

Two types of multi-frame methods exist: multiple frame and two frame cross-correlation (Hassan et al. 1992a). In the multiple frame technique at least four frames are needed and the technique involves prediction and verification of particle displacements. This procedure is less desirable than a two frame technique since it requires more images to be stored and analyzed. The two frame cross-correlation technique involves matching a particle from one image to the proper particle on a second image by means of a correlation coefficient. The basic assumption for this method is that each particle is surrounded by a particular pattern of other particles and this pattern is assumed to remain nearly constant over the time interval of the two sequential frames. A correlation coefficient can therefore be calculated for a particle in one frame with a candidate in the second frame by means of how well their patterns of surrounding particles match. Hassan et al. (1992a) found that the cross-correlation technique generally performed better than the multiple frame technique, although it required more CPU time. The cross-correlation technique was used in this research project, but with a modification allowing analysis of multiple frames in order to assure accurate velocity measurements for both slow and fast particles in the same field of view. The cross-correlation method is described in more detail in Chapter 3.

2.3 Interpolation Algorithm

In order to complete a PTV analysis of a fluid flow it is convenient to interpolate a complete velocity field from randomly spaced vectors. Two types of algorithms were examined and a modification of one of them was incorporated into a velocity field interpolation program. One algorithm considered was used by Cho and McLachlan (1987) for interpolating a velocity field for flow around a cylinder. This method involved a simple convolution technique with an adaptive Gaussian window. In this method the size of the averaging window, h(x,y), is inversely proportional to the square root of the density of the velocity vectors. Equation (2.3.1) gives the interpolated velocity vector at a grid point (x,y), where x(i) and y(i) are the coordinates of a velocity vector, $\vec{V}(i)$, within the averaging window. This exponential weighting function seems

$$\vec{V}(x,y) = \frac{\sum_i \vec{V}(i) e^{-\{[x-x(i)]^2+[y-y(i)]^2\}/h^2(x,y)}}{\sum_i e^{-\{[x-x(i)]^2+[y-y(i)]^2\}/h^2(x,y)}} \qquad (2.3.1)$$

to give a nearly even weighting distribution for velocity vectors which are within a typical interpolation window (see Figure 2.3.1).

Another algorithm considered was used by Kawasue and Ishimatsu (1991) in their experiments on fast measuring techniques for PTV analysis of water flows. This algorithm incorporates all of the velocity vectors in the field of view and weights them according to the inverse of their distance squared from the interrogation point. Equations (2.3.2) and (2.3.3) are used to determine the velocity vector at each grid point (x,y), where x_k and y_k are the coordinates of some velocity vector and r_k^2 is the square of the distance of this vector from a node point.

$$V(x,y) = \frac{\sum_{1}^{n} \frac{V(x_k y_k)}{r_k^2}}{\sum_{1}^{n} \frac{1}{r_k^2}} \qquad (2.3.2)$$

$$r_k^2 = (x - x_k)^2 + (y - y_k)^2 \qquad (2.3.3)$$

For the purposes of interpolating a heterogeneous flow field it is apparent that not all of the vectors in the field of view need to be used to determine a nodal velocity. Instead, an interpolation window is used which excludes vectors which are far away from the node. The actual window size should be based on the raw vector density and reliability, the interpolation grid density, and the degree of heterogeneity of the flow field. The searching window size is not extremely important for the $1/r_k^2$ method, however, since distant vectors already have very little influence on the nodal velocity. The searching window simply reduces computation time by eliminating certain vectors from the computations. Figure 2.3.1 shows a plot of relative weighting of five vectors within a searching window which is twenty pixels on edge for both types of interpolation algorithms. The five vectors are located 1, 3, 5, 7 and 10 pixels away from the node point. The value of the relative weighting for each vector indicates its influence on the interpolated nodal velocity. From Figure 2.3.1 it can be seen that the $1/r_k^2$ weighting distribution gives most of the weighting to the vector which is closest to the node point. This seems most appropriate and therefore this equation was chosen as the weighting distribution function. An additional criteria, however, was applied to the interpolation procedure which required that there be at least two vectors within each averaging window in order to obtain a valid interpolated nodal velocity.

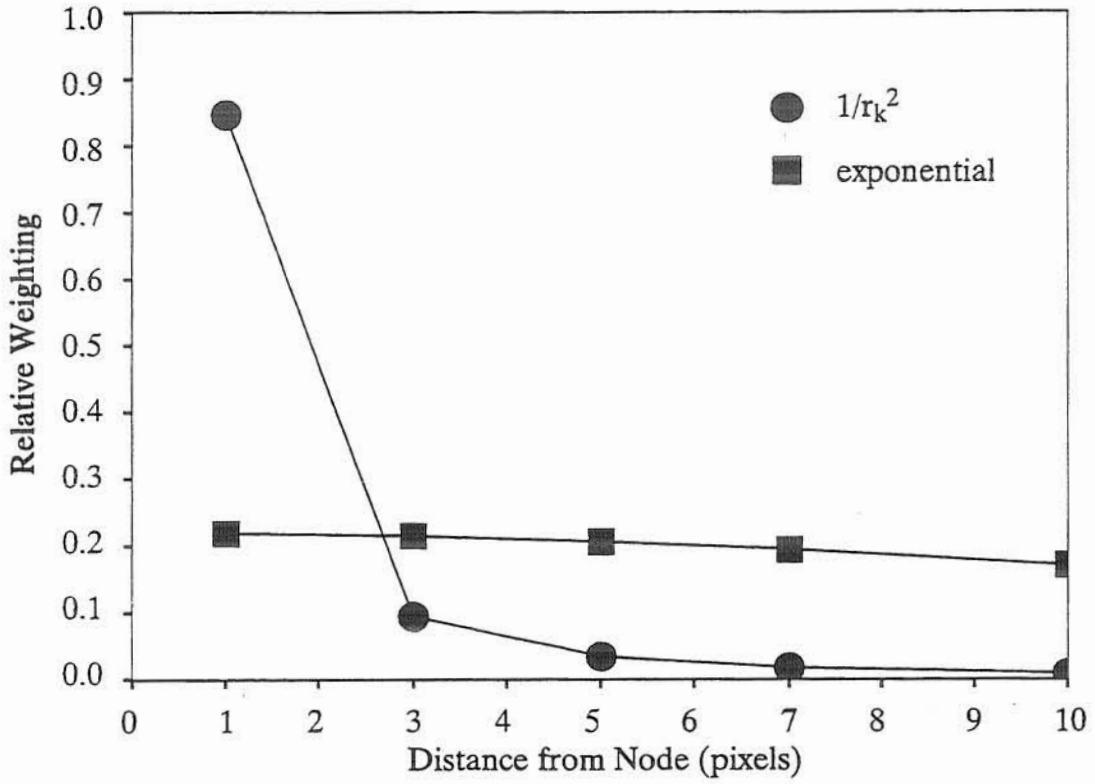

Figure 2.3.1 Relative Weighting for $1/r_k^2$ and Exponential Interpolation Functions

2.4 Nuclear Magnetic Resonance Techniques

The methods for measuring flow velocities in a porous media previously mentioned in this thesis rely upon optical index-matching to allow for the undistorted passage of light rays. The necessity of refractive index-matching is a disadvantage to these techniques because it limits the types of media and fluid that can be used. In nuclear Magnetic Resonance (NMR) techniques, on the other hand, imaging and three-dimensional velocimetry can be performed in a non-index-matched system with no particle seeding. The magnetic response of the water molecules is analyzed instead of the optical images of tracer particles. Apparently, the first application of NMR to porous media was performed by Shattuck et al. (1991) at Duke University. In this experiment, measurements of three-dimensional pore-water velocities and porosity were made in a non-index-matched system of acrylic spheres and water in a Plexiglass column. The column to media diameter ratio was 10 for the experiment and the effect of the wall on axial velocities was found to penetrate a significant distance into the column. In a related experiment by Nakagawa and Jeong (1992), NMR was used to study rotating granular flow. The analysis of mustard seeds in a rotating acrylic column showed the distribution of the mustard seeds depended upon the fluid that was present with the seeds, either water or air.

Furthermore, the seeds were tagged in an additional experiment and the relative motion of the seeds was observed from deformation of the tagged regions of seeds.

NMR has also been used by Hinedi et al. (1993) to measure porosities in aquifer materials. It was found that the technique is biased towards large pores when saturation times are short since it takes a long time for small pores to become completely saturated with water. In addition, the pore shape factor strongly influences the NMR porosity results and must be determined independently from the NMR analysis. Although NMR has the significant advantage over conventional optical velocimetry of not requiring an index-matched system, it does require the use of much more sophisticated and expensive equipment. The lower capital cost and level of complexity of the PTV system developed in this project is considered a significant advantage, which should encourage a more widespread application of the procedure.

3. PTV Procedure and Computer Programs

3.1 General Procedure and Equipment

The first step in obtaining a velocity field for a plane of flow is to illuminate a plane of the flow field with a laser. The laser used for this project was a 300 mW Ion Laser Technology multi-line Argon ion laser. This laser emits light in the 457 to 514 nm wavelength range. The laser light was transmitted through a fiber optic to a cylindrical lens which created a thin light sheet. In order to capture images of the flow field with sufficient magnification and resolution, a monochrome Sony XC-75 1/2 inch CCD camera (768H x 494V) was used and the images were stored on VHS video tape via a Panasonic AG-1960 VCR. The CCD camera has a standard video capture rate of 30 frames per second, which limits the timestep for PTV analysis to multiples of 1/30 of a second (i.e. 0.03333, 0.06667, 0.1, etc. seconds). Two different lens configurations were used with the CCD camera throughout the experiments: a 4X microscope objective with extension tubes and a 75 mm telephoto lens with extension tubes. The amount of extension tube used with the different lenses determined the overall magnification, working distance, and field of view. After recording the images on video tape, they were transferred to a Macintosh IIci where a Perceptics frame grabber was used to capture and digitize images into arrays of 640H x 480V pixels. This array size is smaller than the array size output from the CCD camera because apparently the 640H x 480V is a standard array size for recording video images and the frame grabber will only capture video images of this size or smaller. After the images were digitized, they were enhanced and converted to a binary format. (Examples of both raw and enhanced video images are shown in Chapter 6). The binary matrices of a series of frames were then transferred to a Hewlett Packard workstation where the images were analyzed for particle centroids. Subsequently, the cross-correlation particle tracking algorithm was executed to determine velocity vectors for the flow field. The particle tracking program yielded a two-dimensional velocity vector for each particle tracked from an initial frame to one at some later time. Since steady flow existed in the experiments, other sets of images at different times were analyzed and the resulting vectors combined to achieve a more complete velocity profile. Finally, the interpolation program was executed to yield the complete velocity profile for the flow field. A detailed explanation of all steps involved in capturing, transferring, and analyzing video images of particles is provided in Appendix A and a schematic of the image capture and transfer procedure is shown in Figure 3.1.1.

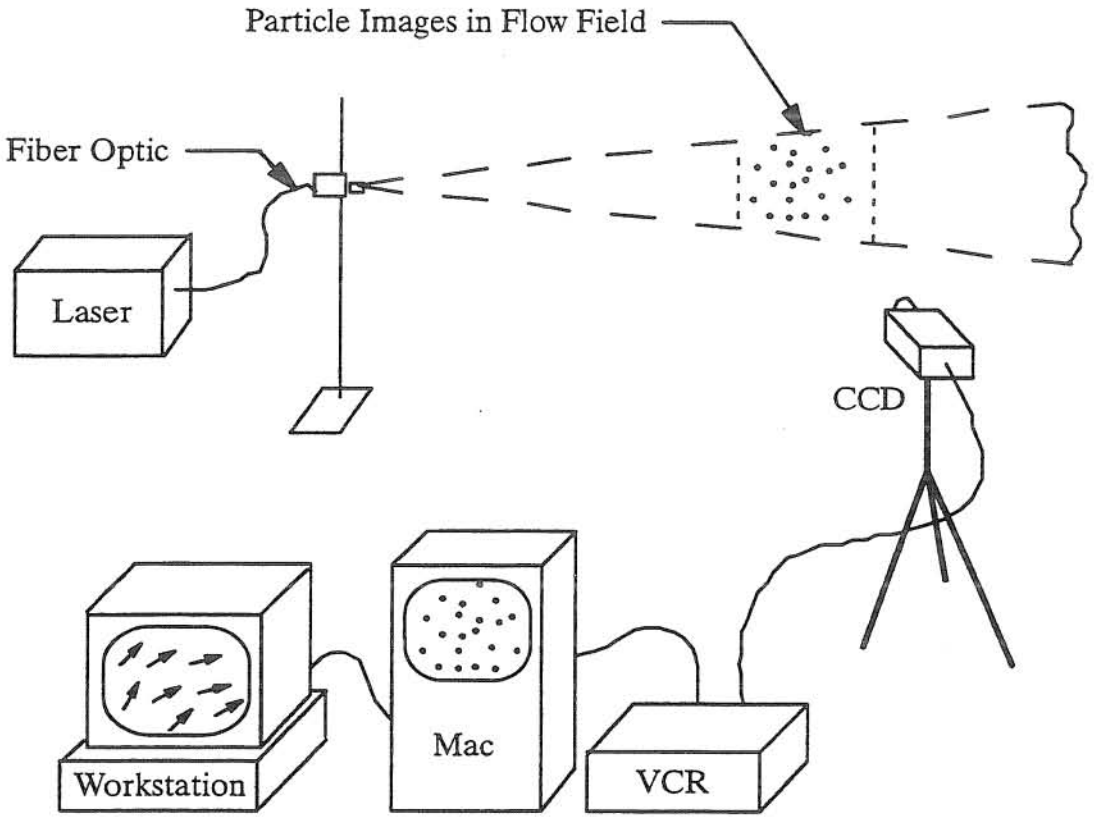

Figure 3.1.1 Image Capture and Transfer Procedure

3.2 Computer Programs

In order to make the analysis of a series of frames simple and fast, the particle identification program, particle tracking program, and several supporting fortran programs were linked together by one Unix script file called "Track." This script file requires an input file which contains all of the information necessary to perform the particle tracking analysis. A detailed explanation of the contents of the input file is provided in Appendix B along with explanations of all of the computer programs and input and output files generated during the analysis. After "Track" is executed, there are two additional script files which may be executed. First, is the "Combine" script file which takes information files from two independent PTV analyses and combines their vector information in order to get a more complete velocity field. "Combine" should therefore only be used for files from the same field of view and flow rate. The "Combine" file also links several fortran programs together for quicker, easier analysis. Combining vector fields is only possible when steady, laminar flow exists. The final script file to

be executed is called "Interpolate." This file takes an information file and generates an interpolated velocity field at regularly spaced grid points. The last program to be executed is a fortran program called "Vavg2.ftn." This program calculates an average pore-water velocity for an interpolated velocity field, including average vertical and horizontal velocities. Details about the use of all of the computer programs are given in Appendix B.

3.3 Particle Identification Algorithm

Once a series of binary image files have been transferred from the Macintosh computer to the workstation, the first required analysis is the particle identification and centroid calculation step. This is performed by a computer program which scans each image and identifies groups of connected black pixels as particles. Since the images are binary, a white pixel is considered background and a black pixel is considered to be part of a particle. While scanning the binary image matrix, each time a black pixel is found a particle number is put into that location in the image matrix to denote the particle to which that pixel belongs. The appropriate particle number is determined by checking the current pixel's neighboring pixels which have already been scanned. If a particle number exists in any of the neighboring pixels then that particle number is assigned to the current pixel and is entered into the image matrix at the location for the current pixel. The current pixel is then considered to be part of a previously identified particle. If there is no previously identified particle number in the neighboring pixels, then a new particle number is created and inserted into the matrix at the current pixel location. If more than one neighboring pixel has a particle number and they are different, all connected pixels are given the lowest particle number and are then considered to be part of the same particle. Once the entire image is scanned, the area centroid of each particle within a specified size range is calculated and output to a file to be used by the particle tracking program.

3.4 Cross-Correlation Method

The cross-correlation particle tracking program is the key to turning a series of binary image matrices into a velocity field. Once the image files have been transferred to the workstation and the centroids of all particles in each frame have been determined, the cross-correlation particle tracking program is executed to properly identify tracer particles from the first frame to another frame at some later time. The cross-correlation method uses a correlation window centered over a particle as a template by which to identify that particle and its immediate neighbors at a later timestep. The basic assumption of this method, therefore, is that the orientation of the tracer particles relative to each other does not change much in one

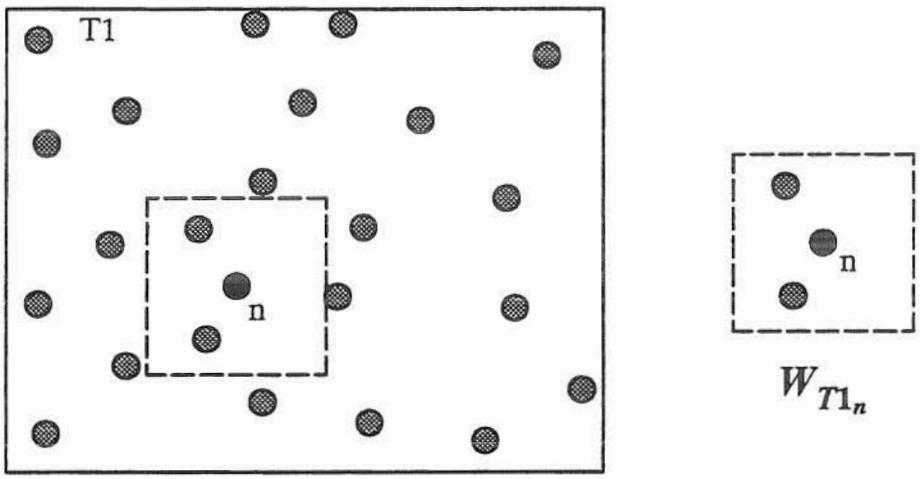

Figure 3.4.1 Sample Image Field and Correlation Window for Particle n at Time = T1

timestep. If it is found that the orientation of the particles relative to each other is changing significantly between consecutive frames, then the timestep between the frames is too large or the flow rate is too high. The specific binary cross-correlation method used in this project is based on the method described by Hassan et al. (1992b).

In order to fully understand how the cross-correlation method can be used to properly identify a particle at a later timestep when it is among other candidate particles, a series of sample images and correlation windows have been drawn that illustrate the cross-correlation technique. Figure 3.4.1 shows an image of a flow field at some time T1. It is assumed that the particle tracking program is currently attempting to track particle n from T1 to some later time T2. The first step the program takes is to draw a correlation window around particle n at time T1. This correlation is denoted as W_{T1n} and also serves as the searching window for candidate particles in the T2 frame. The size of this window should therefore be large enough to ensure that the tracer particles will remain within the searching window from the initial time to the final time when displacements are calculated. Some knowledge about the maximum expected displacement of the particles should be known in order to choose an appropriate correlation window size. This correlation window will be used to see how well the candidate particles at the next timestep correlate with particle n and its immediate neighbors. Figure 3.4.2 shows the same flow field but at some later time T2. The window drawn in this image is in the same location as in T1 and denotes the area in T2 which is searched for candidate particles which correspond to particle n. The asterisk denotes the previous location of particle n at T1. From Figure 3.4.2 it is apparent that three particles are within the searching window and all three will be considered as possible locations of particle n at T2. These particles are denoted as i, j, and k.

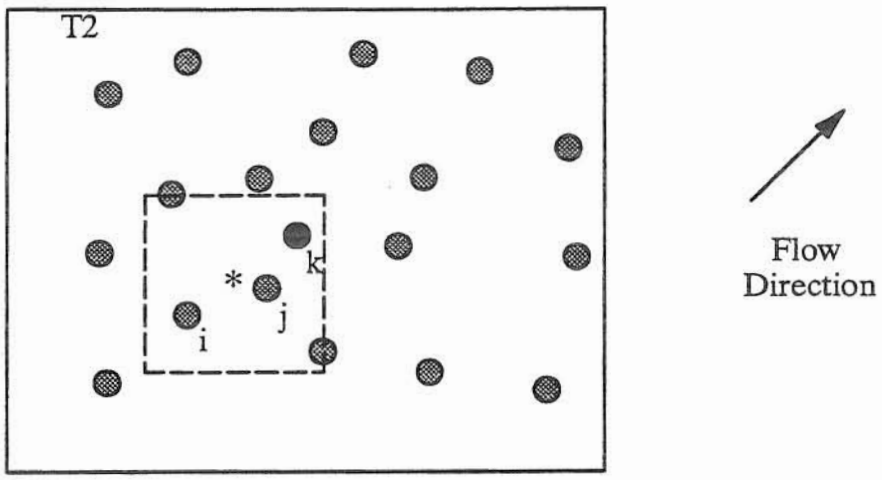

Figure 3.4.2 Sample Image Field at Time = T2

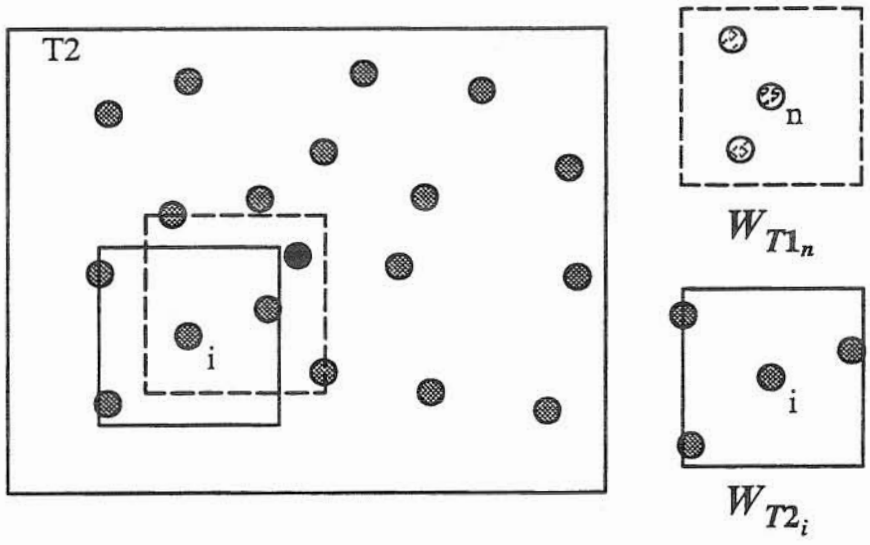

Figure 3.4.3 Correlation Window for Candidate Particle i at Time = T2

The first candidate particle to be analyzed is particle i at T2. In order to determine the correlation between i and n, a correlation window must be drawn around i (W_{T2i}) and compared to the correlation window around n from T1 (W_{T1n}). These two correlation windows must be the same size in order to properly determine their correlation. From Figure 3.4.3 it is apparent that the correlation windows drawn around n and i are not very similar. This potential match would therefore have a low correlation. The same approach is used to compare a correlation window around particle j (W_{T2j}) with W_{T1n}. Again, it is apparent from Figure 3.4.4 that j does not correlate well with particle n. Finally, a correlation window around

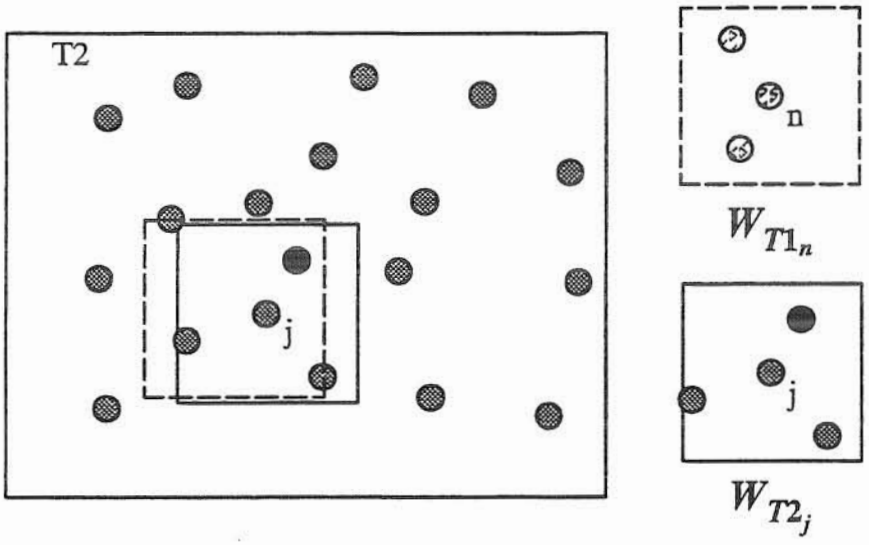

Figure 3.4.4 Correlation Window for Candidate Particle j at Time = T2

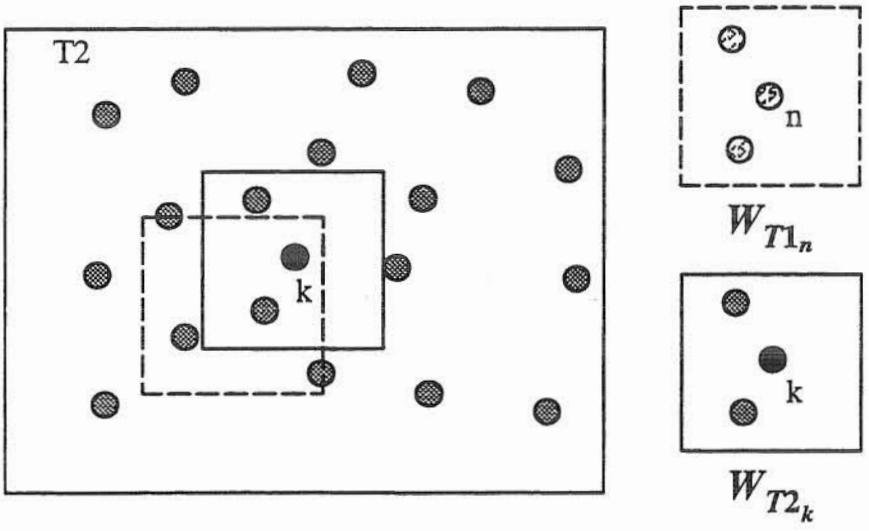

Figure 3.4.5 Correlation Window for Candidate Particle k at Time = T2

candidate particle k is compared with W_{T1n} and a very good match is observed (see Figure 3.4.5). Particle k would therefore have the highest correlation of the three candidate particles and be chosen as the correct location of particle n at T2. The location of particle k is then used to calculate a displacement for particle n and a corresponding velocity vector can be calculated. Figure 3.4.6 shows frames from T1 and T2 superimposed and a velocity vector which indicates that particle n was correctly identified at T2. This analysis can be repeated for

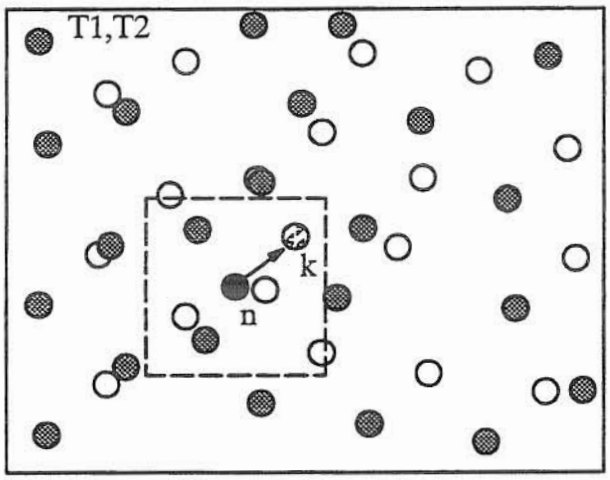

Figure 3.4.6 Computed Velocity Vector for Particle n

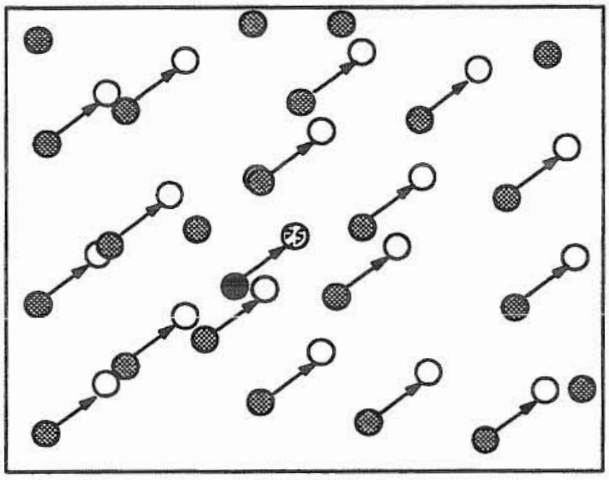

Figure 3.4.7 Velocity Vectors for all Particles in Field of View

all of the particles in the field of view and a field of velocity vectors can be found as shown in Figure 3.4.7.

In order to have a quantitative means for comparing one potential particle match with another it is essential to evaluate a correlation coefficient which gives a numerical value between zero and one for each potential match. A correlation coefficient of one would indicate a perfect match, whereas a correlation coefficient of zero would represent no match at all. The potential match yielding the highest correlation coefficient would therefore be chosen as the correct match, as long as it is greater than some minimum required correlation

coefficient which helps to reduce erroneous vectors. The appropriate minimum correlation coefficient is determined by trial and error for a given series of images. If a required correlation coefficient is too low, erroneous vectors may result and if the coefficient is too high, valid vectors may be eliminated. Different values should be tried and the resulting vector field inspected in order to determine an appropriate correlation coefficient for a given series of images. This minimum value will be influenced by overall image quality. Equation (3.4.1) was used to calculate the correlation coefficient for all potential matches, where $C(T1_n,T2_i)$ is the correlation coefficient for the potential match between n at T1 and i at T2, W_{T1n} and W_{T2i} are the correlation windows described above, B_{T1n} and B_{T2i} are the number of black (or particle containing) pixels in W_{T1n} and W_{T2i}, and x and y are the coordinates of a pixel in the correlation windows. The value of $W_{T1n}(x,y)$ or $W_{T2i}(x,y)$ would therefore be one when the

$$C(T1_n, T2_i) = \frac{\sum_{x=0}^{nx}\sum_{y=0}^{ny} W_{T1_n}(x,y)W_{T2_i}(x,y)}{\sqrt{B_{T1_n}B_{T2_i}}} \qquad (3.4.1)$$

pixel at (x,y) is black (part of a particle) and zero when the pixel is white (background). The correlation windows are compared pixel by pixel and every incidence of black pixel overlap is recorded and the sum of these incidents of overlap comprises the numerator of the fraction in Equation (3.4.1). The denominator is a value somewhere between B_{T1n} and B_{T2i}. If both correlation windows have the same number of black pixels, the denominator is equal to B_{T1n} which is equal to B_{T2i}. For perfect correlation to occur, each correlation window must have the same number of black pixels and all of these pixels must overlap each other when the two correlation windows are compared pixel by pixel.

3.5 Minimum Displacement Criteria

Because the PIV technique developed in this project is video-based, there is an inherent problem of limited resolution and therefore limited accuracy in tracer particle centroid determination. Figure 3.5.1 shows an example of a slight error in centroid determination of a discretized particle image versus the actual particle image due to the approximation of the particle's actual shape with small square pixels. This discretization of the actual image in video analysis limits the accuracy of centroid calculations and encourages the use of some minimum displacement criteria for particle centroids in order to minimize the relative error in velocity measurements. For example, if a given particle has a 0.2 pixel error in its displacement measurement and it only displaces one pixel, it would have a 20% relative error in

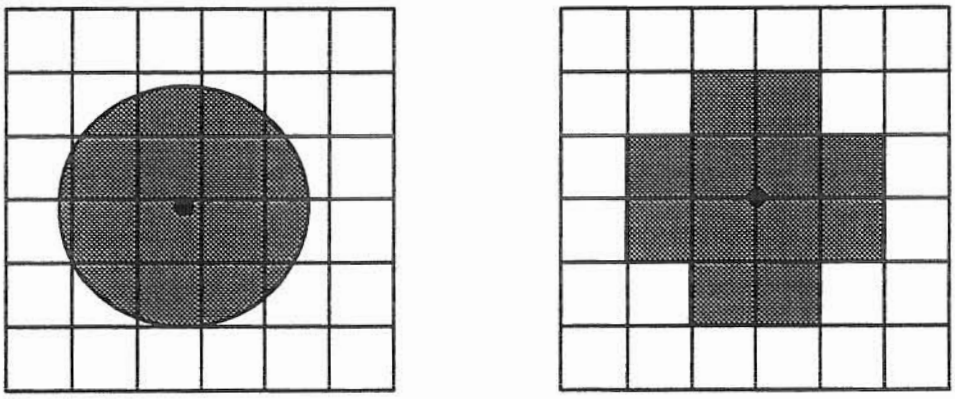

Actual Image Discretized Image

Figure 3.5.1 Particle Centroid Error Due to Limited Video Resolution

$$\textit{Relative Error (\%)} = \frac{\textit{Absolute Displacement Error (pixels)}}{\textit{Displacement (pixels)}} \qquad (3.5.1)$$

displacement and corresponding velocity according to Equation (3.5.1). However, if that same particle travels 5 pixels, the relative error is reduced to 4%, although the absolute error in displacement measurement remains constant.

In order to minimize relative error in velocity determination for all of the tracer particles in a field of view, it was necessary to develop a procedure to analyze a series of video images which would allow velocity determination for fast particles with a small timestep, and slow particles with a large timestep. The analysis begins by analyzing two consecutive frames and calculating velocity vectors for all tracers displacing a distance greater than or equal to a specified minimum displacement criteria. For all of the particles which are correlated at this step but did not travel the minimum displacement criteria, the analysis proceeds to the next frame to allow the tracer to displace further before calculating a final displacement. A file is created to store the location, displacement angle, and velocity magnitude of each particle which correlated but did not displace the minimum displacement criteria. This procedure continues stepping forward in time until all of the particles have displaced a sufficient distance, until they no longer correlate, or until no frames remain to be analyzed. Figure 3.5.2 shows a velocity vector being determined for both a fast and slow particle in the same field of view. The fast particle can be accurately analyzed by measuring its displacement after just one timestep (T1 to T2),

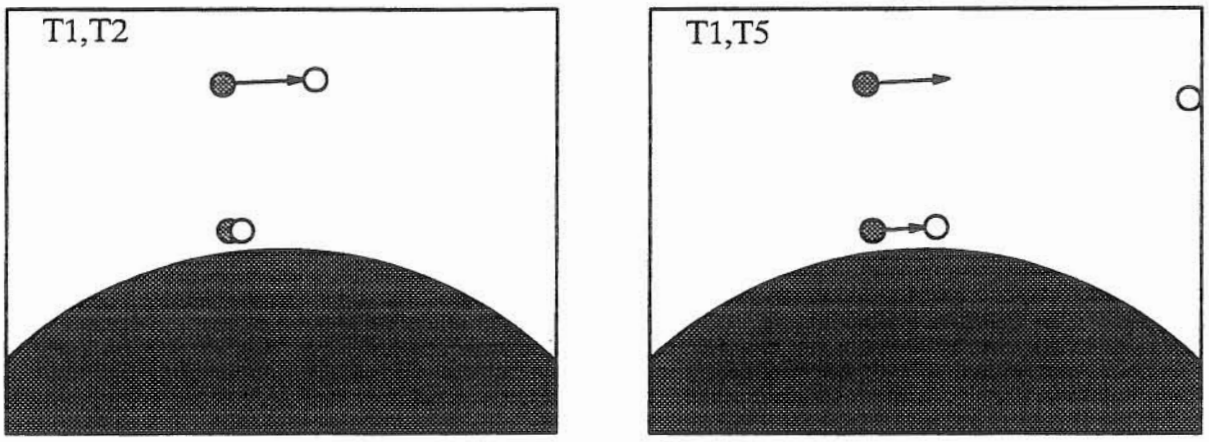

Figure 3.5.2 Tracking a Fast and Slow Particle with Multiple Frames

but the slow particle must advance four timesteps (T1 to T5) before it displaces the minimum displacement criteria. The errors resulting from choosing different minimum displacement criteria are discussed in Chapter 4, where trials with different minimum displacement criteria were performed and average relative errors in velocity were calculated.

When the particle tracking program tracks particles beyond the first timestep forward it uses some of the preliminary displacement data in order to make the next search more efficient and accurate. For example, when a particle displacement calculated from the first timestep is found to be smaller than the minimum displacement criteria, the calculated displacement is used to determine the searching window size in the next iteration. The searching window size becomes the greater of either three times the expected displacement of the particle or three times the particle diameter. This searching window size determination is graphically depicted in Figure 3.5.3, where Dp is the tracer particle diameter, De is the expected particle displacement, and SW is the searching window. Furthermore, the correlation window size is also determined as the greater of 60% of the searching window size or three times the particle diameter. The correlation window size determination is also shown graphically in Figure 3.5.4, where CW is the correlation window. In the first iteration, the size of the searching and correlating windows are equal and are the same size for all tracer particles. This window size is specified by the user based on some information about the maximum expected tracer displacements in the flow field. Finally, the angle of displacement from the previous iteration is also recorded and the tracer particle is required to remain along a similar path to be considered the correct particle. This path was chosen to be within $\pm 65°$ of the previous displacement angle and appears to be a suitable criteria which further ensures the same

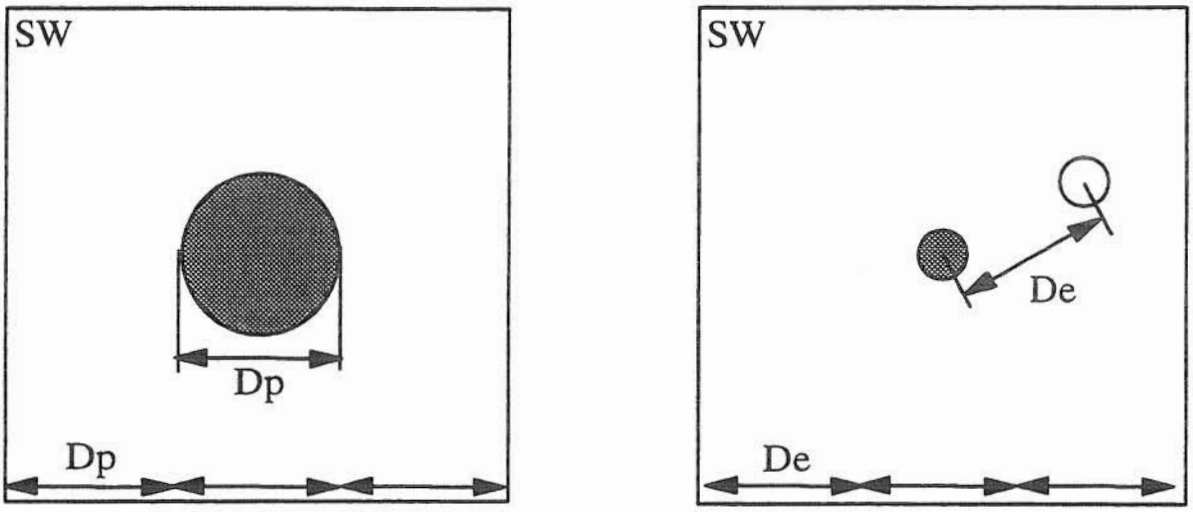

Figure 3.5.3 Determining Searching Window Size (for Iteration > 1)

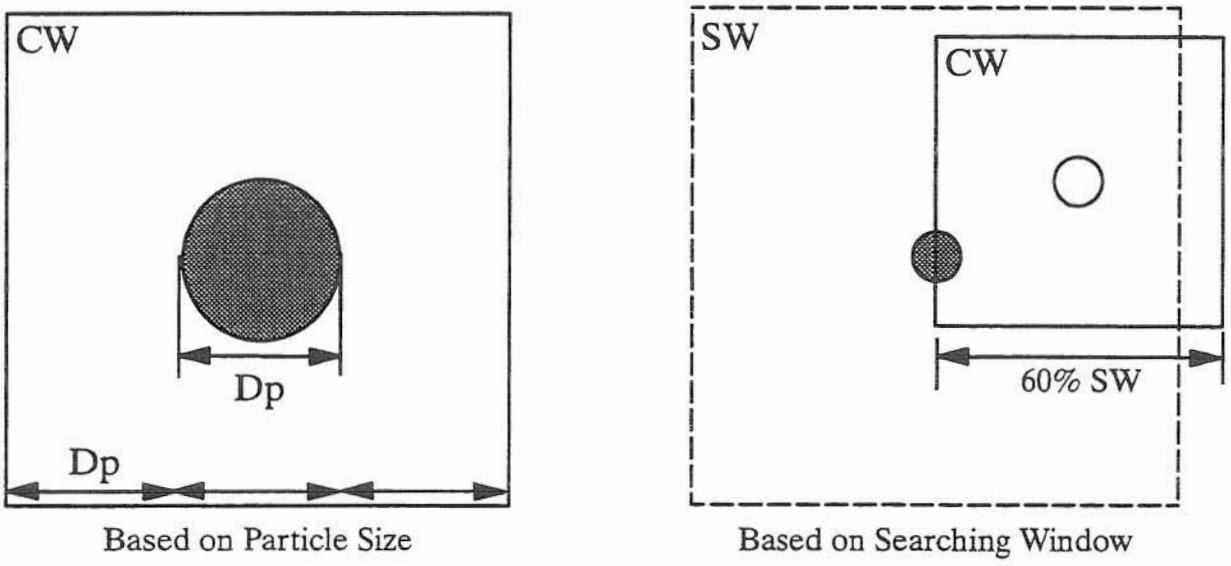

Figure 3.5.4 Determining Correlation Window Size (for Iteration > 1)

particle tracked at the previous iteration is correctly followed at the next iteration. This displacement path criteria is also shown graphically in Figure 3.5.5.

3.6 Interpolation Procedure

After the video images have been analyzed to obtain raw velocity vectors, a Unix script file called "Interpolate" is executed on an information file to generate an interpolated velocity

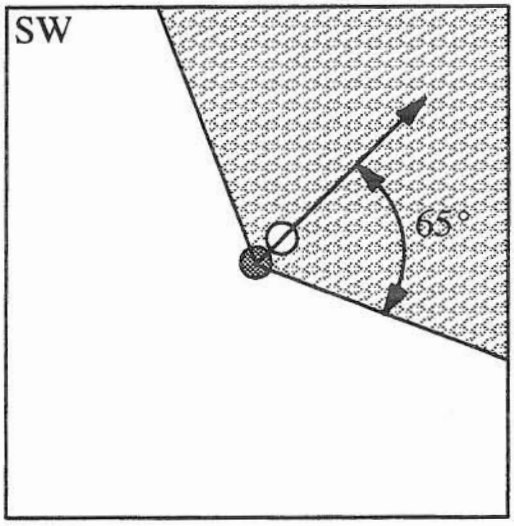

Figure 3.5.5 Displacement Path Criteria (for Iteration > 1)

field at grid points. The velocity field is scanned at regularly spaced node points and a velocity vector is calculated for all qualifying node points using the $1/r^2$ weighting function discussed in Section 2.3. A qualifying node is one that has at least two velocity vectors within a searching window around that node and is also located within a fluid region of the field of view. The size of the searching window is specified by the user and is entered into the input file for "Track" along with the node spacing. These parameters, however, are only used by "Interpolate." In order to determine wether or not a node point is within a fluid region of the field of view, a media file is used by the interpolation program to compare the location of the node point with the location of the media in the field of view. If there is no media within the field of view, all nodes with two or more vectors within the specified interpolation window size will have an interpolated velocity vector. If the locations of the media were not checked, the interpolation program would generate velocity vectors inside the media, which is obviously undesirable. The name of the media file is also entered into the input file for "Track," but is only used by "Interpolate."

3.7 Sources of Experimental Error

There are several sources of experimental error which can affect the PTV analysis of a flow field. These errors can be broken down into two main categories: errors in determining raw velocity vectors and errors in interpolating a velocity field at regular grid points. One significant source of error in determining raw velocity vectors is the centroid determination for each particle image. As discussed in Section 3.5, a round tracer particle must have its shape

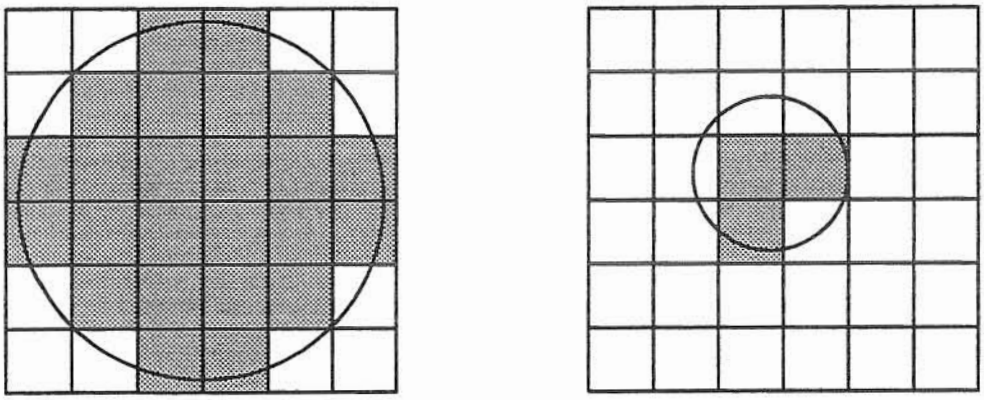

Large Particle Small Particle

Figure 3.7.1 Effect of Particle Size on Error in Centroid Estimation

approximated with square pixels and the centroid of the approximated image may have some error associated with it. This error will be greater for small images and less for large images since the relative effect of approximating a particle's perimeter with small squares decreases as particle size increases. Essentially, the larger a particle image is, the more the approximated image looks like the real image and the more accurate the centroid calculation will be. This effect is shown graphically in Figure 3.7.1. In order to minimize this error, only particle images with 10 or more pixels were analyzed and a minimum displacement criteria was imposed on all particles to make the centroid error small relative to total displacement. The actual error in centroid calculation, therefore, is a function of image size and is difficult to quantify since the "real" centroid for any images particle is actually unknown. Based on typical particle image size of about 30 to 40 pixels, the error in centroid is assumed to be less than 0.25 pixels. This corresponds to a maximum error in particle displacements of 0.5 pixels. The selection of an appropriate minimum displacement criteria is discussed in further detail in Section 4.3.

Another source of error in the raw velocity vector calculations is the conversion of the particle displacements from pixels to length units. This must be done by imaging an object with a known dimension (such as a ruler) and calculating a conversion factor based on the size of that object in pixels. In the porous media experiments, however, there was some magnifying effect of the porous media and fluid such that the focal distance of the lens configuration changed when the field of view was inside the column. This caused some uncertainty in the calibration of the flow field since the calibration of the field of view was performed outside of the column where a ruler could be imaged. Because of the apparent magnifying effect of the porous media, the distance from the lens to the plane of focus was different inside and outside the column. Although the exact effect of the porous media on image size is unknown, it is

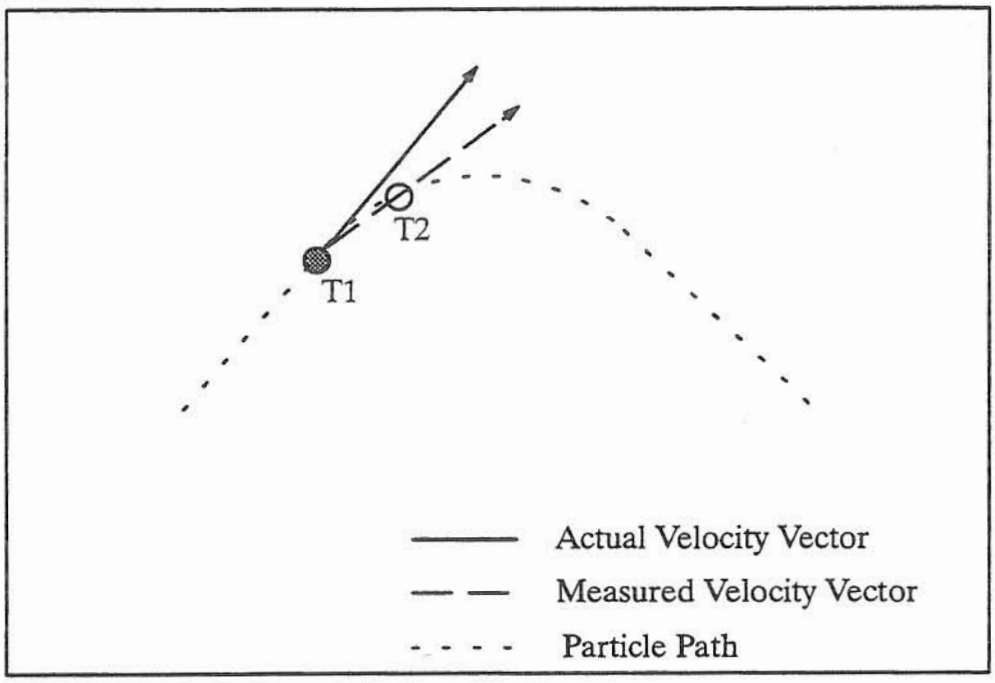

Figure 3.7.2 Velocity Vector Angle Error for Large Displacements

assumed that the effect is small since the distance to the focal plane was greater inside the column, which likely offsets the magnifying effect of the media.

A major error in raw velocity vector determination would be the improper tracking of a particle from one frame to the next. This error would likely be very large since the wrong particle image would be used to determine displacement. These occasional "false" velocity vectors, however, are usually easy to identify since they are inconsistent with either the magnitude or direction of its neighboring velocity vectors. The number of occurrences of "false" vectors will increase as the minimum required correlation coefficient is reduced to allow poorly correlated image pairs to be accepted.

A final source of error in raw vector determination would be for flow fields with highly curved streamlines. In these situations, there should be an upper limit on particle displacement in order to prevent large errors in the measurement of displacement angles over too large a timestep (Figure 3.7.2). The upper limit on displacement would typically be much greater than the minimum displacement criteria discussed above since under most flow conditions it is unlikely that the angle of the particle's path would change greatly over just one or two particle diameters, which corresponds to a relatively large minimum displacement criteria. The physical limit on particle displacement is incorporated into the PTV program by the searching window size which is entered into an initial input file for the PTV program called

"Track," which is discussed in Appendix B. Any particle which travels outside of the initial searching window in the second timestep will not be tracked.

Errors in the interpolation of the velocity field at regular grid points have two major sources. First is the actual approximation of a nodal velocity by vectors located some distance away. The magnitude of these errors will depend on the density of the neighboring velocity vectors and how large the searching window is to find a sufficient number of neighboring velocity vectors. In order to ensure some minimum level of accuracy in interpolated velocity values, a two vector minimum was required to be within each searching window around a node in order for a nodal velocity vector to be determined. Furthermore, the size of the searching windows were kept significantly smaller than the average pore size such that the vectors used in the interpolation window had some relevance to the nodal velocity. The actual values for the errors in the interpolated nodal velocities are difficult to quantify. The other major source of error in the interpolation procedure is specific to porous media flow: the presence of no-slip boundaries. Because the fluid/media interfaces have zero velocities, but are not measured (since there are no moving particles at the interface), nodal velocities near fluid/media interfaces may be biased towards higher fluid velocities which are some distance from the fluid/media interface. These errors are assumed to affect only the node points which are very close to the media surfaces and again, are not easily quantified.

From the previous discussion it is apparent that the errors in the calculated velocity vectors are difficult to quantify and it becomes necessary to compare the calculated velocity values with some theoretical values or values obtained from an independent experimental analysis. In Section 5.3 the resulting velocity vectors in a square column flow are compared to a theoretical velocity profile and the average relative error in the measured velocities was approximately 5%.

4. 2-D Washer Experiment

The purpose of the first experiment was to show that the PTV procedure and all of the equipment were functioning properly. Small particles were videotaped as they flowed around rubber washers which separated glass plates. The images were analyzed and the resulting velocity vectors were overlaid on the particle images to check to see that the vectors properly indicated the displacement of the particles. Furthermore, details of the PTV procedure were developed and some error analysis was performed at this early stage in the research project.

4.1 Experimental Setup

The model for generating the 2-D flow field consisted of two glass plates separated by small rubber washers. A sucrose solution containing 400 μm dyed polystyrene microspheres (Polysciences, Inc.) flowed between the plates and the particles were videotaped with the CCD camera. The sucrose solution was approximately 13% sucrose by weight, which caused the polystyrene particles to be neutrally buoyant (Weast 1983). The solution and the particles had a density of approximately 1.05 g/mL. The glass plate model was illuminated from the back by a lamp and the light was diffused with a piece of opaque white plastic to provide a uniform, white background to contrast the blue particles. A constant flow rate was obtained by recirculating the fluid with a Peristaltic pump. After preliminary observations, however, it was noticed that the pump was causing a pulsing nature to the flow rather than a steady, smooth flow. This problem was solved by introducing intermediate reservoirs which effectively isolated the pump from the model. The pump removed fluid from the low-level reservoir and injected it into the high-level reservoir which maintained a constant head difference across the model. Since the head difference between the models was kept constant, a constant, steady flow was maintained. Figure 4.1.1 shows the major features of the experimental setup.

4.2 Procedure and Results

Analysis of the washer model began with videotaping a 3 by 4 centimeter region of the model containing several 2-D pores. After videotaping for several minutes, portions of the video tape were played back frame by frame to the Macintosh computer where successive images were captured and stored. The images were then enhanced and thresholded to a binary format and transferred to a Hewlett Packard workstation where particle identification and tracking were performed. Preliminary analysis of the video images yielded velocity vectors corresponding to the movement of individual tracer particles. These velocity vectors were then overlaid on top of two of the particle images to visually confirm that the vectors properly corresponded to the movement of the particles (Figure 4.2.1). Once visual confirmation of the

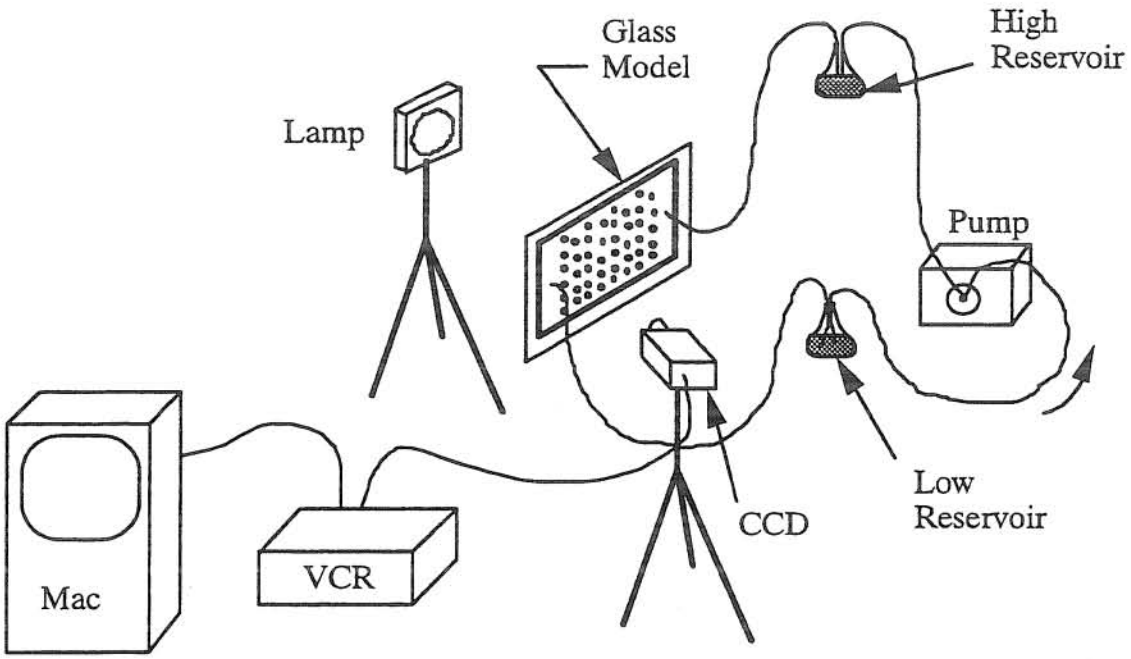

Figure 4.1.1 Experimental Setup for Washer Experiment

PTV procedure had been performed on single sets of images, it was necessary to overlay the results of several series of images in order to provide a velocity vector density sufficient to proceed with the interpolation program (Figure 4.2.2). The interpolation program was then executed with a searching window size of 60 pixels or 3.7 millimeters, as shown in Figure 4.2.2, and a more complete velocity profile was generated. The interpolated velocity profile is shown in Figure 4.2.3.

After confirming that the PTV and interpolation programs were properly functioning, it was important to examine the sensitivity of the procedure to a minimum displacement criteria. A minimum displacement criteria is important because of the error in displacement calculations for a particle with small displacements. The errors for small displacements arise since each particle image is broken down into a small number of square pixels. This discretization of the particle image causes slight errors in centroid calculations since the smooth edges of the particle are approximated by adjacent square blocks. The errors in centroid calculations become less important as total displacement increases. However, as total displacement increases, the velocity measured at a point shifts from an instantaneous velocity to an average velocity measured over the total displacement of a particle. Since the goal of all PIV methods is to measure instantaneous velocities at discrete locations in a flow

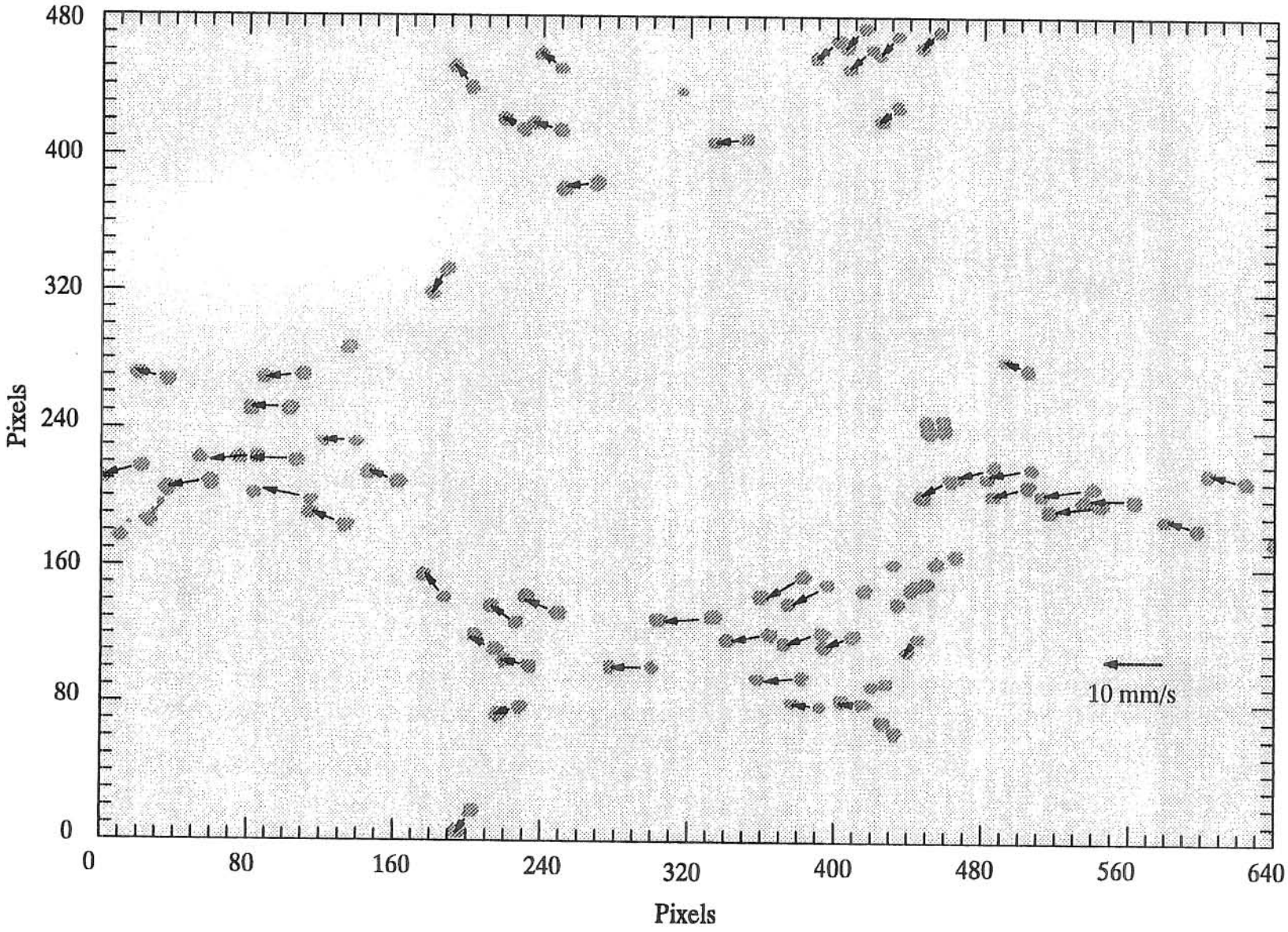

Figure 4.2.1 Overlay of Velocity Vectors on Two Particle Images

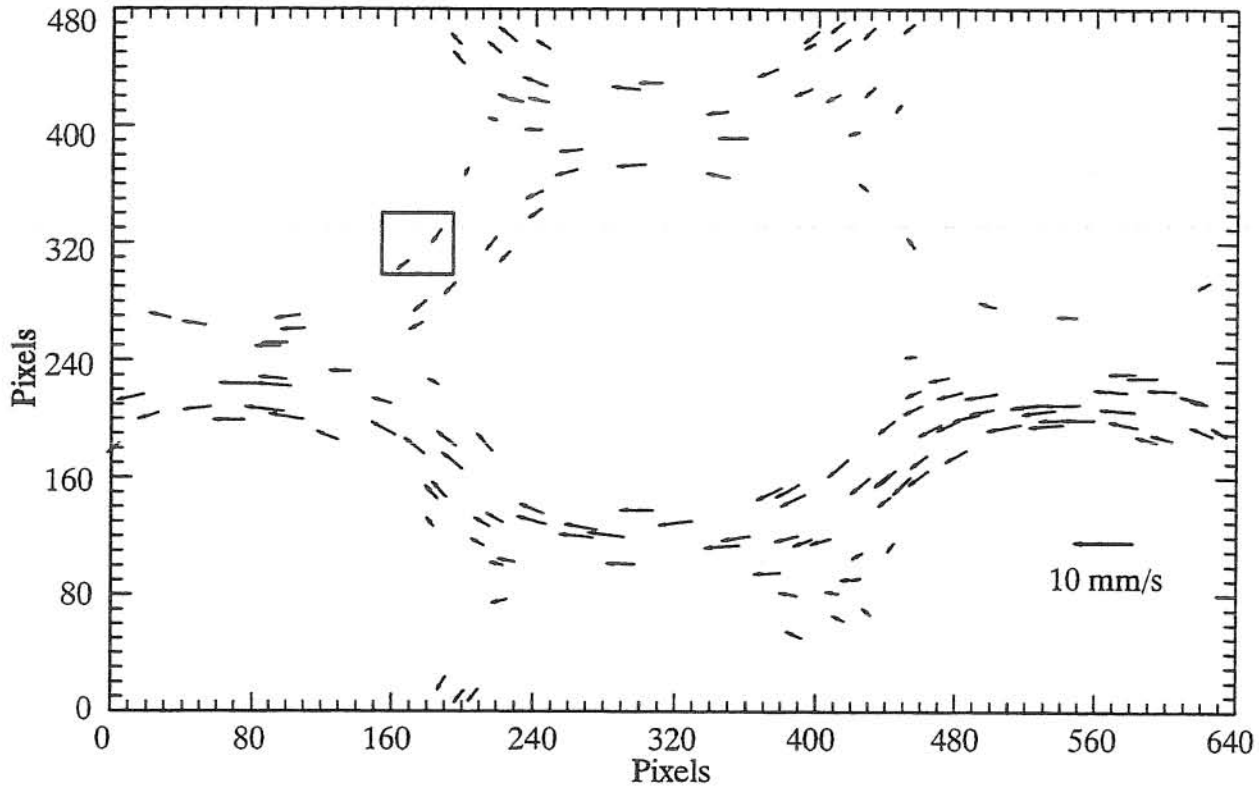

Figure 4.2.2 Overlay of Velocity Vectors from a Series of Images

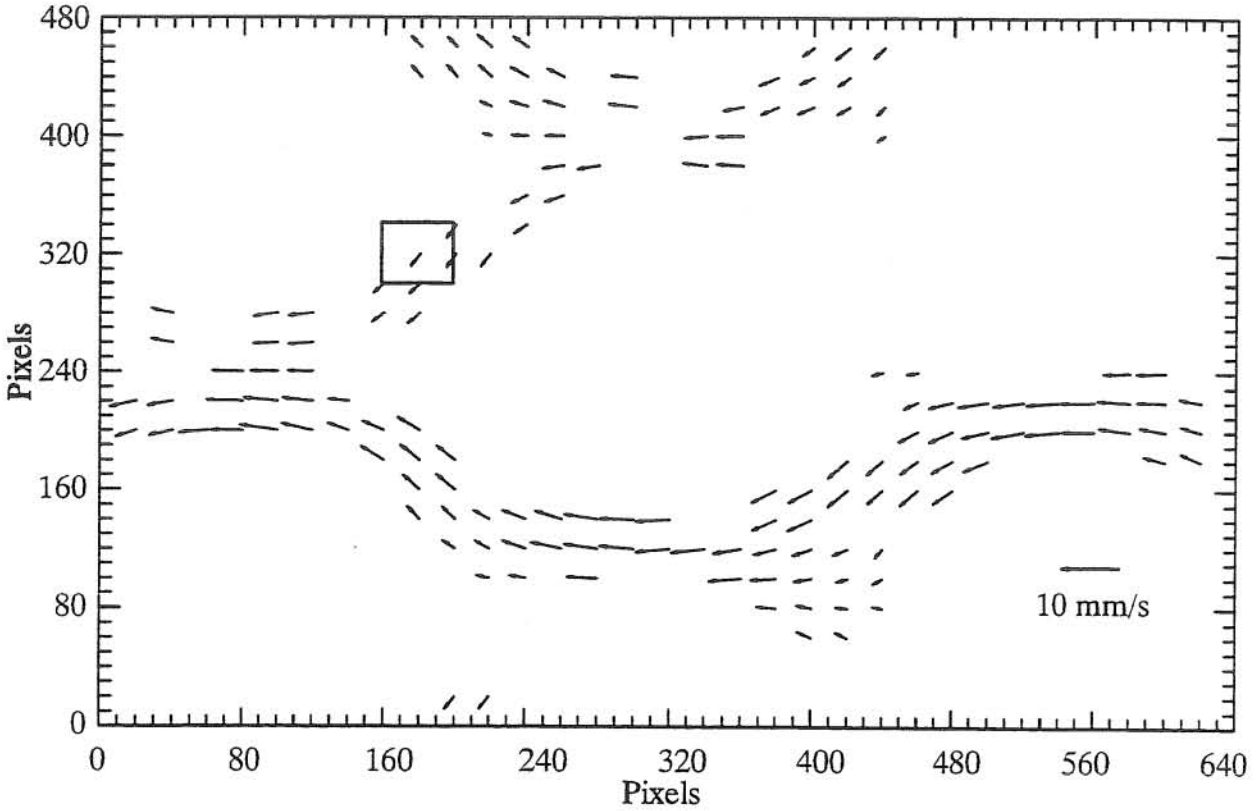

Figure 4.2.3 Interpolated Velocity Field

field, large displacements are generally undesirable. Care must be taken, therefore, to minimize the errors from small displacements, while keeping displacements small enough to obtain a valid velocity vector at a point.

Application of a minimum displacement criteria to all of the particles in a field of view typically demands the analysis of several frames. The faster moving particles will be measured between frames with a smaller time interval than will the slower moving particles. If 10 consecutive images are captured, for instance, PTV analysis of frame one and frame two will yield velocity vectors for only those particles which have displaced a distance greater than or equal to the minimum displacement criteria. In order to obtain velocity vectors for the remaining particles, frame one must be analyzed with frame three, which increases the time interval and observed displacement of the remaining particles. This process of stepping forward one additional frame is repeated until all of the particles have moved a distance equal to or greater than the minimum displacement criteria, all of the remaining particles fail to meet the minimum correlation criteria, or all of the available frames have been analyzed. This procedure should yield the most consistent level of reduced error in the displacement of each particle, as well as the corresponding velocity values.

In order to determine an appropriate minimum displacement criteria, a series of images was processed ten times with a different minimum displacement criteria for the particles for each iteration. The minimum displacement criteria chosen were 1, 2, ...,10 pixels. The average velocity for each particle was calculated from all ten iterations and assumed to be the true velocity of that particle. Then the individual velocities for each particle were compared to the true velocities. The average difference from the true velocity for each particle was recorded as the relative error for each iteration (Figure 4.2.4). The average relative error for each iteration was then compared in order to choose the optimum minimum displacement criteria.

4.3 Conclusions and Error Analysis

In Figure 4.2.1, visual confirmation of the ability of the PTV procedure to accurately track particles is made. From Figure 4.2.3, however, it can be seen that the interpolated velocity field is incomplete which is due to a lack of velocity vectors in certain regions, as seen in Figure 4.2.2. Proper particle seeding density and tracer distribution can alleviate this problem. In the final porous media experiments a higher seeding density was used which allowed for a more complete velocity field. For the purposes of this portion of the experiment, however, the results were sufficient to illustrate the proper functioning of the interpolation program.

The relative error results from the minimum displacement criteria analysis are presented in Figure 4.2.4 It is evident that a minimum displacement criteria of at least three pixels is

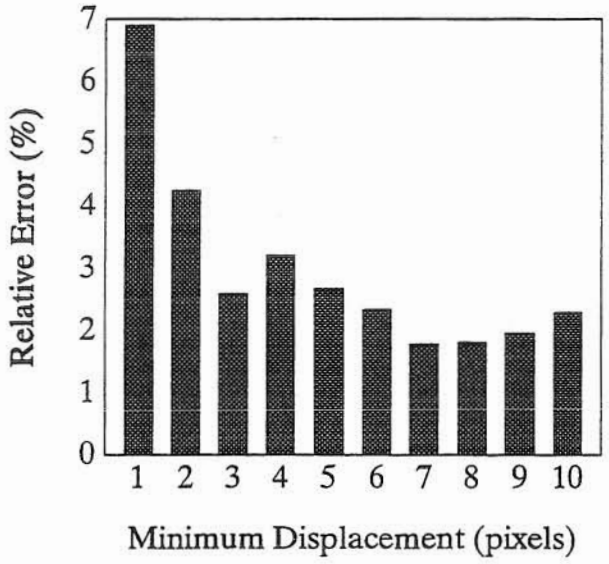

Figure 4.2.4 Relative Error vs. Minimum Displacement for 1 to 10 Pixel Displacements

important and ideally a minimum displacement criteria of seven to nine pixels should be maintained. Due to the large relative velocity errors for the minimum displacement criteria of one and two pixels, another analysis was performed using the iterations with minimum displacements of three to ten pixels only. The average value of the velocity for each particle, therefore, was computed using only the trials for three to ten pixels minimum displacement. The results from this analysis are shown in Figure 4.3.1 and also indicate that a minimum displacement criteria of seven to nine pixels is optimum. This criteria should be applicable to most observed flow conditions. A flow field with highly curved streamlines, however, may have a limit on maximum particle displacement which is close to the value of the minimum displacement criteria. This upper limit on displacement would be to prevent large errors in the measurement of displacement angles over too large a timestep. The errors associated with large particle displacements were discussed previously in Section 3.6.

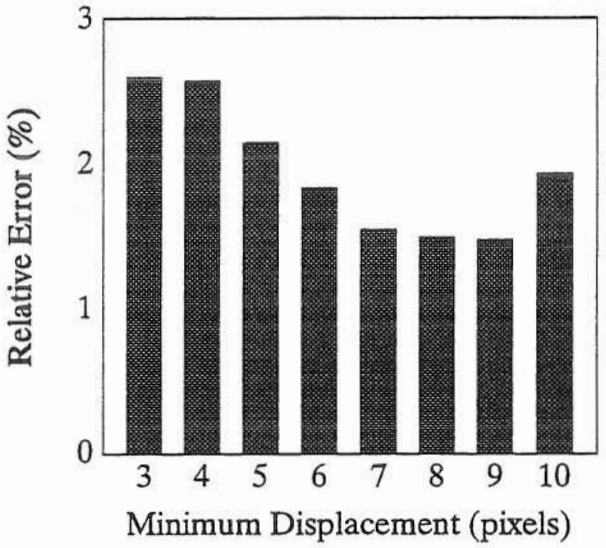

Figure 4.3.1 Relative Error vs. Minimum Displacement for 3 to 10 Pixel Displacements

5. 1-D Laminar Flow in a Square Column

Before applying the video PTV technique developed in this project to a 3-D porous media, it was important to ensure that the technique gave quantitatively accurate results with a simpler and verifiable flow regime. An example of such a flow regime is laminar flow in a square column as described by Camp et al. (1990) and Langlois (1964). A sheet of laser can be used to illuminate a plane of flow which can be analyzed to see if the procedure developed in this project verifies the theoretical velocity profile in the square column. After verification, the technique can be applied to a porous medium. Due to the complexity of the geometry, theoretical verification of the porous medium results can only be done by checking the average pore-water velocity obtained with that expected from macroscopic calculations based on flow rate, area, and porosity. Other velocimetry techniques, such as laser Doppler velocimetry, could possibly be used to verify point velocity vectors within the porous medium.

5.1 Theoretical Solution

In order to confirm that the velocity vectors found from the PTV procedure are reliable, it is important to know the expected velocity profile for laminar flow in a square column. Langlois (1964) presents the equation for axial velocity for a rectangular pipe. This velocity equation can be simplified for flow in a square pipe (Figure 5.1.1), which results in the following equation:

$$V(x,y) = \frac{G}{2\mu}\left[a^2 - y^2 + \frac{32a^2}{\pi^3}\sum_{n=0}^{\infty}\frac{(-1)^{n+1}\cosh\left[(2n+1)\frac{\pi x}{2a}\right]\cos\left[(2n+1)\frac{\pi y}{2a}\right]}{(2n+1)^3\cosh\left[(2n+1)\frac{\pi}{2}\right]}\right] \qquad (5.1.1)$$

where V is the flow velocity at a given point, G is the pressure gradient, and μ is the viscosity. Figure 5.1.2 shows a three-dimensional plot of the theoretical dimensionless velocity profile for laminar flow in a square column.

5.2 Experimental Setup

In order to obtain velocity measurements for a vertical plane in a column of fluid, a planar section must first be illuminated with a sheet of laser light. The laser used in this project was a 300 mW Argon ion laser with a cylindrical lens providing a laser sheet approximately 1 mm thick. The fluid, tracer particles, and pumping setup from the washer experiments were reused in the square column experiment. The glass column was a 22 mm inside diameter column

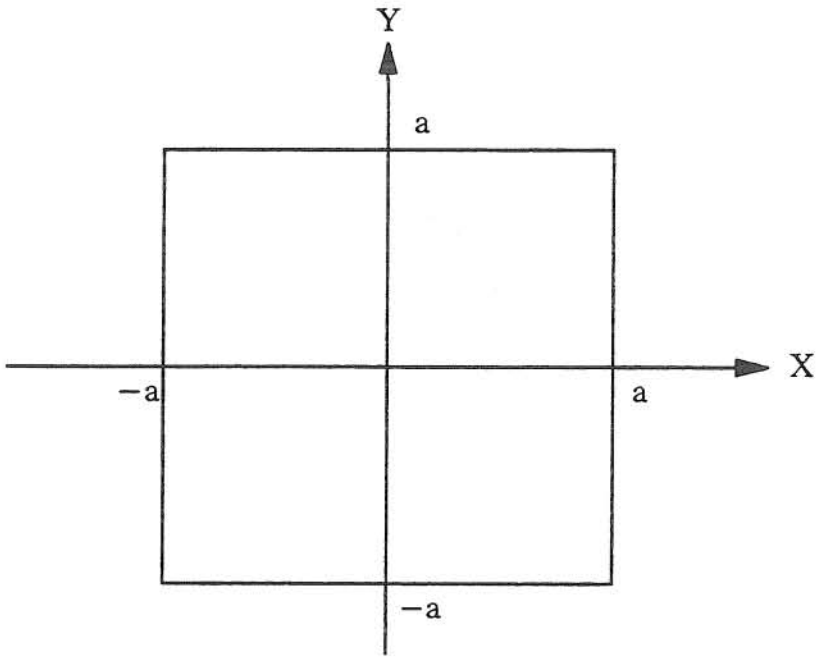

Figure 5.1.1 Cross-section of Square Pipe

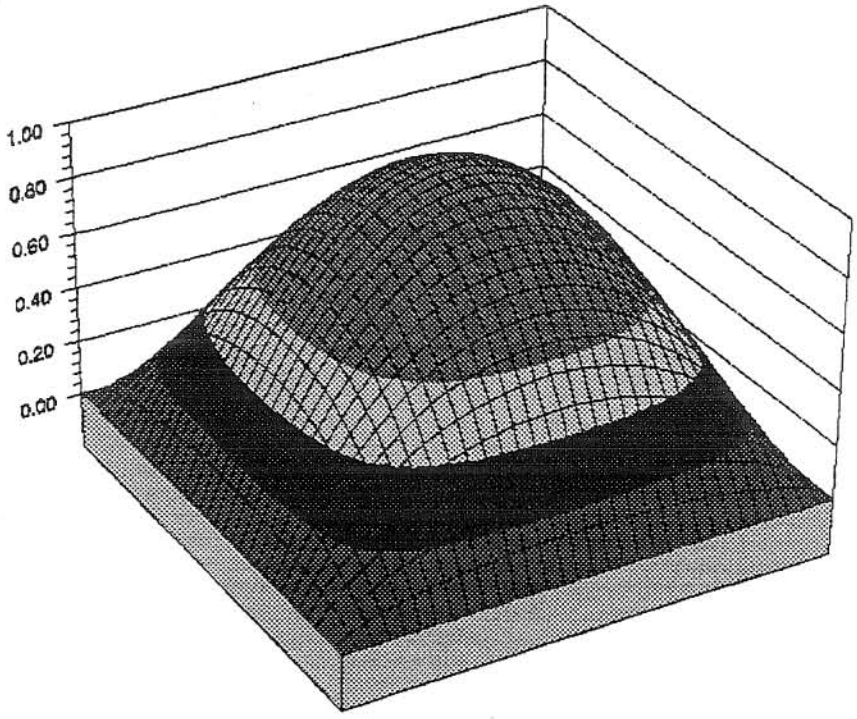

Figure 5.1.2 Theoretical Dimensionless Laminar Velocity Profile for a Square Column

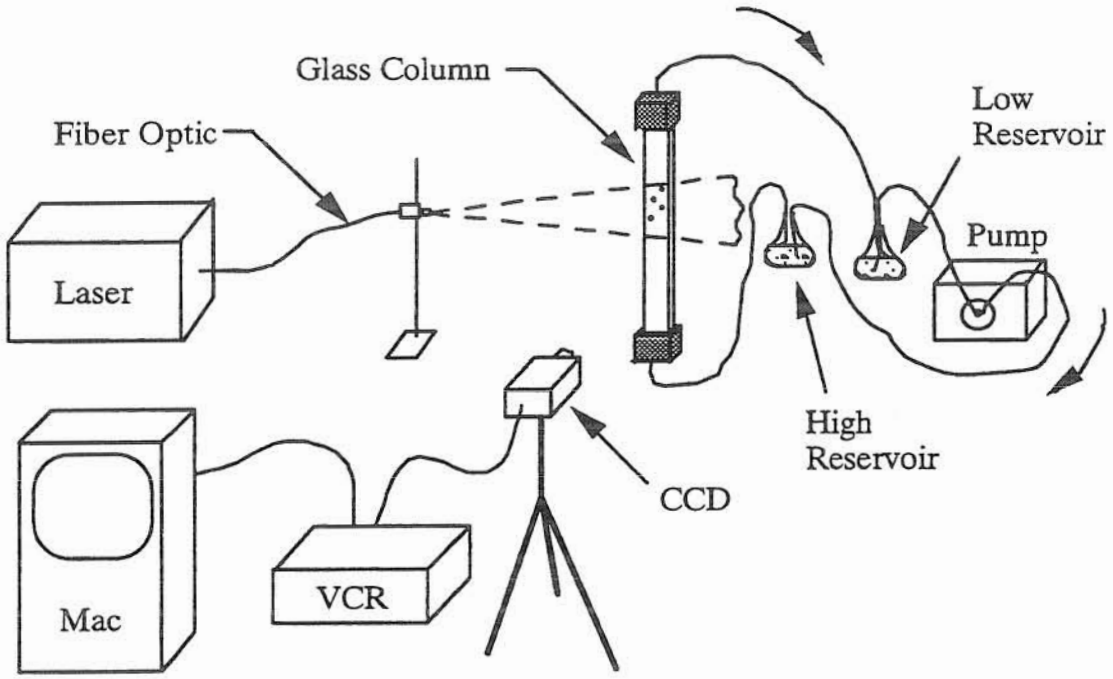

Figure 5.2.1 Experimental Setup for Glass Column Experiment

made by Vitro Dynamics, Inc. The energy was dissipated at the entrance of the square column with 3 mm glass beads and the flow direction was upwards. Scratch marks were etched on the sides of the column to aid in alignment of the laser sheet and to determine the centerline of the column for velocity profile analysis. Figure 5.2.1 shows the major features of the experimental setup.

The kinematic viscosity of the sucrose solution used in this experiment was approximately 1.4 centistokes (Weast 1983) and the flow rate was 76 mL/min, resulting in a Reynolds number of approximately 40, which ensured laminar flow conditions since the transition to turbulence begins at a Reynolds number of approximately 2100 (Denn 1980). The Reynolds number was calculated with the following expression:

$$\mathbf{Re} = \frac{vd}{\nu} \qquad (5.2.1)$$

where Re is the Reynolds number, v is the average fluid velocity, d is the inside edge length or hydraulic diameter of the pipe (four times the area divided by wetted perimeter), and ν is the kinematic viscosity of the fluid (Denn 1980). Based on flow through a circular pipe, the entrance length in which the laminar profile is still developing is given by:

$$\frac{Le}{D} \approx 0.59 + 0.055Re \qquad (\mathrm{Re} < 2100) \qquad (5.2.2)$$

where Le is the entrance length, and D is the pipe diameter (Denn 1980). The entrance length for the column used in this experiment, therefore, is approximately 6.1 centimeters or 2.8 column diameters. Since the column was approximately 14 diameters long, there should have been sufficient distance for the velocity profile to become fully developed.

5.3 Procedure and Results

Three different vertical planes were videotaped in the column: the center of the column and half the distance to the front and back walls (Figure 5.3.1). For each plane, the velocity vectors obtained from the analysis of several series of frames were overlaid to obtain enough velocity vectors for a complete analysis of each cross-section. The resulting particle velocities for each of the three planes were normalized by a peak central velocity which was determined by a least-square error minimization procedure that determined the best-fit surface for the velocity vectors from all three planes. The dimensionless velocity values were then plotted against the theoretical dimensionless velocity profile for each of the planes; no interpolation of the velocity vectors was performed (Figures 5.3.2, 5.3.3, 5.3.4). As seen in these figures, no velocity data were measured near the wall. This was due to a slight roundedness of the corners of the column which caused distortion of the images at the edges of the column. For this reason, only the central 80% of the width of the column was videotaped. An average relative error in the experimental velocity measurements of 5.3% was calculated for the front plane, 2.9% for the middle plane, and 6.4% for the back plane when each plane was compared to the

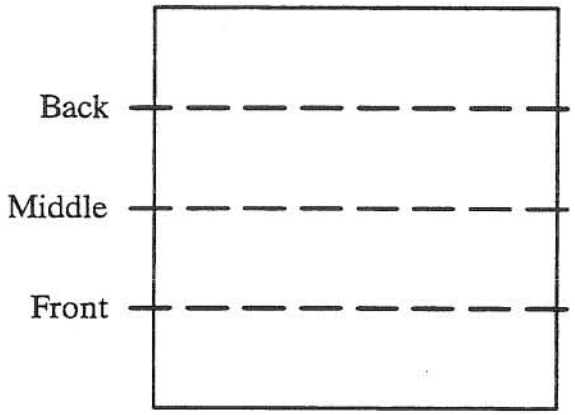

Figure 5.3.1 Vertical Planes in Square Column Chosen for Analysis

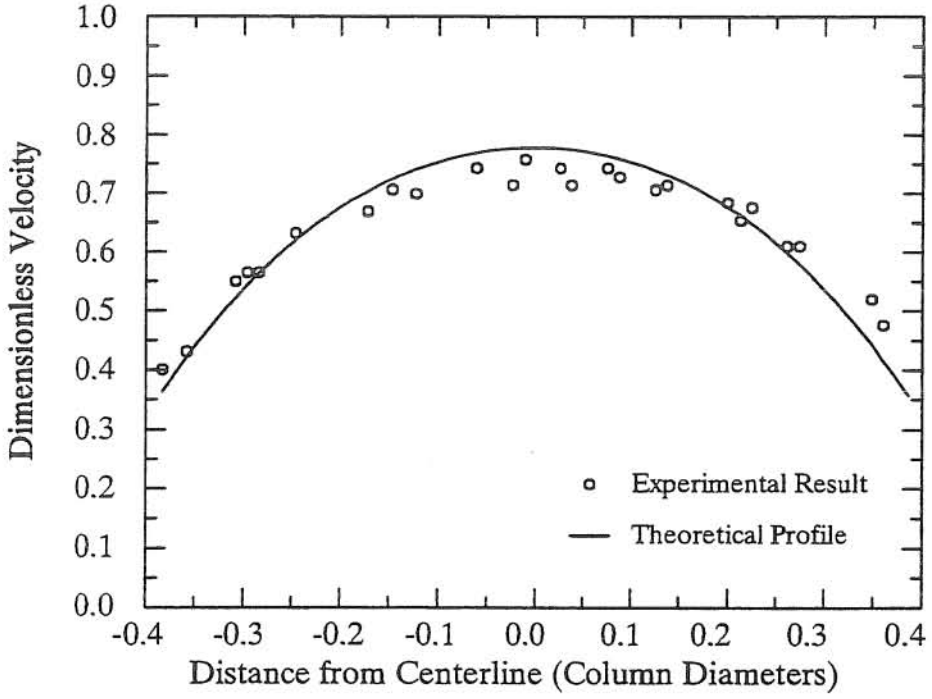

Figure 5.3.2 Experimental vs. Theoretical Velocities for 1/2 Distance to Front Wall

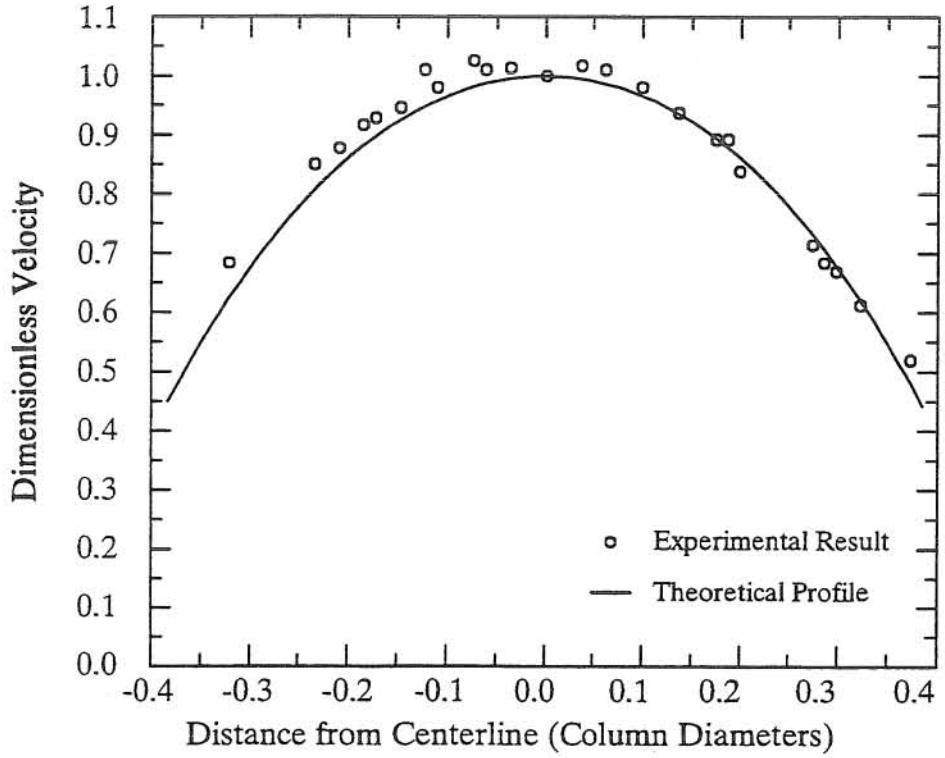

Figure 5.3.3 Experimental vs. Theoretical Velocities for Central Plane

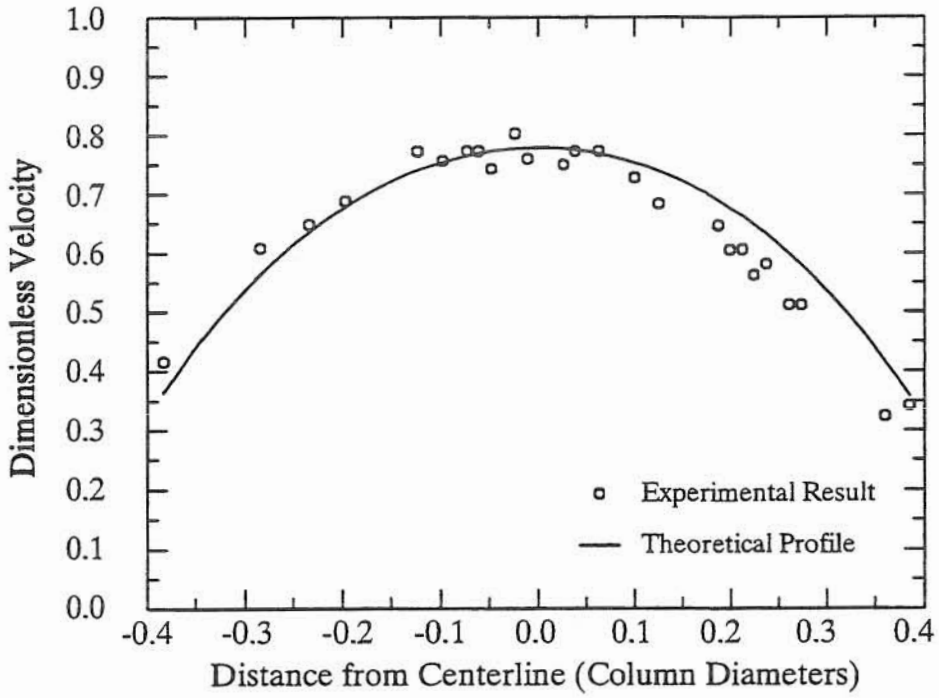

Figure 5.3.4 Experimental vs. Theoretical Velocities for 1/2 Distance to Back Wall

best-fit planar laminar velocity profile. An average relative error of 5.3% was calculated for the entire column when experimental data was compared to a best-fit surface for all three planes.

5.4 Conclusions

From observation of the experimental results it is evident that the measured velocities in the square column correlate fairly well with the theoretical plots. The errors present in the data are most likely due to problems with the experimental setup rather than the analytical procedure. If the column is too short, for example, the entrance and exit affects may interfere with the flow and prevent fully developed laminar conditions to exist. The length to width ratio of the column used in this experiment was approximately 14 to 1 which is apparently much less than the ratio used by Camp et. al (1990). The 14 to 1 ratio, however, should have provided sufficient length for the development of a fully developed laminar profile, although equation (5.2.2) was developed for a circular pipe and the column in this experiment was square. This may require a slightly greater entrance length for full development of the laminar profile. Since the length to width ratio for the column was relatively small, the flow might not have been fully developed which would be responsible for the imperfect agreement between theoretical and experimental results. Furthermore, there may have been some slight error in determining

the centerline of the column on the images, which could have resulted in a slight shift of the data to the right or left of the actual center of the column. This shift is apparent in the back plane (Figure 5.3.4), where the experimental data seems to be skewed to the left. Despite these errors, the velocities calculated were very close to the theoretical profile and ensured that the PTV procedure was properly functioning.

6. 2-D Analysis of Porous Media

The previous experiments were designed to verify the procedures and computer algorithms developed for PTV and velocity field interpolation. The following experiment applies these procedures to an idealized index-matched porous medium system. The goal of this experiment is to obtain a two-dimensional velocity field for a plane passing through a pore of the porous medium. The experimental setup is very similar to the previous square column experiments, however the column is filled with polymethylmethacrylate (PMMA) beads and an index-matching fluid is used to allow undistorted viewing of the interior of the column.

6.1 Experimental Setup

The physical setup for this experiment is nearly identical to the 1-D Laminar Flow in a Square Column experiment. However, the square column used in this experiment was made from Plexiglass and was 30 inches long and 3.75 inches square on the inside. The media used was 3/8 inch diameter PMMA spheres obtained from Spex Industries and the fluid was a Laser Liquid purchased from Cargille Laboratories. The fluid was seeded with hollow glass microspheres (Potters Industries, Inc.) which had a mean diameter of 8 μm and a range of 2 to 30 μm. The tracers had a nominal density of 1.1 g/cm^3. The entire experiment was also performed in a temperature controlled room in order to assure that the refractive indices of the PMMA beads and the Laser Liquid could be matched. The details about refractive index matching and materials selection are discussed in Section 6.2.

In addition to the PMMA beads, 9 mm glass beads (Cataphote, Inc.) were used to fill the upper and lower portions of the column since they were significantly cheaper than PMMA. The optical properties of the glass beads were unimportant since the glass beads were not in the section of the column in which videotaping and velocimetry were performed. The glass beads simply filled the ends of the column to allow the flow to develop before reaching the test section where the PMMA beads were placed. Another difference between the porous media experiment and the previous experiment is the type of flow control. In this experiment, the flow was controlled by a valve on the bottom of the column and the driving force was the gravitational head of the fluid in the column. The direction of flow, therefore, was downwards. A pump was used to recirculate the fluid into the top of the column and the pumping rate was adjusted to match the discharge rate from the bottom of the column in order to achieve a steady state flow condition. Figure 6.1.1 shows the major features of the experimental setup.

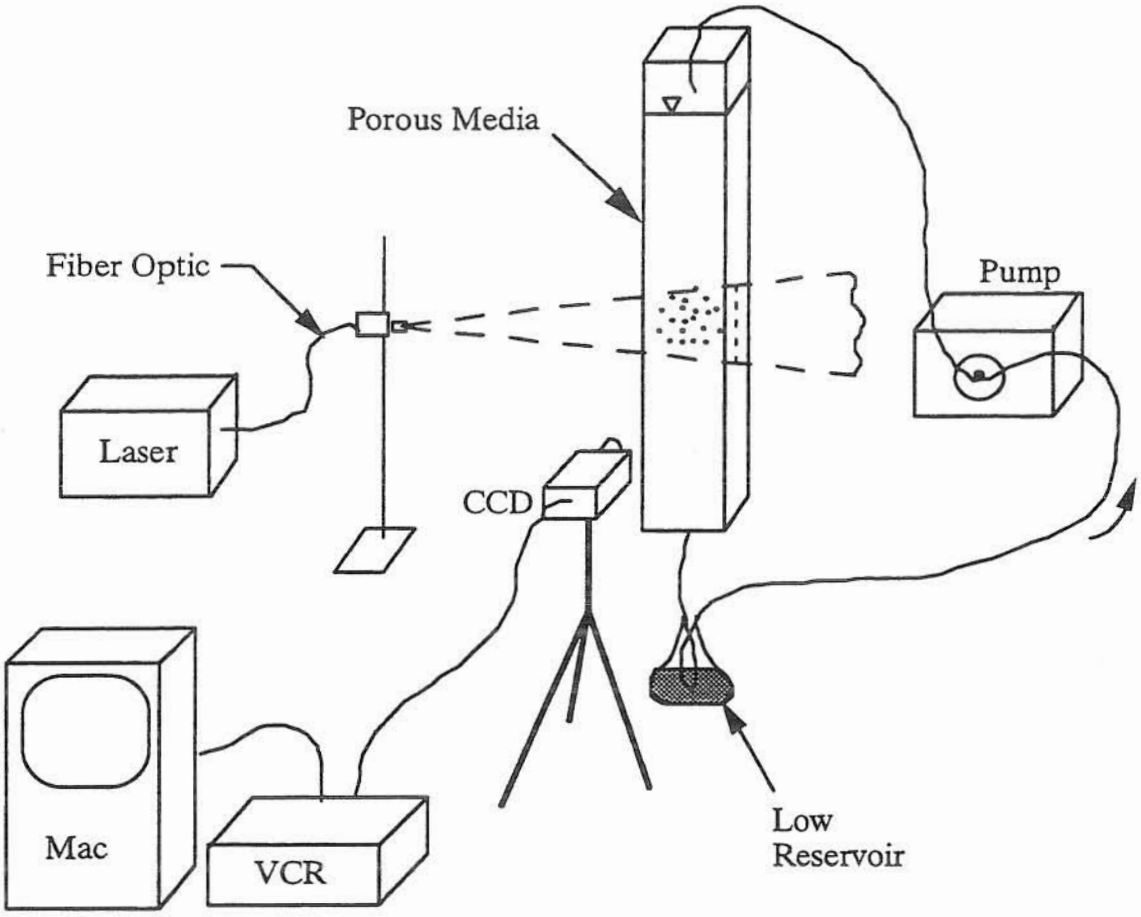

Figure 6.1.1 Experimental Setup for Porous Medium Experiments

6.2 Refractive Index Matching

In order to be certain that the media and fluid would have the appropriate indices of refraction and form a transparent matrix, it was important to study the nature of refractive indices before purchasing the required materials. First, it was necessary to realize that the refractive index for a medium is a function of the wavelength of the light passing through the medium, as well as the temperature of the medium. Furthermore, the laser used in these experiments was a multi-line laser with emissions ranging from 457 to 514 nm. Because the laser emits light at many different wavelengths, unlike a single-line laser, it was important that the media and fluid not only have a matching refractive index at a specified wavelength and temperature, but that they also had a similar optical dispersion, or shape to their respective

refractive index versus wavelength plots. This would ensure that all of the light emitted from the laser would be able to pass through the fluid-media matrix undistorted.

For the PMMA, ICI Acrylics, Inc. (manufacturer of the raw PMMA) provided a plot of refractive index versus wavelength at 23°C. Because this temperature provides a convenient working environment, it was selected to be the design temperature for the experiment. The appropriate Cargille fluid was then selected such that it would have the same refractive indices at 23°C for the emission wavelengths of our laser. In addition to refractive index and optical dispersion, chemical compatibility was also considered. Before purchasing the Laser Liquid and tracers it was necessary to be sure that they would not react and become unusable in the experiment. Cargille provided a catalog of all of their fluids and in the catalog they listed many known compatibilities and incompatibilities with the fluids. Based on these criteria, a Laser Liquid (formula code 5610) was chosen to match our refractive index and compatibility requirements. Chemical compatibility with polystyrene was an original requirement for the fluid since polystyrene tracer particles were initially chosen for the experiment. After preliminary testing, however, it appeared that the polystyrene tracers were sticking to the PMMA and coating the beads rather than staying in the fluid. Hollow glass microspheres were then chosen as tracers instead of the polystyrene.

The specifications for the Cargille fluid ordered were n_d (refractive index at λ = 589.3 nm)= 1.4895 at 25°C. Cargille provided a plot of the refractive index versus wavelength for the 5610 Fluid. Figure 6.2.1 shows a plot of refractive index versus wavelength for both the Laser Liquid and the PMMA at 23°C. It is clear that the refractive indices of the fluid and the media are very similar throughout the emission spectrum of our laser, although they are not exactly identical. The close match of the optical dispersion between these two materials was thought to ensure that all of the light emitted from the laser and reflected by the tracers would pass through the media-fluid matrix undistorted. Furthermore, since the refractive index of PMMA increases with temperature and the refractive index of the 5610 Fluid decreases with temperature, temperature control is crucial and can be adjusted to fine-tune the refractive indices of the two media.

After some initial inspection of the PMMA/fluid matrix, it was apparent that the index matching was not perfect for 23°C since blurring of the images was occurring in the column. The temperature of the column was therefore adjusted to attempt to get a better match between media and fluid. Adjusting the temperature, unfortunately seemed to make little difference in the quality of the images. This is possibly due to the fact that the laser emits a range of wavelengths and the media and fluid have optical dispersion curves which are slightly different. This would mean that the refractive indices only truly match for one wavelength and

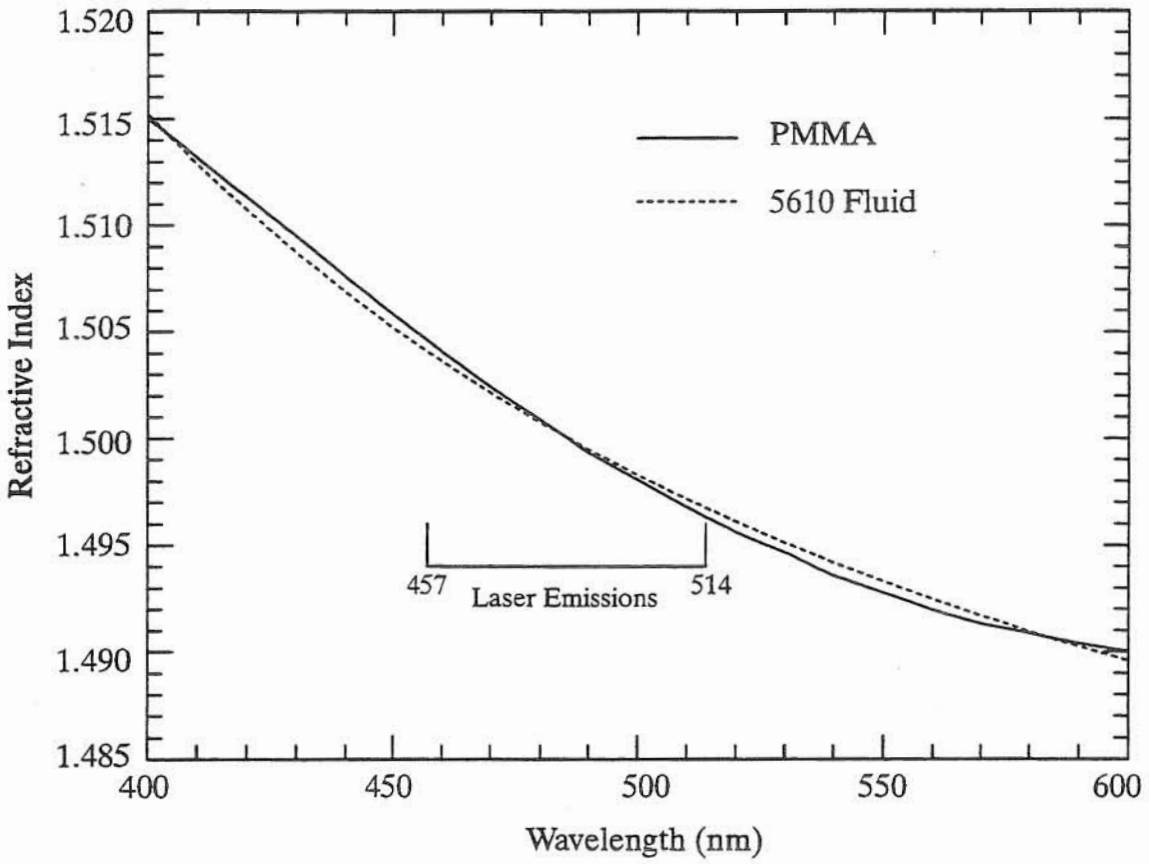

Figure 6.2.1 Refractive Indices vs. Wavelength for PMMA and 5610 Fluid at 23°C

the other wavelengths would be subject to some deflection and blurring of the images. Furthermore, the PMMA may not be perfectly homogeneous and have some variation in optical properties. Possibly selection of an optical quality glass would have eliminated concerns about inhomogeneities in optical properties of the medium. Also, filters or prisms could be used to reduce the laser to a single-line such that index matching would only be necessary for one wavelength of light and not a range of wavelengths. The final temperature used in the experiments was 24°C, which appeared to provide the best index matching.

6.3 Seeding Density and Flow Rate Calculations

The proper seeding density of the tracer particles was determined by simply adding a small amount of tracers to the fluid and observing the resulting tracer concentration in a plane of the fluid which was illuminated by the laser. Tracers were then added until the number of tracers in a field of view seemed appropriate. The optimum density should be high enough to provide a large number of vectors to make the velocity field analysis more complete, but also be low

enough to minimize incidence of particle overlap or such high densities that accurate tracking becomes difficult.

In order to determine the appropriate flow rates to use for the column three criteria were examined. First, the packed bed Reynolds number (Re_p) for the experiment was specified to be in the laminar flow range. This required a Re_p less than 10 (Denn 1980). In order to provide a safety factor against transition flow patterns, a maximum Re_p of 0.1 was chosen for the experiment. Equation (6.3.1) gives the definition of Re_p, where D_p is the media diameter, V_∞ is the apparent velocity or specific discharge, ε is the void fraction or porosity, and ν is the kinematic viscosity. The apparent velocity is defined by equation (6.3.2), where Q is the flow

$$\mathrm{Re}_p = \frac{D_p V_\infty}{(1-\varepsilon)\nu} \qquad (6.3.1)$$

$$V_\infty = \frac{Q}{A} \qquad (6.3.2)$$

$$Q = \frac{A(1-\varepsilon)\nu\,\mathrm{Re}_p}{D_p} \qquad (6.3.3)$$

rate through the column and A is the cross-sectional area of the column (Denn 1980). Combining these equations yields equation (6.3.3) which expresses the flow rate through the column in terms of the desired Re_p. Using this equation and a maximum Re_p of 0.1, a maximum flow rate of 32,800 mL/min was determined for the column, using an average porosity of 0.38, which was determined when the column was filled with media. The porosity was actually determined for the different sections of the column and the section containing PMMA had a porosity of 0.38, and the upper and lower glass bead sections had porosities of 0.37 and 0.39, respectively. These porosity calculations are discussed further in Section 6.4.

Another constraint applied to the flow rate was the maximum velocity of the tracers across the field of view. It is desirable to be able to track the fastest particles in the pores of the porous medium such that high velocity vectors are not lost. In order to convert this constraint into a maximum allowable flow rate, an assumption about the ratio of the maximum pore-water velocity to the average pore-water velocity ($\overline{V}_{max}/\overline{V}_{avg}$) had to be made. Based on the data from Northrup et al. (1993) and Shattuck et al. (1991), it appears that typically the maximum pore-water velocity is approximately two to five times the average pore-water velocity. Therefore, it was assumed that the maximum particle velocities would be no more than five times the average pore-water velocity in the column. In addition to estimating $\overline{V}_{max}/\overline{V}_{avg}$, it was necessary to specify the maximum allowable displacement (d_{max}) of each tracer per frame

(1/30 second) in units of tracer diameters. This value was chosen to be 4 tracer diameters, or 18 pixels based on an assumed magnification yielding a minimum of 4.5 pixels per tracer diameter. Once these assumptions were made, the maximum allowable $\overline{V}_{max}$ could be determined from equation (6.3.4), where D_t is the tracer particle diameter. Then, the

$$\overline{V}_{\max} = d_{\max} D_t \left(30 \frac{frames}{second} \right) \qquad (6.3.4)$$

$$\overline{V}_{avg} = \frac{\overline{V}_{\max}}{\left(\frac{\overline{V}_{\max}}{\overline{V}_{avg}} \right)} \qquad (6.3.5)$$

$$V_\infty = \overline{V}_{avg} \varepsilon \qquad (6.3.6)$$

$$Q = V_\infty A \qquad (6.3.7)$$

maximum allowable $\overline{V}_{avg}$ could be determined according to equation (6.3.5), where ($\overline{V}_{max}/\overline{V}_{avg}$) was 5. The maximum apparent velocity could then be determined from equation (6.3.6) and the maximum flow rate was found from equation (6.3.7) (Denn 1980). From the above assumptions, it was calculated that the maximum flow rate should be 190 mL/min to assure that all particles were moving slow enough to be tracked. Clearly the criteria of maximum displacement would control the maximum flow rate used in the experiment since the maximum allowable flow rate based on Re_p was 170 times higher than the maximum allowable flow rate based on maximum allowable tracer displacement. A flow rate of 190 mL/min corresponds to a Re_p of $5.8*10^{-4}$.

The final constraint on the flow rate was that the average tracer velocity (equal to $\overline{V}_{avg}$) be greater than 100 times the settling velocity of the tracers such that the velocities of the tracers could be representative of the velocity of fluid elements. Stokes' Law was used to calculate the settling velocity of the particles:

$$V_s = \frac{(\varrho_t - \varrho_f) D_t^2 g}{18\mu} \qquad (6.3.8)$$

where V_s is the tracer settling velocity, ϱ_t is the density of the tracer, ϱ_f is the density of the fluid, g is the gravitational force constant, and μ is the dynamic viscosity of the fluid (Denn 1980). The maximum diameter of the tracer particles (30 μm) was used in determining the settling

velocity since the largest tracers would have the largest settling velocities and be the "worst case" for a minimum required flow rate. Equation (6.3.9) was then used to find the minimum

$$\overline{V}_{avg} = 100V_s \qquad (6.3.9)$$

required $\overline{V}_{avg}$ and equations (6.3.6) and (6.3.7) were used to calculate the minimum apparent velocity and flow rate. The minimum required flow rate was calculated to be 0.072 mL/min based on the settling velocity requirements. A flow rate of 0.072 mL/min corresponds to a Re_p of $2.2*10^{-7}$. Therefore, based on the previous three criteria, the flow rate was required to be between 0.072 and 190 mL/min and the experiment was required to be within the Re_p range of $2.2*10^{-7}$ and $5.8*10^{-4}$.

This range of Re_p is actually relevant to the study of groundwater flow since two well-known field studies were conducted in sandy, unconfined aquifers with Re_p in the same range as our experiments. First, it was estimated from available data that the Re_p for a sandy aquifer in Borden, Ontario was approximately 10^{-6} (Ball and Roberts 1991, Mackay et al. 1986). For a similar aquifer in Cape Cod, Massachusetts a Re_p of 10^{-5} was estimated from available data (Wood et al. 1990, LeBlanc et al. 1991). From these estimations, it is evident that the Re_p of our experiments is representative of some types of aquifers and flow conditions in nature.

6.4 Procedure and Results

Before interrogation of the flow patterns in the column of porous media could begin, it was necessary to fill the column with media and properly seeded fluid, and to determine the porosities of the different sections of the column. First, both the glass and PMMA beads were washed with water and dried in a low temperature oven. Then, the glass beads were dumped into the bottom 20 cm of the column, followed by an eight cm layer of PMMA and then an additional 22 cm of glass beads. The porosities of the different sections of the column were determined by equation (6.4.1), where V_m is the actual volume of the media in a section and V_b is the bulk volume of the column section. The actual volume of media added to a section was

$$\varepsilon = 1 - \frac{V_m}{V_b} \qquad (6.4.1)$$

determined by dividing the mass of media in the section by the density of the media. The density of the glass was determined to be approximately 2.51 g/cm^3 and the density of the

PMMA was found to be approximately 1.18 g/cm^3. These densities were determined by measuring the volume of displaced water in a graduated cylinder when a given mass of beads was added to the cylinder. As reported in the previous section, the measured porosities of the column sections were 0.381 ± 0.019 for the PMMA section and 0.387 ± 0.007 and 0.369 ± 0.009 for the lower and upper glass sections, respectively. The errors in the porosity measurements are due to errors in determination of material density and bulk volume of the column sections.

Before video taping of the column began, the fluid was removed from the column and tracers were added to the fluid. Before the fluid was returned to the column a sample of the fluid was illuminated with a laser and observed with the video camera to determine if the tracer concentration was suitable. Once a suitable tracer concentration was achieved, the fluid was returned to the column and the PTV experiments were begun. For each PTV experiment the temperature of the fluid, the flow rate, the lens configuration and resulting magnification, and the location of the pore were recorded. Several minutes of video tape were usually recorded for each experiment and then the video tape was analyzed to obtain an interpolated velocity field for the specific flow conditions and location.

The first pore videotaped was located about 1.9 cm or two bead diameters from the inside of the front face of the column. The flow rate for this preliminary experiment was 71.6 ± 0.8 mL/min which corresponded to an average pore-water velocity for the PMMA section of the column of 0.34 ± 0.02 mm/s and a Reynolds number of approximately $2.2 * 10^{-4}$. The laser sheet thickness for this experiment was approximately one millimeter, which was determined to be too thick to be representative of a plane of flow, but results are still reported for this initial experiment. In subsequent experiments the laser sheet was made thinner by passing it between two sheets of black construction paper which were separated by about 0.4 mm. The first step in analyzing the porous media flow was to videotape the column for approximately four minutes and then begin the capturing and analysis procedure described in Section 3.1. Figure 6.4.1 shows a raw image captured by the Macintosh computer. This image was then inverted (Figure 6.4.2), converted to a binary format (Figure 6.4.3), and enhanced with a noise reduction feature (Figure 6.4.4). Finally, the images of the interfaces between the media and the fluid were erased such that they would not dominate the correlation windows used by the cross-correlation algorithm to track particles from one frame to the next (Figure 6.4.5). The tracer concentration in this initial porous media experiment was apparently too low and resulted in a fairly sparse vector field requiring superposition of velocity vectors from different time steps in order to provide a sufficiently dense vector field.

Several series of images were analyzed for this experiment and the resulting velocity vectors were overlaid to form a more complete vector field (Figure 6.4.6). The minimum

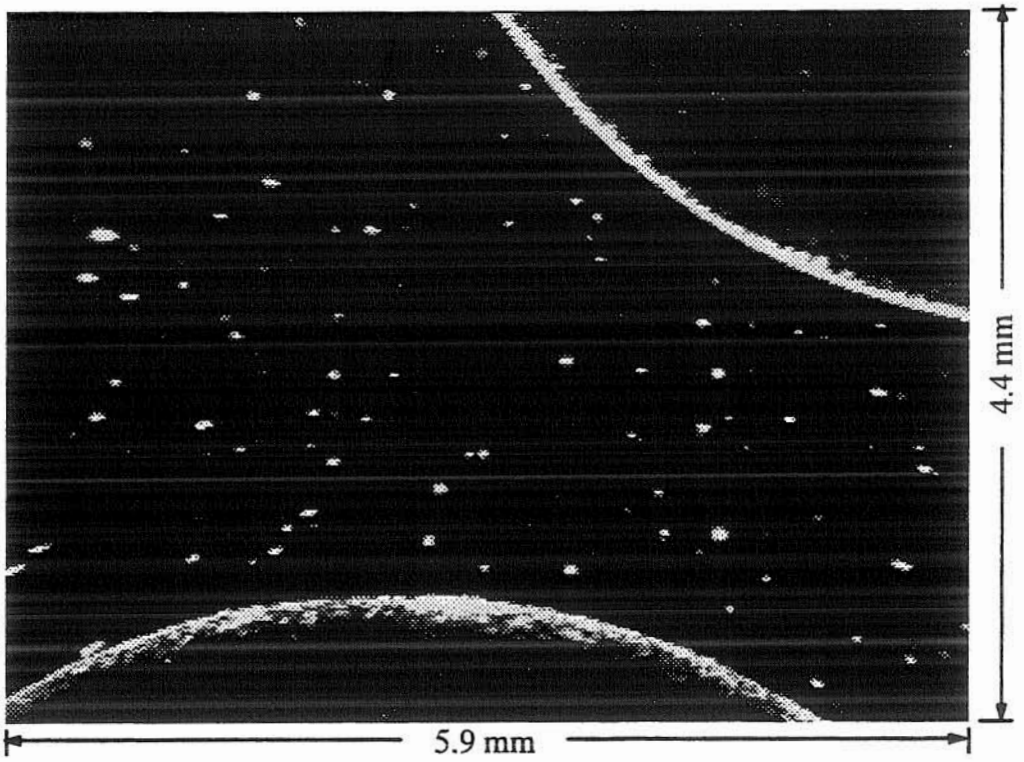

Figure 6.4.1 Raw Image of Captured Flow Field in Preliminary Porous Media Experiment

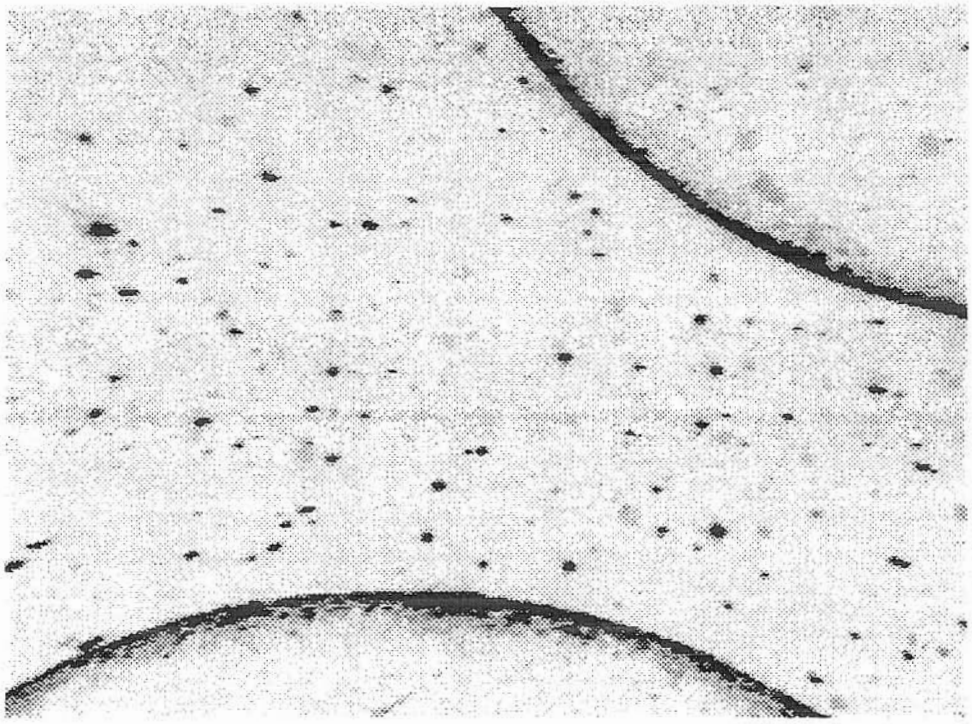

Figure 6.4.2 Inverted Image of Captured Flow Field in Preliminary Porous Media Experiment

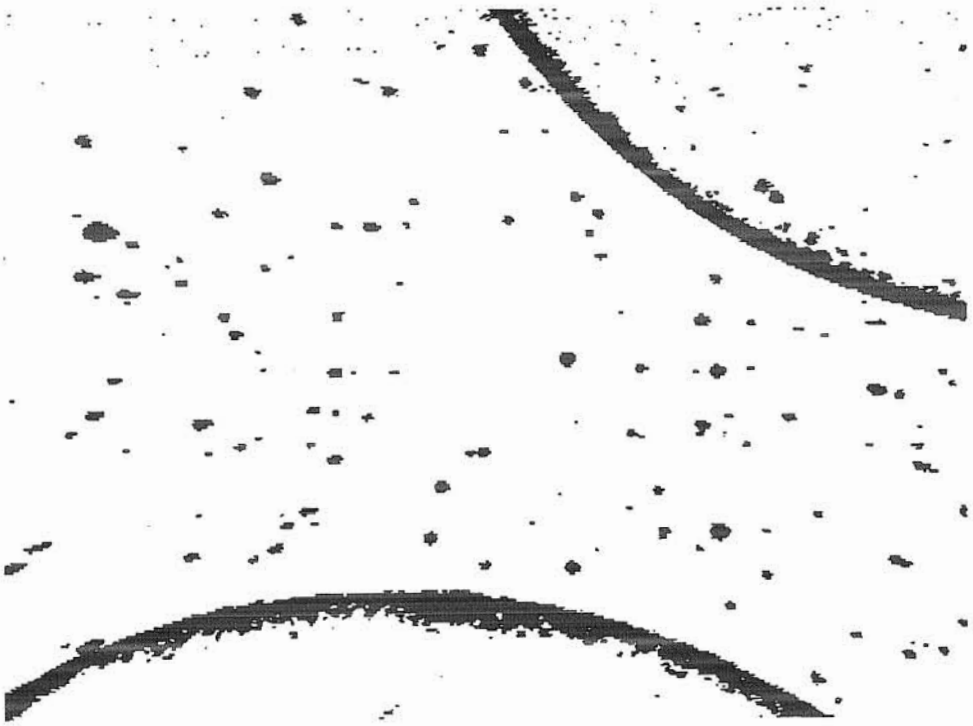

Figure 6.4.3 Binary Image of Captured Flow Field in Preliminary Porous Media Experiment

Figure 6.4.4 Enhanced Image of Captured Flow Field in Preliminary Porous Media Experiment

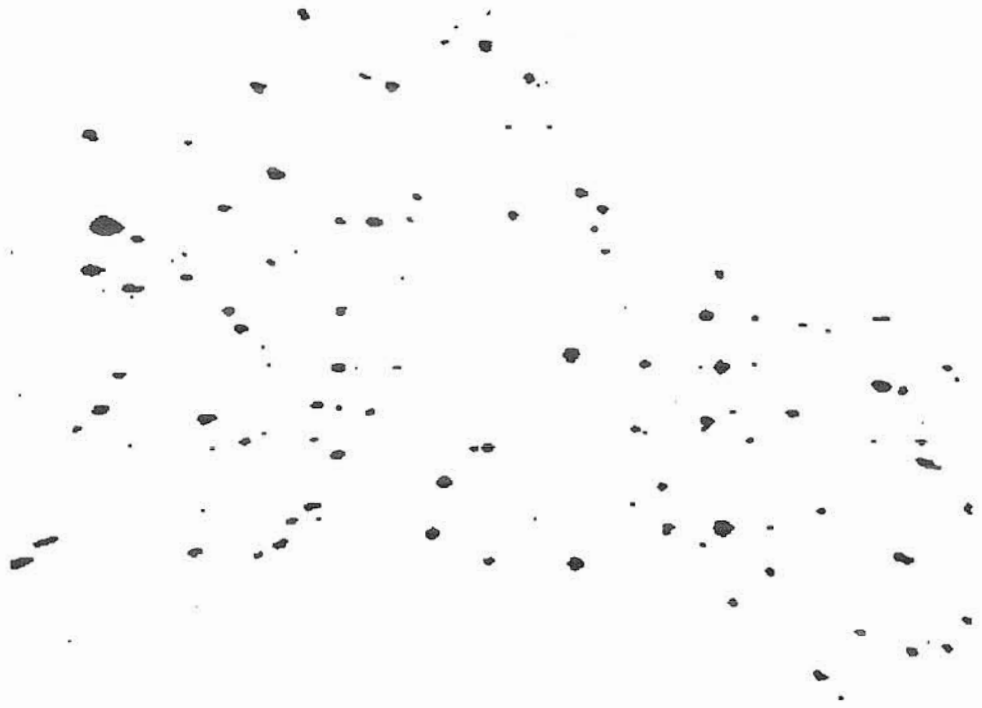

Figure 6.4.5 Image of Tracer Particles Only in Preliminary Porous Media Experiment

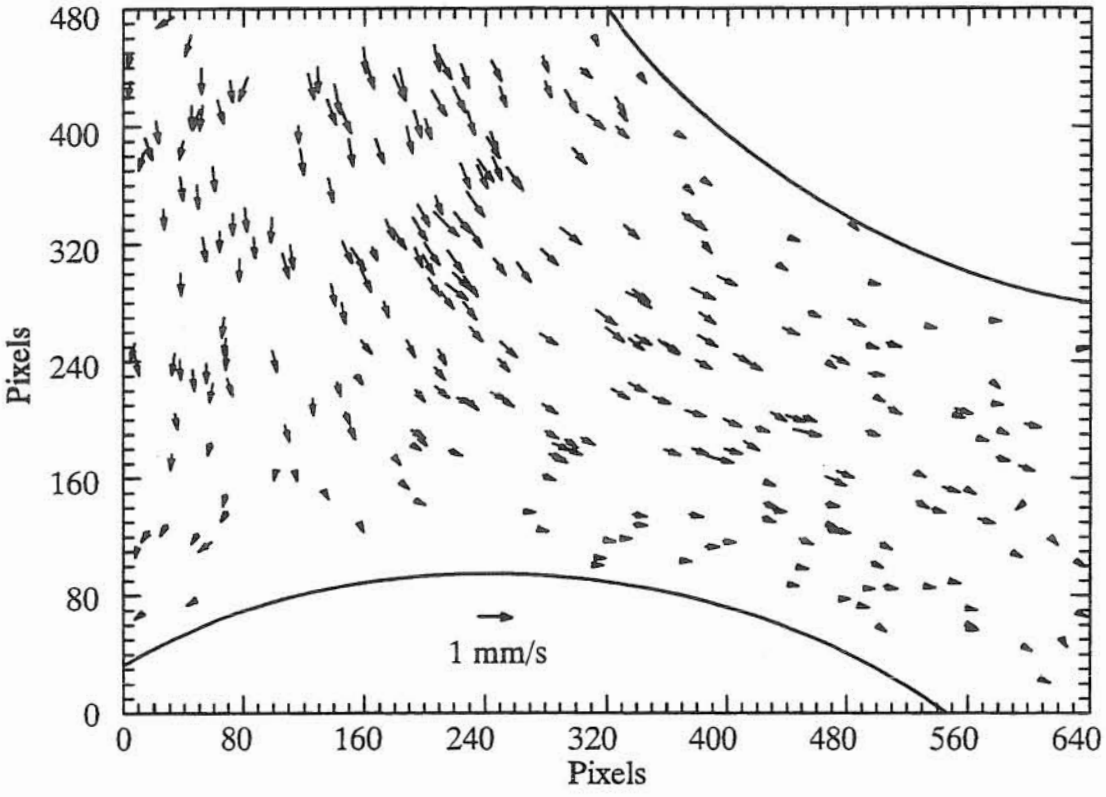

Figure 6.4.6 Raw Vector Field for Preliminary Porous Media Experiment

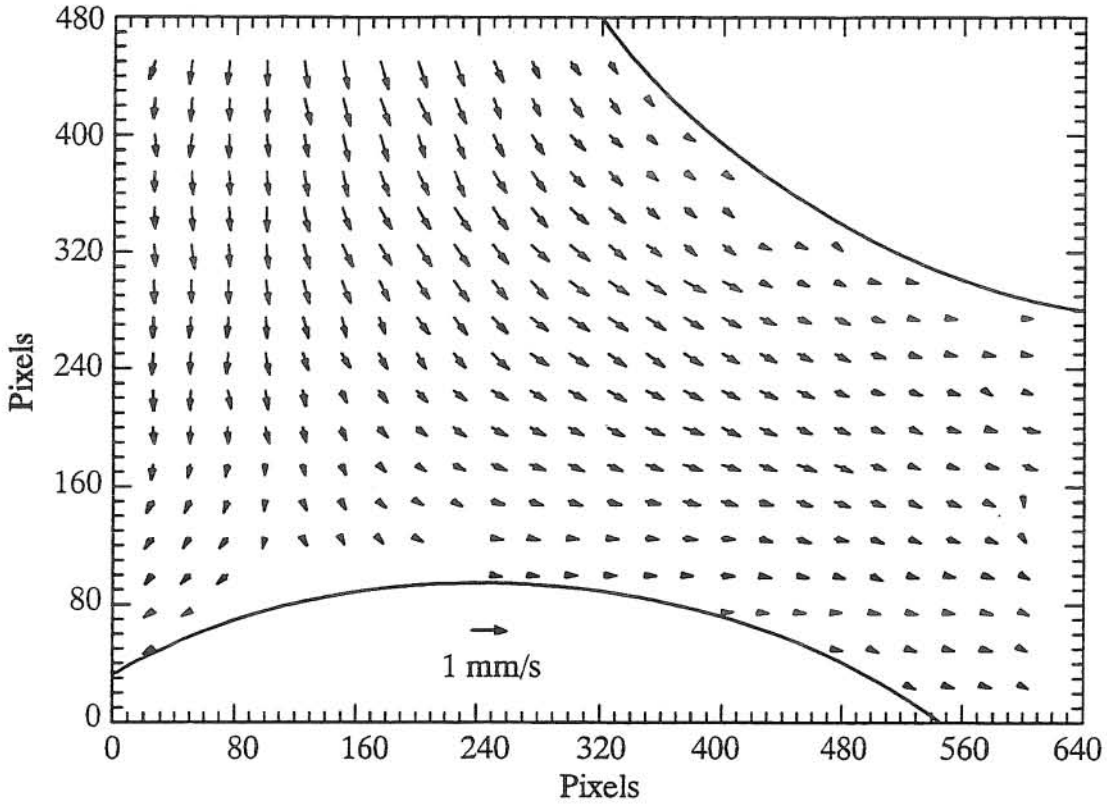

Figure 6.4.7 Interpolated Vector Field for Preliminary Porous Media Experiment

required correlation coefficient required for these experiments was 0.65, which was chosen by trial and error because it yielded a large number of vectors without many erroneous ones. Also, the minimum displacement criteria used in these experiments was 4 pixels since the flow had a large variation between the fast and slow moving particles and a large minimum displacement criteria was impractical. The vector field was then analyzed to obtain an interpolated velocity field at regularly spaced grid points (Figure 6.4.7). The grid spacing for this plot was 25 pixels (0.23 mm) and the interpolation window size was 80 pixels (0.74 mm).

The interpolated vector field was analyzed and the average magnitude of the velocity vectors ($\overline{V}$) was found to be 0.32 mm/s. The average vertical ($\overline{V}_y$) and horizontal ($\overline{V}_x$) velocities were found to be 0.25 and 0.19 mm/s respectively. The average pore-water velocity observed in the experiment agrees with the expected average velocity based on the bulk flow rate and porosity, 0.34 ± 0.02 mm/s. A slight variation of the the local average pore-water velocity from the bulk average pore-water velocity is expected since the PMMA beads were placed randomly in the column, resulting in an irregular pore structure. Therefore, the measured pore-water velocity is less than the predicted value due to the particular shape of this pore which probably has a significant out-of-plane velocity component.

Flow Condition	Q (mL/min)	$\overline{V}$ (mm/s)	Re
High	84.5±0.9	0.41±0.03	$2.6*10^{-4}$
Medium	57.5±0.6	0.28±0.02	$1.8*10^{-4}$
Low	36.3±0.4	0.17±0.01	$1.1*10^{-4}$

Table 6.4.1 Three Flow Conditions for First Porous Media Experiment

The next set of porous media experiments were on a different pore in the column which was located just 1.2 cm or 1.2 bead diameters from the inside front face of the column. This pore was videotaped for three different flow rates and analyzed to check for consistency of the flow structure over these different flow rates. However, the CCD camera was accidentally shifted slightly for the third or "low" flow rate condition and therefore the velocity fields for this condition may possibly display some slightly different characteristics than the first two flow conditions. The three flow rates used and the corresponding expected average pore-water velocities and Reynolds numbers are presented in Table 6.4.1. The pore was videotaped for approximately three minutes for each flow rate and several series of images were analyzed for each flow rate to generate velocity vector fields (Figures 6.4.8, 6.4.9, and 6.4.10). Subsequently, interpolated velocity fields for each flow rate were generated and are shown in Figures 6.4.11, 6.4.12, and 6.4.13.

Analysis of the average pore-water velocities is shown in Table 6.4.2 and indicates that the flow structure remains similar for the three different flow rates. This analysis was performed on the interpolated velocity fields such that the velocity vector distribution would be similar for each flow condition. Since the "low" flow condition was for a slightly shifted field of view, however, the velocity vector distribution was slightly different and can be seen by comparing Figure 6.4.13 with Figures 6.4.11 and 6.4.12. In particular, it is important to note that the field of view for the "low" flow condition was shifted slightly upwards where lower flow velocities dominated. This is likely responsible for the lower ratio of observed average pore-water velocity to the predicted value ($\overline{V}/\overline{V}_{theoretical}$) since the slower velocity vectors tend to bias the average pore-water velocity calculation towards these "slower" values. Furthermore, the slightly lower $\overline{V}/\overline{V}_{theoretical}$ for the "high" flow condition compared to the "medium" flow condition is likely due to the fact that the interpolated velocity field for the "high" flow rate condition had more velocity vectors in the upper right and left regions of the flow field than the "medium" flow rate condition. These were slow flow regions and also tended to bias the average pore-water velocity calculations towards a lower value.

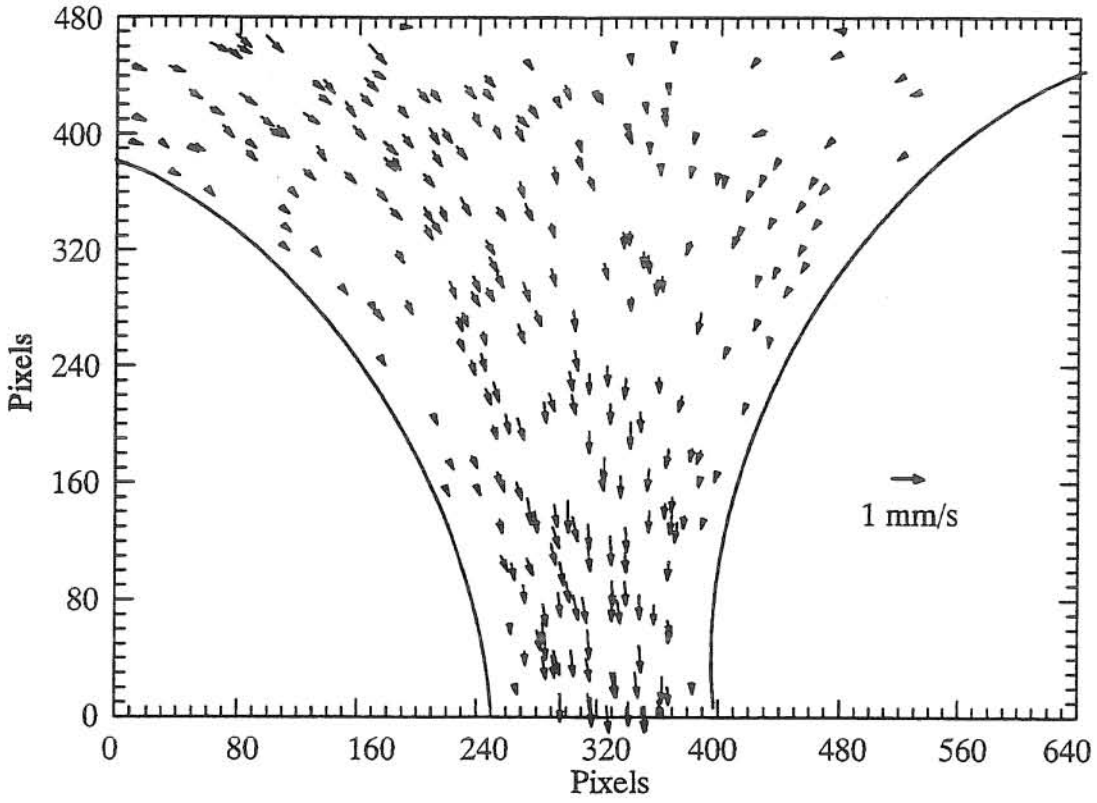

Figure 6.4.8 Raw Vector Field for High Flow Rate from First Experiment

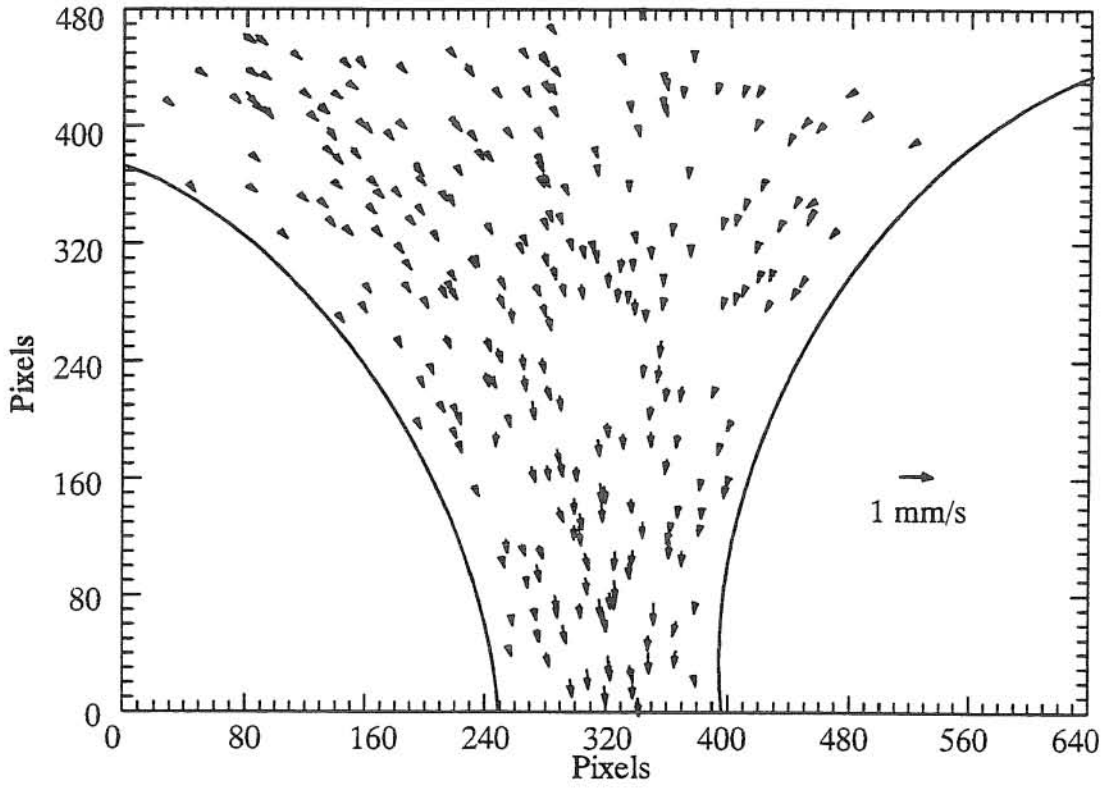

Figure 6.4.9 Raw Vector Field for Medium Flow Rate from First Experiment

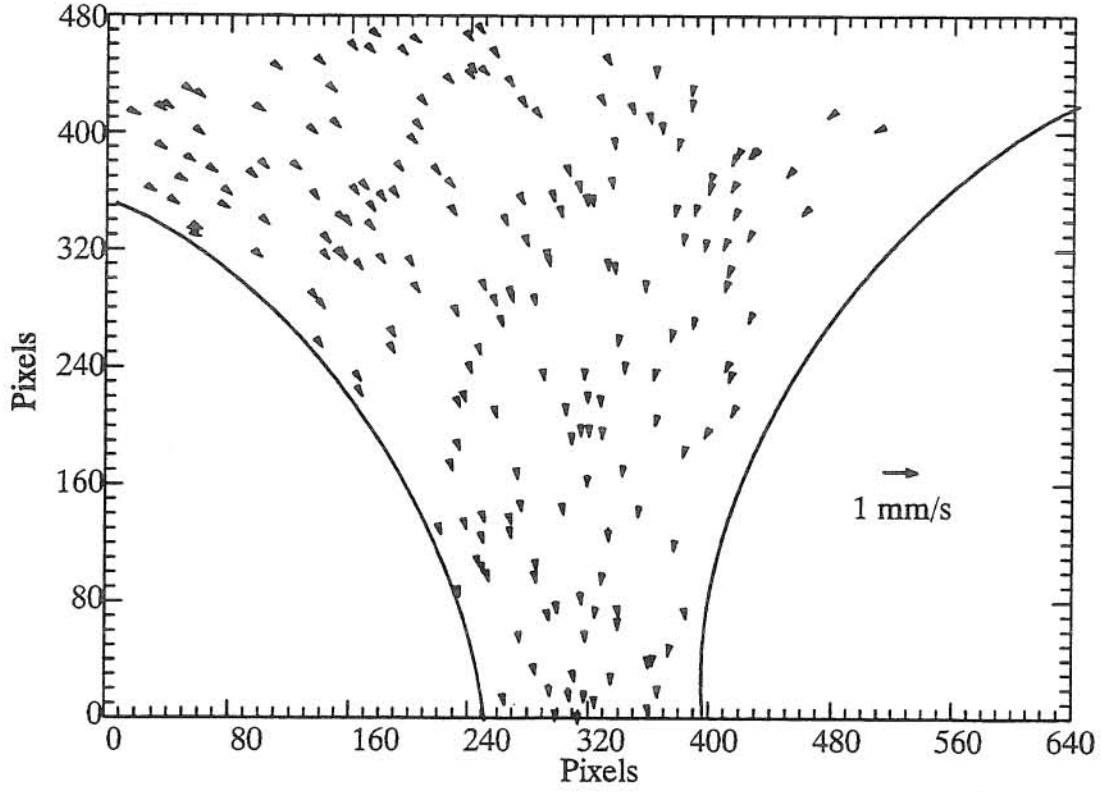

Figure 6.4.10 Raw Vector Field for Low Flow Rate from First Experiment

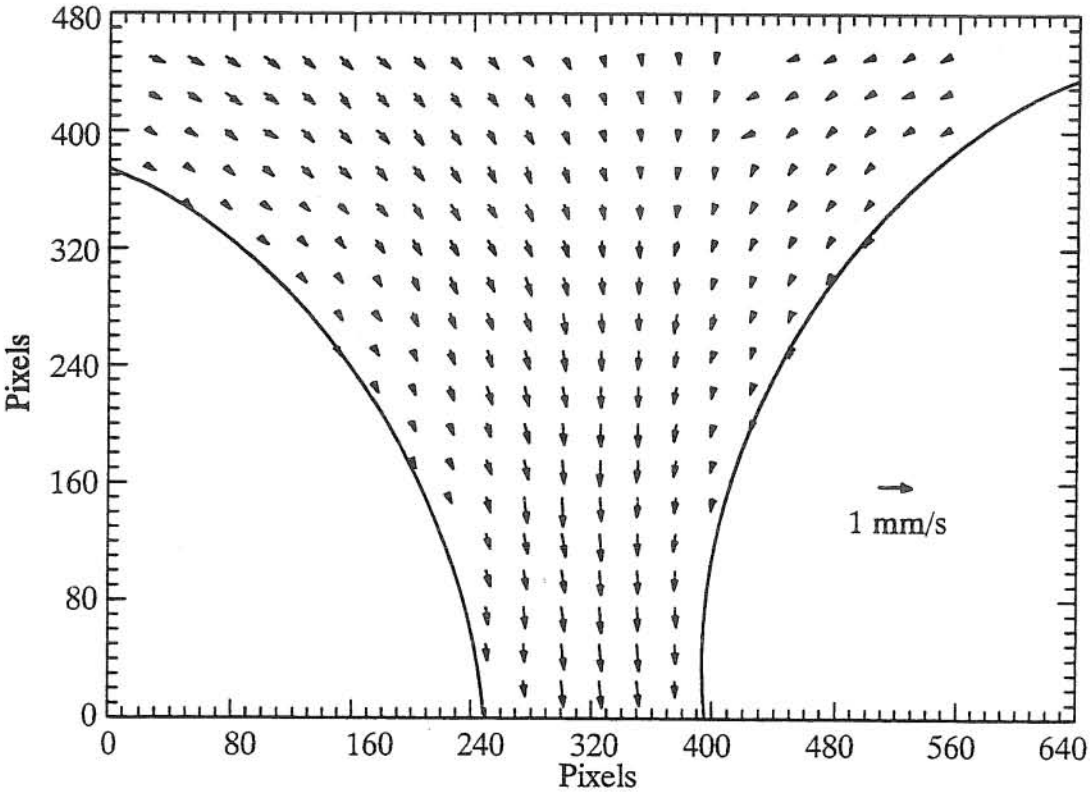

Figure 6.4.11 Interpolated Velocity Field for High Flow Rate from First Experiment

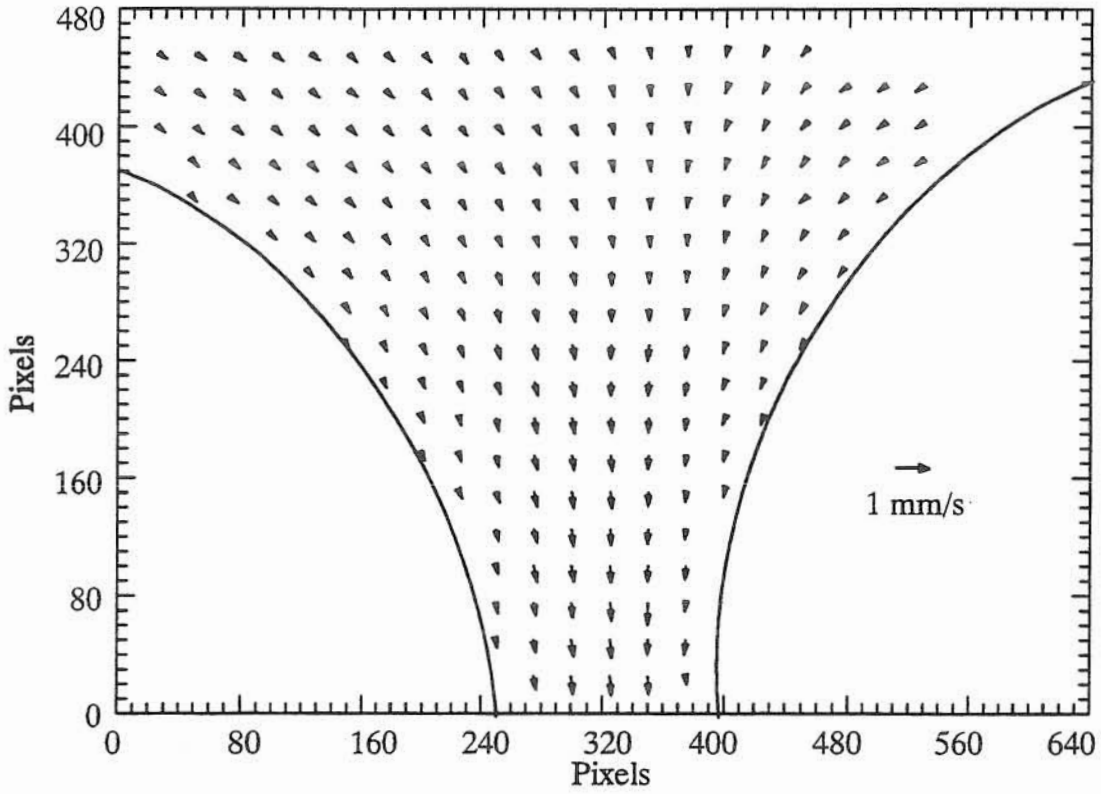

Figure 6.4.12 Interpolated Velocity Field for Medium Flow Rate for First Experiment

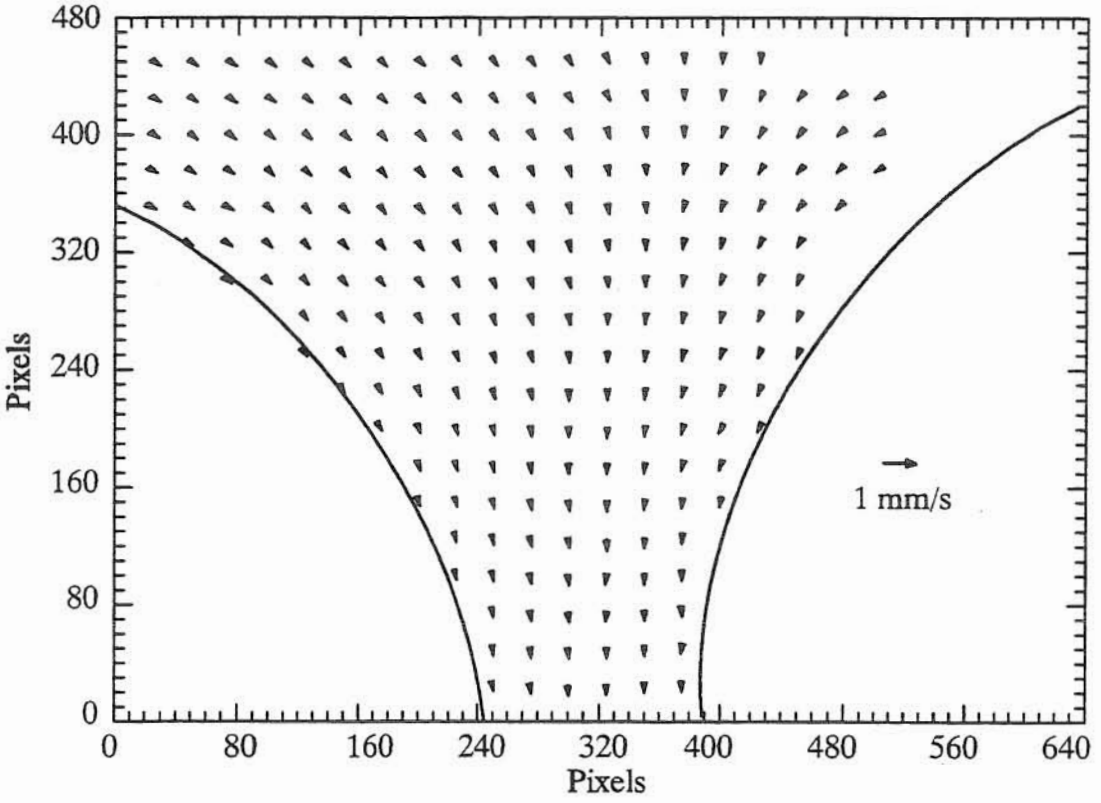

Figure 6.4.13 Interpolated Velocity Field for Low Flow Rate for First Experiment

	Flow Condition		
	High	Medium	Low
$\overline{V}_{theoretical}$ (mm/s)	0.41	0.28	0.17
$\overline{V}$ (mm/s)	0.52	0.37	0.22
$\overline{V}_y$ (mm/s)	−0.51	−0.36	−0.21
$\overline{V}_x$ (mm/s)	0.12	0.09	0.06
$\overline{V}/\overline{V}_{theoretical}$	1.27	1.35	1.24
$\overline{V}_y/\overline{V}_{theoretical}$	−1.24	−1.32	−1.20
$\overline{V}_x/\overline{V}_{theoretical}$	0.28	0.31	0.34

Table 6.4.2 Observed Pore-water Velocities for Three Flow Rates from First Experiment

Another pore in the column was also analyzed in order to confirm that the PTV procedure can accurately measure a flow field which has flow divergence. This pore was also videotaped for three different flow rates to check for consistency of the measured flow field structure over different Reynolds numbers. The location of this pore was approximately 1.0 cm or 1.1 bead diameters from the inside front face of the column. The three flow rates used and the corresponding expected average pore-water velocities and Reynolds numbers are presented in Table 6.4.3. The pore was videotaped for approximately three minutes for each flow rate and

Flow Condition	Q (mL/min)	$\overline{V}$ (mm/s)	Re
High	164.7±1.8	0.79±0.05	$5.0*10^{-4}$
Medium	105.0±1.1	0.50±0.03	$3.2*10^{-4}$
Low	54.2±0.6	0.26±0.02	$1.7*10^{-4}$

Table 6.4.3 Three Flow Conditions for Second Porous Media Experiment

several series of images were analyzed for each flow rate to generate velocity vector fields (Figures 6.4.14, 6.4.15, and 6.4.16). Subsequently, interpolated velocity fields for each flow rate were generated and are shown in Figures 6.4.17, 6.4.18, and 6.4.19.

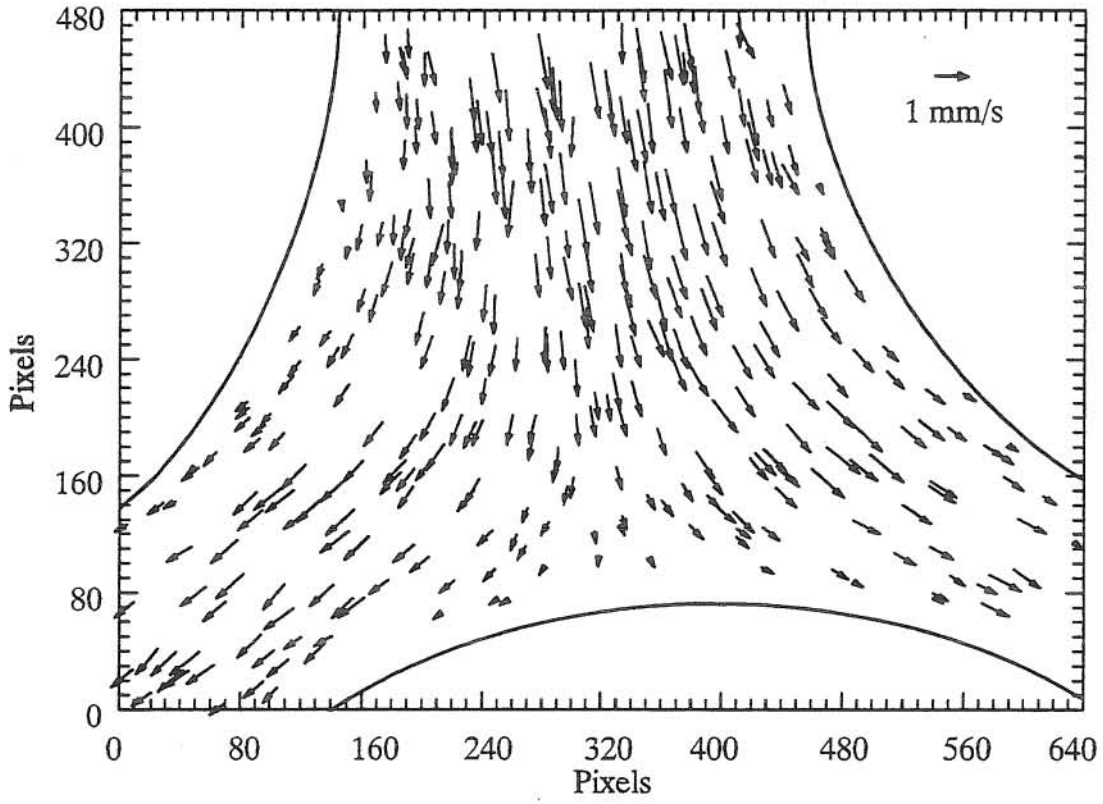

Figure 6.4.14 Raw Vector Field for High Flow Rate from Second Experiment

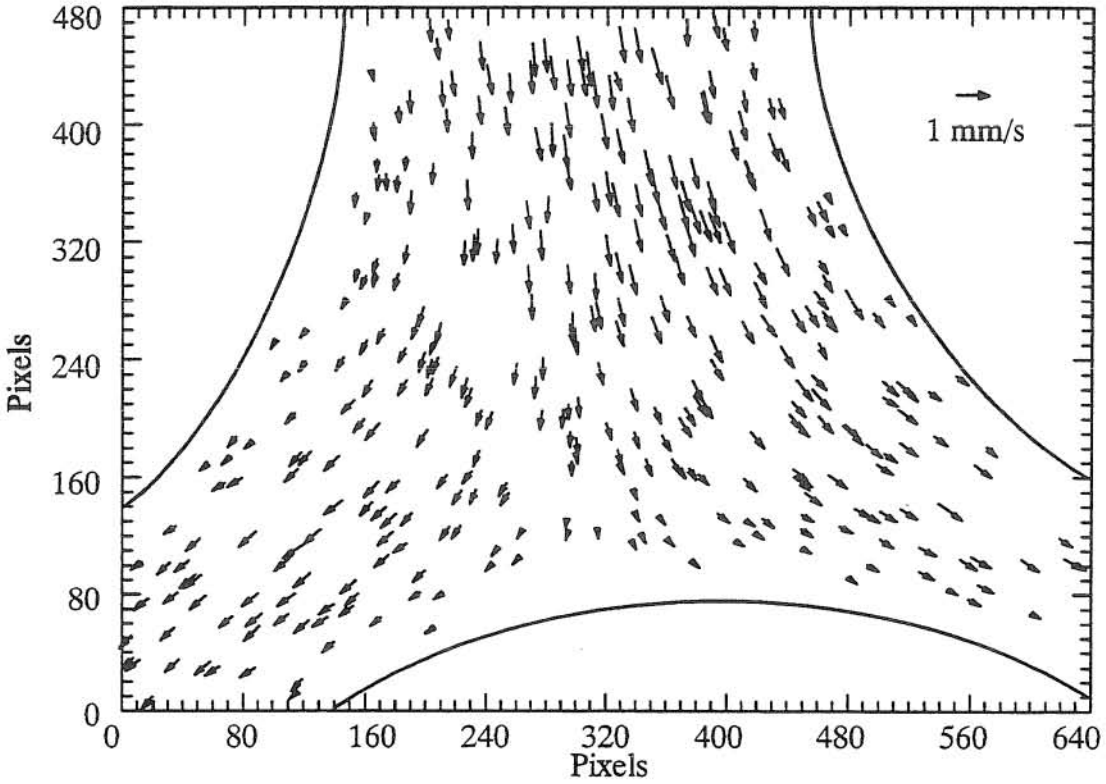

Figure 6.4.15 Raw Vector Field for Medium Flow Rate from Second Experiment

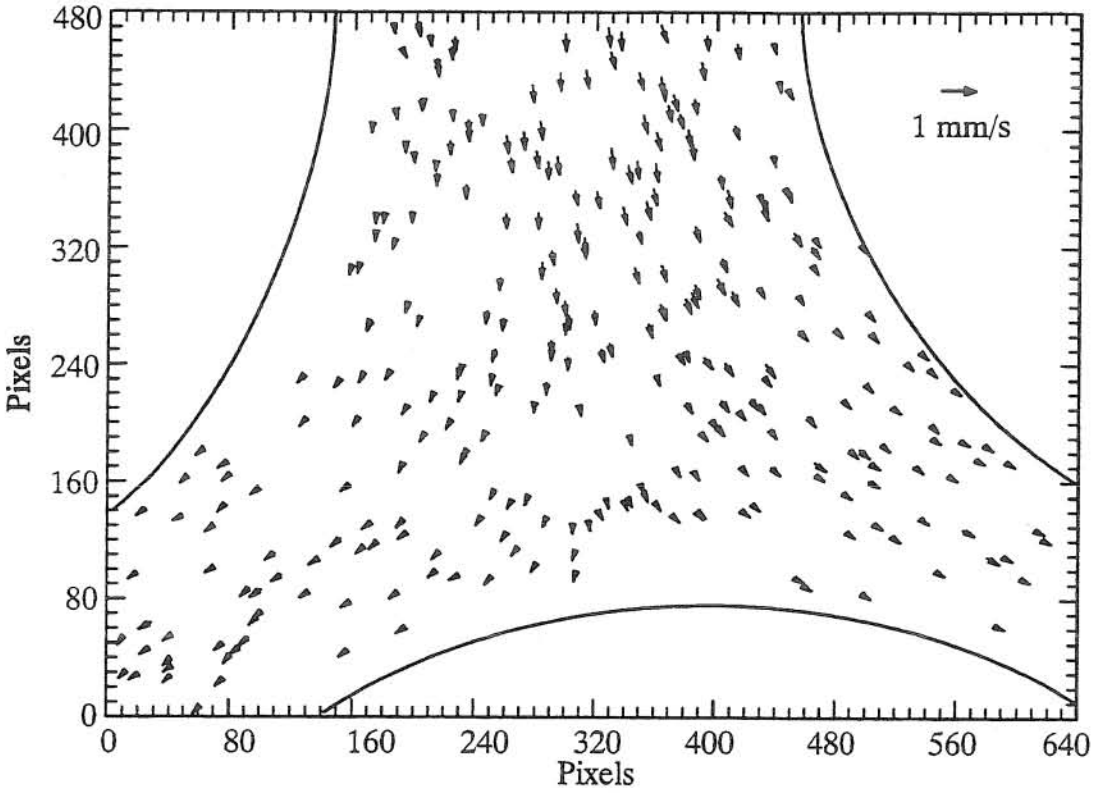

Figure 6.4.16 Raw Vector Field for Low Flow Rate from Second Experiment

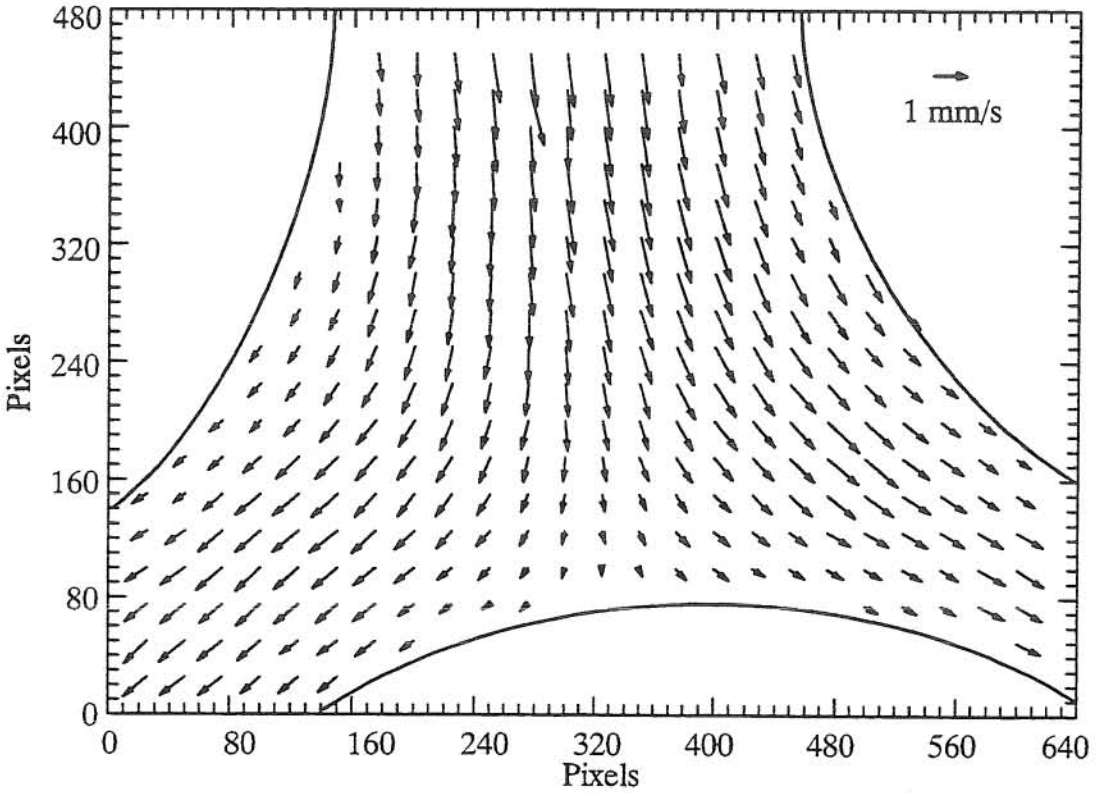

Figure 6.4.17 Interpolated Velocity Field for High Flow Rate from Second Experiment

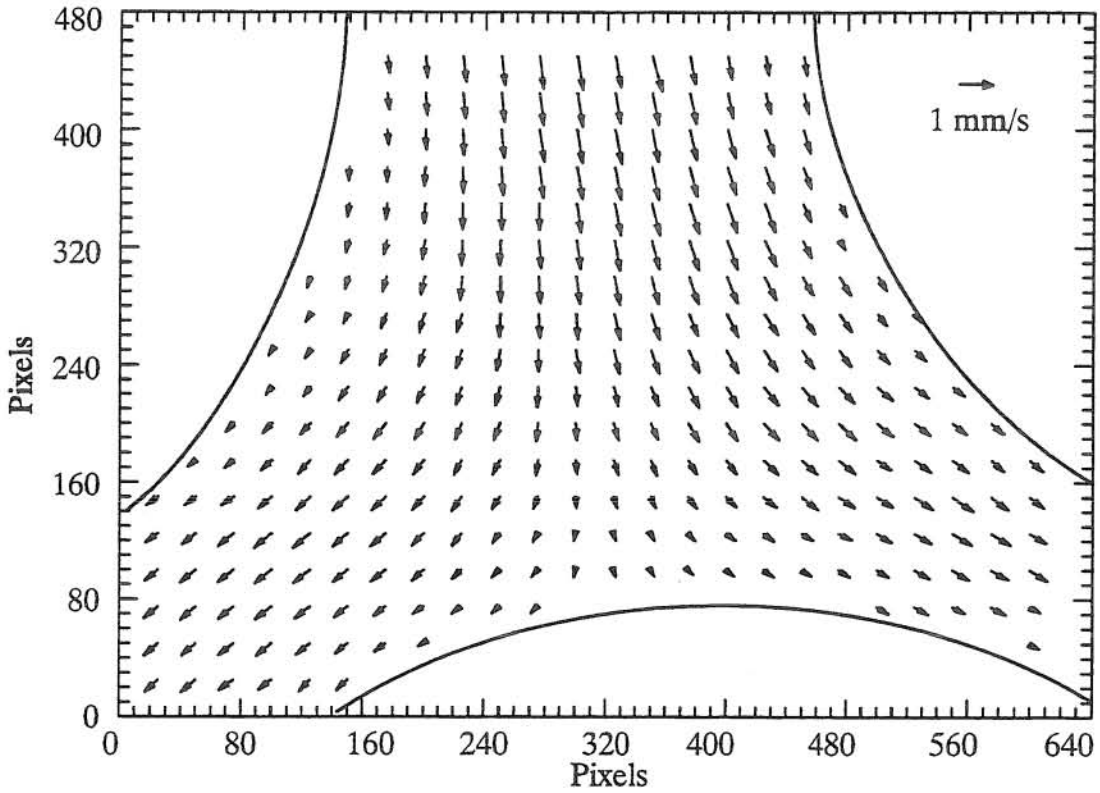

Figure 6.4.18 Interpolated Velocity Field for Medium Flow Rate for Second Experiment

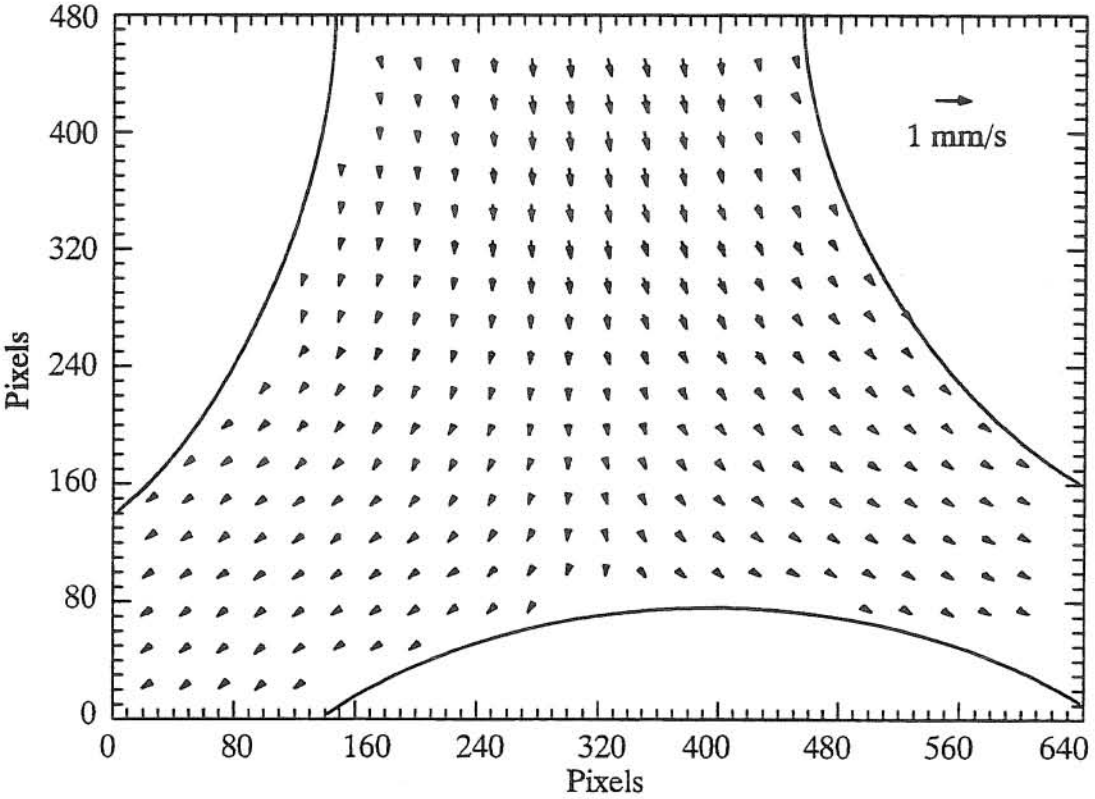

Figure 6.4.19 Interpolated Velocity Field for Low Flow Rate for Second Experiment

	Flow Condition		
	High	Medium	Low
$\overline{V}_{theoretical}$ (mm/s)	0.79	0.50	0.26
$\overline{V}$ (mm/s)	1.09	0.70	0.37
$\overline{V}_y$ (mm/s)	−1.09	−0.70	−0.37
$\overline{V}_x$ (mm/s)	0.08	0.07	0.03
$\overline{V}/\overline{V}_{theoretical}$	1.39	1.39	1.43
$\overline{V}_y/\overline{V}_{theoretical}$	−1.38	−1.38	−1.42
$\overline{V}_x/\overline{V}_{theoretical}$	0.11	0.14	0.11

Table 6.4.4 Observed Pore-water Velocities for Three Flow Rates from Second Experiment

Analysis of the average pore-water velocities for the second set of porous media results is shown in Table 6.4.4 and indicates that the flow structure remains similar for the three different flow rates as was the case with the previous experiment. Furthermore, the PTV program seems to be accurately measuring a flow field with strong divergence. If the displacements are small enough between consecutive frames, the PTV program developed should be able to generate a velocity field for even the most chaotic flow conditions.

6.5 Conclusions

It has been demonstrated that the PTV procedure developed in this project can track particles in a fluid inside a porous medium and produce a two-dimensional velocity field for a plane in the porous medium. The limitations on the procedure appear to be primarily of an optical nature. These limitations required that the selected pores for videotaping be close to the column surface since blurring of the images occurred when pores at greater distances into the column were observed. For the pores which were analyzed, the average pore-water velocities calculated closely matched the predicted values based on bulk flow rate and column porosity. These values, however, were for individual pores and did not represent a representative elementary volume of the porous media and therefore can not be used to truly confirm that the procedure can accurately measure a flow rate in the column.

Suggestions for possible improvement of the experimental apparatus would include the selection of a higher quality media such as optical quality glass since it is possible that there

were some inhomogeneities in the media which caused some distortion of the images. Also, a single-line laser would likely assist the index matching since the refractive indices of the materials would only have to match for one wavelength of light as opposed to a range for the multi-line laser. In addition, it would be advisable to develop a more reliable method for calibrating the flow field since the current method requires imaging of a ruler outside of the column and any possible magnifying effects of the media-fluid matrix on the image field. A calibration technique internal to the column may be more accurate.

7. Overall Conclusions and Future Applications

The PTV procedure developed in this project is an effective means for measuring flow velocities and can be used with porous media if optimum refractive index matching is achieved. Furthermore, a video based system has been demonstrated to have some advantages over photographic techniques for measuring laminar, steady flow velocity fields which have a large difference between minimum and maximum velocity within a field of view, as in porous media. A series of video frames can be analyzed which allows for a minimum displacement criteria to be met for all of the tracer particles within a field of view, such that relative errors in velocity measurement are minimized for all particles in a field of view. Also, for laminar, steady flow superposition of velocity vectors from different times can be used to help overcome the limited resolution of video to obtain a more complete velocity field.

Future applications of this research could be used in the field of colloid transport in groundwater. This is an area of emerging concern particularly with the transport of pollutants from landfills as described by McCarthy and Zachara (1989). Compounds which were thought to be immobile due to their sorption properties may bind to colloids as well as to fixed aquifer solids and be transported at near groundwater velocities. Examples of radionuclide transport due primarily to mobile colloids have been documented at Las Alamos National Laboratory, where radionuclides were known to strongly adsorb to the aquifer solids and were therefore thought to be essentially immobile, but instead the radionuclides adsorbed to some mobile colloids and were transported much farther than originally predicted (McCarthy and Zachara 1989). In order to predict contaminant transport in groundwater it is necessary to understand and model all modes of transport. The parameters governing the transport of colloids are not fully understood and this area of research could benefit from the PTV technique developed in this project. For example, the influence of heterogeneity on colloid transport and the presence of preferential flow paths for colloids could be identified with an index-matched PTV system.

Visualization of colloids in glass micromodels has been recently used to study the influence of the gas-water interface on colloid transport in unsaturated porous media flow (Wan and Wilson 1994). In these experiments different types of colloids, including latex particles, clay, and bacteria, were introduced into a network of small connected pores, some of which contained entrapped air bubbles. The gas-water interfaces were found to attract both hydrophobic and hydrophilic colloids. The degree of sorption at the interfaces was affected by particle hydrophobicity, solution ionic strength, and particle charge. Furthermore, the sorption process was found to be essentially irreversible, which indicates that a "static gas-water interface [in an unsaturated soil] behaves as a sorbent phase retarding the transport of particulate contaminants" (Wan and Wilson 1994).

Another area of research which this project hopes to benefit is the modeling of dispersion. The dispersive flux of a chemical is a function of variations in the chemical concentration and velocity on the microscopic scale. The dispersive flux, therefore, is a function of the point-level velocities of the fluid as described by Northrup et al. (1993) as:

$$J_a = \frac{1}{U_\beta}\int (C_a - < C_a >^\beta)(V - < V >^\beta)dU \qquad (7.1)$$

where J_a is the dispersive flux of compound a, U_β is the bulk fluid volume, C_a is the concentration of a at a point, $<C_a>^\beta$ is the bulk average concentration of a, V is the fluid velocity at a point, and $<V>^\beta$ is the bulk average pore-water velocity. Measuring the point velocities in the pores of a porous medium(V) should assist verification of the dispersive flux equation, which has been largely theoretical to this point. Furthermore, the PTV analysis procedure could be coupled with local concentration measurements by counting tracer particles in a sampling volume or using laser induced fluorescence and correlating the intensity of a fluorescent dye with concentration. Particle counting, however, will likely have limited application to concentration measurements since the maximum density of identifiable tracer images is fairly small with normal video imaging.

References

Adrian, R. J., (1991), "Particle-Imaging Techniques for Experimental Fluid Mechanics," *Annu. Rev. Fluid Mech.*, vol. 23, 261-304.

Arroyo, M. P., and C. A. Greated, (1991), "Stereoscopic Particle Image Velocimetry," *Meas. Sci. Technol.*, vol. 2, 1181-1186.

Ball, W. P., and P. V. Roberts, (1991), "Long-term Sorption of Halogenated Organic Chemicals by Aquifer Material - Part 1. Equilibrium," *Environmental Science & Technology*, vol. 25, no. 7, 1223-1236.

Camp, C. E., W. B. Kolb, K. L. Sublette, and R. L. Cerro, (1990),"The Measurement of Square Channel Velocity Profiles Using a Microcomputer-Based Image Analysis System," *Experiments in Fluids*, vol. 10, 87-92.

Chen, R. C. , and J. R. Kadambi, (1990),"LDV Measurements of Solid-Liquid Slurry Flow Using Refractive Index Matching Technique," *Particulate Science and Technology*, vol. 8, 97-109.

Chen, R. C., and L. S. Fan, (1992), "Particle Image Velocimetry for Characterizing the Flow Structure in Three-Dimensional Gas-Liquid-Solid Fluidized Beds," *Chemical Engineering Science*, vol. 47, no. 13/14, 3615-3622.

Cho, Y-C, and B. G. McLachlan, (1987), Personal Computer (PC) Based Image Processing Applied to Fluid Mechanics Research, SPIE Vol. 829, *Applications of Digital Image Processing X*, 253-257.

Cui, M. M., and R. J. Adrian, (1992), "Mass Distribution of a Granular Suspension in Couette Shear Flow: Heavy Particles," Department of Theoretical and Applied Mechanics, University of Illinois at Urbana-Champaign.

Denn, M. M., (1980), *Process Fluid Mechanics*, Englewood Cliffs: Prentice-Hall, Inc., 34-37.

Dybbs, A., and R. V. Edwards, (1982), "A New Look at Porous Media Fluid Mechanics Darcy to Turbulent," Departments of Mechanical and Aerospace and Chemical Engineering, Case Western University.

Dybbs, A., and R. V. Edwards, (1984), "An Index Matched Flow System for Measurements of Flow in Complex Geometries," *Laser Anemometry in Fluid Mechanics-II: Selected Papers from the Second International Symposium on Applications of Laser Anemometry to Fluid Mechanics, Lisbon, Portugal*, 171-184.

Fingerson, L. M., R. J. Adrian, R. K. Menon, and S. L. Kaufman, (1991), "Data Analysis, Laser Doppler Velocimetry and Particle Image Velocimetry," *TSI Short Course Text*.

Hassan, Y. A., T. J. Blanchat, and C. H. Seeley, Jr., (1992), "PIV Flow Visualization Using Particle Tracking Techniques," *Meas. Sci. Technol.*, vol. 3, 633-642.

Hassan, Y. A., T. J. Blanchat, C. H. Seeley, Jr., and R. E. Canaan, (1992), "Simultaneous Velocity Measurements of Both Components of a Two-Phase Flow Using Particle Image Velocimetry," *Int. J. Multiphase Flow*, vol. 18, no. 3, 371-395.

Hinedi, Z. R., Z. J. Kabala, T. H. Skaggs, D. B. Borchardt, R. W. K. Lee, and A. C. Chang, (1993), "Probing Soil and Aquifer Material Porosity With Nuclear Magnetic Resonance," *Water Resources Research*, vol. 29, no. 12, 3861−3866.

Kawasue, K., and T. Ishimatsu, (1991), "Fast Measuring Technique of Velocity Distribution of Water Flow," *FLUCOME* '91, 595-600.

Langlois, W. E., (1964), *Slow Viscous Flow*, New York: Macmillan, 121-124.

LeBlanc, D. R., S. P. Garabedian, K. M. Hess, L. W. Gelhar, R. D. Quadri, K. G. Stollenwerk, and W. W. Wood, (1991), "Large-Scale Natural Gradient Tracer Test in Sand and Gravel, Cape Cod, Massachusetts 1. Experimental Design and Observed Tracer Movement," *Water Resources Research*, vol. 27, no. 5, 895-910.

Mackay, D. M., D. L. Freyberg, P. V. Roberts, and J. A. Cherry, (1986), "A Natural Experiment on Solute Transport in a Sand Aquifer 1. Approach and Overview of Plume Movement," *Water Resources Research*, vol. 22, no. 13, 2017-2029.

McCarthy, J. F., and J. M. Zachara, (1989), "Subsurface Transport of Contaminants: Mobile Colloids may Alter the Transport of Contaminants," *Environ. Sci. Technol.*, vol. 23, no. 5, 496-502.

Nakagawa, M., and E. K. Jeong, (1992), "Application of NMR to Rotating Granular Flow," Proceedings of the 9th Conference on Engineering Mechanics, 644-647.

Northrup, M. A., T. J. Kulp, S. M. Angel, (1993), "Direct Measurement of Interstitial Velocity Field Variations in a Porous Medium Using Fluorescent-Particle Image Velocimetry," *Chemical Engineering Science*, vol. 48, no. 1, 13-21.

Rosenstein, N. D., (1980), *Non-Linear Laminar Flow in a Porous Medium*. Ph. D. Thesis, Case Western Reserve University, 45-52.

Salch, S., J. F. Thovert, and P. M. Adler, (1992), "Measurement of Two-Dimensional Velocity Fields in Porous Media by Particle Image Displacement Velocimetry," *Experiments in Fluids*, vol. 12, 210-212.

Shattuck, M., R. Behringer, J. Geordiadis, and G. A. Johnson, (1991), "Magnetic Resonance Imaging of Interstitial Velocity Distributions in Porous Media," *Experimental Techniques in Multiphase Flows, ASME 1991*, FED-vol. 125, 39-45.

Wan, J., and J. L. Wilson, (1994), "Visualization of the Role of the Gas-water Interface on the Fate and Transport of Colloids in Porous Media," *Water Resources Research*, vol. 30, no. 1, 11−23.

Weast, R. C., (1983), *CRC Handbook of Chemistry and Physics*, Boca Raton: CRC Press, D-266.

Wegner, T. H., A. J. Karabelas, and T. J. Hanratty, (1971), "Visual Studies of Flow in a Regular Array of Spheres," *Chemical Engineering Science*, vol. 26, 59-63.

Wood, W. W., T. F. Kraemer, and P. P. Hearn, Jr., (1990), "Intragranular Diffusion: An Important Mechanism Influencing Solute Transport in Clastic Aquifers?," *Science*, vol. 247, 1569-1572.

Appendix A - PTV Imaging Procedure

1.) **Videotape flow field** for future playback and analysis. Be sure to calibrate the image field by recording an image of an object that has a known dimension (i.e. a ruler). This will be used to convert displacements from pixels to length units. Be sure that the appropriate magnification and field of view have been chosen.

In order to determine whether or not your images will be suitable for analysis there are a some guidelines to follow. First, be sure that the particles you are videotaping are in the 4 to 6 pixel diameter range. This will allow for a significant number of tracers (and velocity vectors) in your field of view, but will also keep the images large enough to identify from one frame to the next. Be sure to keep the tracer concentration high enough to get many vectors, but low enough to prevent significant particle overlap. There is no set limit on particle concentration since it will depend on the quality of images and size of particles. Larger particles can be tracked more reliably, but result in lower resolution analysis.

Second, be sure that the velocity of the tracers is not too fast. If the particles are moving large distances between successive frames (1/30 sec.) then they may be difficult to track. There are no set guidelines for the maximum allowable displacement between frames since it is dependent on the concentration of tracers, uniformity of flow, and quality of images. In the case of parallel flow, for example, large displacements may be allowed since the particles are not moving much relative to each other, allowing good correlation. Also, if only a few tracers are present it may be possible to allow greater displacements since fewer candidate particles would be present at the next timestep.

Note: If particles are moving very slow, it may be advisable to analyze only every other frame or every third frame, etc. However, if this is done the timestep in the input file must be appropriately adjusted.

2.) **Capture** a series of successive frames from the VCR to the Macintosh computer via the Image 1.44 software. The VCR should be in the pause mode during image capture and advanced two fields (one frame) for each successive capture. The tracking on the Panasonic VCR must be precisely adjusted in order to obtain useful images. (Adjust tracking in the slow-playback mode and be patient.)

Capture enough images to ensure that all particles have moved the minimum required

distance. This is typically 2 to 10 images depending on maximum and minimum velocities in the flow field. For example, if all of the particles are moving approximately the same speed, then only two images may be required. On the other hand, if some are moving very fast and some very slow, many images may be required in order to allow all particles to travel a minimum required displacement. This minimum displacement criteria is imposed to ensure a certain level of accuracy in the displacement and velocity measurements since measurements of short displacements have high relative errors.

When saving images refer to them in a manner such that they can be located (approximately) on the tape again if necessary. Also, label all frames in a series in a manner such as to keep them in order for further analysis. (i.e. pm.q01.p01.05.21.01, pm.q01.p01.05.21.02, etc.) In this case, "pm" is for porous media, "q01" is for first flow rate, "p01" is for first location of videotaping, "05.21" is for time = 5 minutes and 21 seconds after start of experiment on video tape, and "01" is for the first frame in the series of successive frames.

Note: When capturing images be sure the Gain and Offset settings are consistent for all images in a series.

NOTE: When saving images be sure to use file names that are 5 to 20 digits long. This is because the program "Track" truncates off the last 3 characters to make a root file name used to generate the names of various other input and output files. "Track" assumes these last 3 characters (i.e. ".01") are specific to a particular frame and not representative of the series of frames.

3.) **Determine scale** by analyzing the image of the ruler or other object of known dimensions. Draw a line on the image (on Mac screen) and calculate the pixel to length unit ratio to be entered into the input file for "Track."

4.) **Threshold** captured images and enhance as necessary with options such as *reduce noise* or *smooth*. After image "cleaning," use the *make binary* option to create a file of 0s and 255s. Be sure to use the same procedure for all sets of images in the same experiment. Create a macro to allow easy repetitive operations with TeachText software. Also, erase any fluid/media interfaces or other immobile "noise" in the field of view after image enhancement such that these large areas of black pixels will not be used to determine the correlation of a particle from one frame to the next. This would reduce the importance of neighboring particles since they would have a small total area compared to the large,

black immobile objects in the flow field, such as a media/fluid interface.

NOTE: Images must be black particles on white background. If this is not the case for your images use *invert* on the Mac to reverse the grey scale spectrum before image enhancement.

Note: Before proceeding to the work stations, first create a file with all of the media (no-fluid) regions assigned a pixel value of 100. This file will be used in the interpolation program later to avoid interpolating a velocity field inside the media. When the interpolation program "sees" a 100 in this file it knows that that location is inside the media and not part of the fluid. All other pixels can have any value other than 100. If there is no media in the field of view, then any of the image files can be used as the "media" file instead since they will have no 100-valued pixels and therefore contain no media regions.

5.) **Export** text version of binary files and call them the same name as their source files but with ts at the end. Also export the file containing media locations with pixel values of 100. Example name: pm.qo1.p01.05.21.01t or pm.qo1.p01.mediat

6.) **Transfer** the text files to the cern network via the ftp command. Type "prompt" to turn off the interactive mode and use "mget" to get the whole group of files. For example, "mget pm.qo1.p01.05.21.*" would retrieve all of the files beginning with "pm.qo1.p01.05.21.". Be sure you start the ftp process from the directory to which you want the files to be copied into.

7.) **Create an input file** for the "Track" program which has all of the parameters necessary for performing the particle tracking and interpolation analysis. This input file is described in more detail in Appendix B.

8.) **Execute Track** script file with the input file as the only input. The output files from this program are discussed in Appendix B and include a logos plot for all of the vectors found in the field of view and an information file which contains information necessary to run the interpolation program called "Interpolate."

Example: Track *infile*

9.) **Inspect** logos plot of velocity field. If erroneous vectors exist either change some input parameters such as the minimum required correlation coefficient and rerun "Track" or manually clean the images by deleting the erroneous vectors from the information file

and changing N in the information file (N is the number of vectors in the file). Then, execute "inter4.go" to regenerate a logos plot without the erroneous vectors.

Example: inter4.go < *new_information_file* > *output_file.log*

The new information file can also be combined with other information files or used by "Interpolate" to generate an interpolated velocity field at grid points.

10.) **Repeat** above procedure (steps 2-9) if you wish to generate a more complete velocity field before going on to interpolate a velocity field at grid points. Additional information files (for the same location, flow rate, and magnification) can be combined using the script file "Combine." This should only be done for conditions of laminar, steady flow where superposition is valid.

11.) **Execute Combine** script file if the information file from the current analysis is to be combined with the information file from another analysis at a different time. This should only be done when steady, laminar conditions existed everywhere in the field of view. The combined information file can then be used by "Interpolate" to create an interpolated velocity field for the field of view. "Combine" asks for the name of both information files and the name of the new combined file.

12.) **Execute Interpolate** script file with the name of the information file as the only input. This generates an interpolated velocity field for the field of view at grid points. If the interpolated velocity field is unsatisfactory you can change some of the input parameters in the information file such as the grid spacing or searching window size and rerun "Interpolate."

Example: Interpolate *information_file*

NOTE: If *information_file* is too large "Interpolate" may give an error. In this case use the command: "interp4.go < *information_file* > *information_file.interp4.log*" instead to get the same resulting files.

Note: If no media is located in the field of view and a media file was therefore not created, just substitute the name of one of the text image files for the media file name in the input file. This will work since there should be no 100 valued pixels in any of the

binary image text files and therefore no media will be found in the field of view by "interp4.go," which is called by "Interpolate."

13.) **Execute Vavg2.go** in order to calculate an average pore-water velocity and average vertical and horizontal velocities. The input file for this program is a file generated by "interp4.ftn" called "interp4.vel.out." "Vavg2.out" would contain the average pore-water velocity data.

Example: Vavg2.go < *interp4.vel.out* > *Vavg2.out*

Appendix B - README File (Program and File Listings and Explanations)

FILE NAME: README
WRITTEN BY: TONY DILL

CONTENTS: I. PROGRAM DESCRIPTIONS
II. INPUT/OUTPUT FILE DESCRIPTIONS

I. PROGRAM DESCRIPTIONS

Track

"Track" is the first program to be run after transferring the image files from the Mac. This script file takes an input file which contains all of the parameters necessary to generate a velocity field for a series of frames and creates numerous output files (see the EXAMPLE section below for further explanation). The images are analyzed to determine the particle centroids with sub-pixel accuracy. "locate1.go" is called to determine the centroids of all acceptable particles in an image field. Then, "pr1.go" and "pr2.go" are called to perform the particle tracking. This program can be run with 2 or more frames. Finally, "inter4.go" is called to produce a logos plot of the velocity field for accepted velocity vectors from all frames in a series. "Track" reads in at least 2 binary image matrices of 0s and 255s or 0s and 1s. The file names of these matrices can begin with "WA," "pm," or "SQ" for the type of experiment being performed. Other prefixes can be used, but should be just 2 characters long. These files must end with the extension "t" for "text," although the name of the files entered into the input file should not contain the "t" extension. If measurement files (ending in "m") already exist for the images, "locate1.go" will not be called and the existing centroid values will be used. To recalculate the centroids, delete the "m" files before running "Track."

With the correct input file, "Track" then determines the size of the matrices and begins making names for various output files by truncating the last 3 digits of the file name and adding new extensions. Therefore, file names should be at least 5 characters long, but no longer than 20. (i.e. pm.01 or pm.q01.p01.00.01.01)

Then, after centroids are determined, a combined file is prepared which has all the information required by the particle tracking programs (pr1.go or pr2.go). The name of the combined file is the name of the truncated input file with a number extension corresponding to the iteration number (i.e. ".1") and ".comb" (i.e. pm.q01.p01.00.01.1.comb). The composition

of this combined file is discussed in Section II. INPUT/OUTPUT FILE DESCRIPTIONS.

Finally, a particle tracking program is executed to obtain velocity vectors for the pair of images being analyzed. "pr1.go" is executed for the first iteration and "pr2.go" is used for subsequent iterations. An interrogation program ("inter4.go") is then run on the final data to provide logos plots for all iterations combined. In addition to a logos plot an information file is output which has no extension and can be used by the script file "Interpolate" to get an interpolated velocity field.

Before running "Interpolate," the script file "Combine" can be run to combine two different information files if desired.

---------- EXAMPLE ----------

COMMAND: Track *infile*

CONTENTS of *infile*:

N = Number of frames to be analyzed
frame_1 = Name of first image file in series. (w/out "t" extension)
. (i.e. pm.q01.p01.36.20.01)
.
.
frame_N = Name of last (Nth) image file in series. (i.e. pm.q01.p01.36.20.03)
Mediafile = Name of image file containing media locations which are 100-valued pixels.
S = Scaling factor to determine arrow length on logos plots. A value of 999.9 will cause the program to determine its own S.
Cmin = Minimum acceptable correlation coefficient for a vector.
MINDISP = Minimum displacement criteria (pixels).
R = Ratio of pixels to length units.
TIMESTEP = Time between frames (in Tunits).
Lunits = Length units.
Tunits = Time units.
L = Length of initial searching window (pixels).
Diameter = Average diameter of tracer particles (pixels).
Minarea = Minimum area for a tracer (pixels).

Maxarea = Maximum area for a tracer (pixels).
Spacing = Grid spacing for interpolation program (pixels).
Lint = Length of searching window for interpolation program (pixels).

*note: "Spacing" and "Lint" are not used by "Track," but are required in the information file to be used by "Interpolate."

*note: Text files (ending in "t") must be present for each image.
(i.e. pm.q01.p01.36.20.01t must be present)

SAMPLE OUTPUT (N=3): (details of these files are described in Section II)

divisions −> file containing number of iterations performed and number of vectors found for each iteration

pm.q01.p01.36.20 −> information file to be used by interrogation or interpolation program to make logos plot of vectors

pm.q01.p01.36.20.01 −> frame 1 image file converted to 0s and 1s

pm.q01.p01.36.20.02 −> frame 2 image file converted to 0s and 1s

pm.q01.p01.36.20.01m −> file with X and Y centroids of all tracers found in frame 1.

pm.q01.p01.36.20.02m −> file with X and Y centroids of all tracers found in frame 2.

pm.q01.p01.36.20.01m2 −> file containing the X and Y centroids of all particles in frame 1 which correlated with particles in frame 2 but did not travel the minimum displacement criteria

pm.q01.p01.36.20.01m3 −> file containing the X and Y centroids of all particles in frame 1 which correlated with particles in frame 3 but did not travel the minimum displacement criteria

pm.q01.p01.36.20.1.comb −> combined file (input for "pr1.go")

pm.q01.p01.36.20.1.d −> output file from "pr1.go" containing displacements and angles of all particles in frame 1 which correlated with particles in frame 2 but did not travel the minimum displacement criteria.

pm.q01.p01.36.20.1.log −> logos plot of vectors found for frames 1 and 2

pm.q01.p01.36.20.1.out −> output from "pr1.go" showing statistics

pm.q01.p01.36.20.2.comb −> combined file (input for "pr2.go")

pm.q01.p01.36.20.2.d −> output file from "pr2.go" containing displacements and angles of all particles in frame 1 which correlated with particles in frame 3 but did not travel the minimum displacement criteria.

pm.q01.p01.36.20.2.log −> logos plot of vectors found for frames 1 and 3

pm.q01.p01.36.20.2.out –> output from "pr2.go" showing statistics
pm.q01.p01.36.20.list –> file with no. of iterations and frames analyzed in each iteration
pm.q01.p01.36.20.log –> logos plot of vectors found from all iterations combined

---

locate1.ftn (locate1.go)

Typically, this program is called by the script file "Track" in order to create files with the extension "m" that contain the X and Y centroid values for all of the particles found in binary matrix of 0s and 1s. The 1s indicate presence of a particle.

Program "locate1.ftn" takes an input matrix of 0s and 1s and identifies particles within a specified size range. This range is entered into the input file for "Track." Centroids of the acceptable particles are output to screen or piped into a file. A file called "locate1.out" is also created which is possibly helpful for debugging. This file outputs the total number of 1s found in the matrix and the number of pixels which compose each particle. Some particles have zero pixels because they joined with another particle during scanning. If particles are in the correct size range, then the X and Y centroids are output. Units for centroids are pixels.

EXAMPLE: locate.go < pm.q01.p01.36.20.01 > pm.q01.p01.36.20.01m

---

pr1.ftn (pr1.go)

Program "pr1.ftn" tracks particles between two frames (Hassan et al, 1992 algorithm) and creates a logos plot of the vectors. This program is usually called by the UNIX script file "Track."

In addition to creating a logos plot of the found vectors, this program also outputs several other files which are described in the following example and in more detail in Section II. EXAMPLE also shows how "pr1.go" should be invoked.

---------- EXAMPLE ----------

COMMAND: pr1.go < pm.q01.p01.36.20.1.comb

–note: This command is performed inside the "Track" program, but can be performed independently if the appropriate input file exists.

OUTPUT: (details of these example files are in Section II)

divisions –> File containing number of iterations performed and number of vectors found for each iteration. From "pr1.go" divisions is initially created and always has only one iteration. "divisions" is updated by "pr2.go" to add more iterations.

pm.q01.p01.36.20 –> Information file to be used by interrogation or interpolation program to make logos plot of vectors. This will be appended by "pr2.go."

pm.q01.p01.36.20.01m2 –> File containing the X and Y centroids of all particles in frame 1 which correlated with particles in frame 2 but did not travel the minimum displacement criteria.

pm.q01.p01.36.20.1.d –> Output file containing displacements and angles of all particles in frame 1 which correlated with particles in frame 2 but did not travel the minimum displacement criteria.

pm.q01.p01.36.20.1.log –> Logos plot of vectors found for frames 1 and 2.

pm.q01.p01.36.20.1.out –> Data file showing statistics, used for debugging.

---

pr2.ftn (pr2.go)

Program "pr2.ftn" tracks particles between two frames (Hassan et al, 1992 algorithm) and creates a logos plot of the vectors. This program is usually called by the Unix script file "Track."

In addition to creating a logos plot of the found vectors, this program also outputs several other files which are described in the following example and in more detail in Section II. EXAMPLE also shows how "pr2.go" should be invoked.

---------- EXAMPLE ----------

COMMAND: pr2.go < pm.q01.p01.36.20.2.comb

–note: This command is performed inside the "Track" program, but can be performed independently if the appropriate input file exists.

OUTPUT: (details of these example files are in the README file)

divisions –> File containing number of iterations performed and number of vectors found for each iteration. "divisions" is updated by "pr2.go" to add more iterations.

pm.q01.p01.36.20 –> Information file to be used by interrogation or interpolation

program to make logos plot of vectors. This is appended by "pr2.go."

pm.q01.p01.36.20.01m3 –> File containing the X and Y centroids of all particles in frame 1 which correlated with particles in frame 3 but did not travel the minimum displacement criteria.

pm.q01.p01.36.20.2.d –> Output file containing displacements and angles of all particles in frame 1 which correlated with particles in frame 3 but did not travel the minimum displacement criteria.

pm.q01.p01.36.20.2.log –> Logos plot of vectors found for frames 1 and 3.

pm.q01.p01.36.20.2.out –> Data file showing statistics, used for debugging.

Add.PM.ftn (Add.PM.go)

This program is called by "Track" to help create the file name for the next combined particle tracking input file. Also the ".list" file is updated to keep track of which frames correspond to each iteration. This program can not be run outside of the context of "Track" so no example for its use is given.

---

accmat.ftn (accmat.go)

This program converts a matrix of 0s and positive integers in to a matrix of 0s and 1s. Any integer greater than 0 is given the value of 1. This program is called by "Track" and converts the binary images of 0s and 255s from the Image software into 0s and 1s.

The input file must have the number of columns and rows as the first two items, followed by the matrix. The output file consists of the matrix only.

EXAMPLE: accmat.go < *infile* > *outfile*

---

inter4.ftn (inter4.go)

This program creates a logos plot of all of the velocity vectors found in the multiple iterations performed by "Track." This program is executed by "Track," but can be run separately. The example files below are discussed in the README file.

EXAMPLE: inter4.go < pm.q01.p01.36.20 > pm.q01.p01.36.20.log

---

truncate.ftn (truncate.go)

This program reads in a character variable and truncates off a certain number of digits. The number of digits to truncate is input after the character string. Only the truncated character string is returned. This program is called by "Track" in order to create a root file name for which is used to generate various output file names.

Combine

This program is used to combine information files from different times. The user is prompted for the file names for the two information files and the new combined information file created by the program. It allows a denser raw vector field to be generated for a given field of view and should only be done for laminar, steady flow. This combined information file can then be input into "interp4.go" to get a more complete interpolated velocity field. "Combine" calls "Combine.go" to actually combine the information files and also uses "Check.go" to determine if the timestep between frames is 1/30 sec or not. If the timestep for an information file is not 1/30 sec, then "Convert.go" is called to convert the information file to a 1/30 sec timestep.

Check.ftn (Check.go)

This program is called by "Combine" to see if the timestep for an information file is 1/30 second or not. "yes" or "NO" is returned.

Convert.ftn (Convert.go)

This program reads in an information file and changes the file from one timestep to a video rate timestep of 1/30 second. It is called by "Combine."

Combine.ftn (Combine.go)

This program takes in two information files and combines them into one. It is called by "Combine."

Interpolate

This script file takes in an information file and creates an interpolated velocity field by running "interp4.go." This program also checks to see if the mediafile exists before running "interp4.go."

---

interp4.ftn (interp4.go)

This program interpolates a velocity field at grid points given an appropriate input file of vector information. This program is not called by "Track" and should be executed separately on an information file. The information file may contain vector information from trials at different times for the same location in the flow field if the flow is laminar and steady. This combined file can be created with the script "Combine."

In addition to an information file, another file must exist. It is the file containing media locations, or regions where there is no fluid. It is important to designate these areas so a velocity vector is not put inside a solid, which would not make sense. This file is a matrix with 100s at media locations. The name of the file should be in the input file which was used by "Track." The name of the media file can be changed in the information file (i.e. pm.q01.p01.36.20) before running "interp4.go." If no media is present in the field of view, you can use any of the image files as the media file since they will contain no 100s and therefore no media locations. Output consists of a logos plot of the interpolated velocity field and an output file for debugging ("interp4.out"). A file called "interp4.vel.out" is also output which can be used by "Vavg2.ftn" to calculate avergae pore-water velocities.

Note: There is NO provision for a no-slip condition at media interfaces. Some vectors near media/fluid interfaces may therefore be too high, since there are no "zero-velocity" vectors to influence the interpolated velocity.

---------- EXAMPLE ----------

COMMAND:

interp4.go < pm.q01.p01.36.20 > pm.q01.p01.36.20.interp4.log

OUTPUT: pm.q01.p01.36.20.interp4.log –> Logos plot of interpolated velocity field.
interp4.out –> Output file for debugging
interp4.vel.out –> This file has the grid point X and Y velocities for the interpolated field. To be used by "Vavg2.go" to analyze the pore-water velocities.

–note: The output could be formatted in a different way to allow different analysis if necessary. Just change write statements below and output necessary items.

REFERENCE FOR INTERPOLATION EQUATIONS:
Fast Measuring Technique of Velocity Distribution of Water Flow. K. Kawasue and T. Ishimatsu. FLUCOME '91, 595–600.

Vavg2.ftn (Vavg2.go)

This program calculates the average pore-water velocity for an interpolated velocity field and also calculates an average vertical and horizontal velocity. Input file is an output file generated by the "interp4.ftn" program called "interp4.vel.out."

EXAMPLE: Vavg2.go < interp4.vel.out > Vavg2.out

II. INPUT/OUTPUT FILE DESCRIPTIONS

The following input and output files are examples to help identify what is required by, or output from various programs. In this example it is assumed that initially there are four files created on the Mac and transferred to the cern network for analysis. They are: pm.q01.p01.36.20.01t, pm.q01.p01.36.20.02t, pm.q01.p01.36.20.03t, and media.loc. These files are explained and then different output files are produced by executing several programs. After an example command, the output files created are explained in detail. An input file for the "Track" file must be created which contains all necessary parameters for the particle identification, particle tracking, interrogation, and interpolation programs.

---------- Starting Files ----------

pm.q01.p01.36.20.01t – This text file is the matrix of 0s and 255s created on the Mac for frame 1.

pm.q01.p01.36.20.02t – Text file for frame 2.

pm.q01.p01.36.20.03t – Text file for frame 3.

media.loc – This file contains 100-valued pixels where media exists. At every location a "100" is found, there is no fluid present.

infile – Input file for "Track."

Contents of infile:

N = Number of frames to analyzed

frame_1 = Name of first image file in series. (w/out "t" extension)
(i.e. pm.q01.p01.36.20.01)

.

.

frame_N = Name of last (Nth) image file in series. (i.e. pm.q01.p01.36.20.03)

Mediafile = Name of image file containing media locations which are 100-valued pixels.

S = Scaling factor to determine arrow length on logos plots. A value of 999.9 will cause the program to determine its own S.

Cmin = Minimum acceptable correlation coefficient for a vector.

MINDISP = Minimum displacement criteria (pixels).

R = Ratio of pixels to length units.

TIMESTEP = Time between frames (in Tunits).

Lunits = Length units.

Tunits = Time units.

L = Length of initial searching window (pixels).
Diameter = Average diameter of tracer particles (pixels).
Minarea = Minimum area for a tracer (pixels).
Maxarea = Maximum area for a tracer (pixels).
Spacing = Grid spacing for interpolation program (pixels).
Lint = Length of searching window for interpolation program (pixels)

*note: "Spacing" and "Lint" aren't used by "Track," but are required in the information file to be used by "interp4.go"

*note: Text files (ending in "t") must be present for each image. (i.e. pm.q01.p01.36.20.01t must be present)

EXAMPLE of an infile:

```
3
pm.q01.p01.36.20.01
pm.q01.p01.36.20.02
pm.q01.p01.36.20.03
media.loc
999.9
0.6
4
118.7
0.03333333
mm
s
24
7
10
150
25
80
```

COMMAND: Track *infile*

---------- Resulting Files ----------

divisions
locate1.out
pm.q01.p01.36.20
pm.q01.p01.36.20.01
pm.q01.p01.36.20.01m
pm.q01.p01.36.20.01m2
pm.q01.p01.36.20.01m3
pm.q01.p01.36.20.02
pm.q01.p01.36.20.02m
pm.q01.p01.36.20.03
pm.q01.p01.36.20.03m
pm.q01.p01.36.20.1.comb
pm.q01.p01.36.20.1.d
pm.q01.p01.36.20.1.log
pm.q01.p01.36.20.1.out
pm.q01.p01.36.20.2.comb
pm.q01.p01.36.20.2.d
pm.q01.p01.36.20.2.log
pm.q01.p01.36.20.2.out
pm.q01.p01.36.20.list
pm.q01.p01.36.20.log

divisions – This file has the number of iterations performed on the first line and then the number of vectors found during each iteration on successive lines.

locate1.out – debugging file

pm.q01.p01.36.20 – This is an information file which contains information needed to create a logos plot by an interpolation or interrogation program. It has the following format:

N
dT R S
Xclip Yclip
Lunits Tunits

NX NY
Mediafile
SPACING
LINT
X1 Y1 dX1 dY1
.
:
XN YN dXN dYN
pm.q01.p01.36.20.log
pm.q01.p01.36.20.interp4.log

where: N – Number of vectors found from all iterations.
dT – Timestep between first two frames in seconds. (vectors from all iterations are scaled to this timestep)
R – Ratio of pixels to length units.
S – Scaling factor to size logos arrows.
Xclip, Yclip – Sizing parameters for logos plot.
Lunits, Tunits – Units for time and length.
NX, NY – Number of columns and rows.
Mediafile – Image file with 100–valued pixels that indicate media locations.
SPACING – Spacing between interpolation grid points.
LINT – Size of searching window for interpolation program.
X1, Y1 – Coordinates of first vector in pixels.
dX1, dY1 – Displacements of first vector in pixels.
pm.q01.p01.36.20.log – Title of logos plot created by "inter4.go."
pm.q01.p01.36.20.interp4.log – Title of logos plot created by "interp4.go."

pm.q01.p01.36.20.01 – This text file is the same as pm.q01.p01.36.20.01t but has 255s converted to 1s.

pm.q01.p01.36.20.01m – This text file has the centroids of all of the particles found in frame 1.

pm.q01.p01.36.20.01m2 – This file contains the X and Y centroids of all particles in frame 1 which correlated with frame 2 but did not travel the minimum displacement.

pm.q01.p01.36.20.01m3 – This file contains the X and Y centroids of all particles in frame 1 which correlated with frame 3 but did not travel the minimum displacement.

pm.q01.p01.36.20.02 – see pm.q01.p01.36.20.01

pm.q01.p01.36.20.02m – see pm.q01.p01.36.20.01m

pm.q01.p01.36.20.03 – see pm.q01.p01.36.20.01

pm.q01.p01.36.20.03m – see pm.q01.p01.36.20.01m

pm.q01.p01.36.20.1.comb – This is the input file for "pr1.go." It has the following format:

pm.q01.p01.36.20.1.out
pm.q01.p01.36.20.1.log
pm.q01.p01.36.20
pm.q01.p01.36.20.01m2
pm.q01.p01.36.20.1.d
C
MINDISP
dT R S
Lunits Tunits
L N1 N2
NX NY
COLOR
Mediafile
SPACING
LINT
[Frame 1 0s and 1s image matrix]
[Frame 2 0s and 1s image matrix]
[Frame 1 particle centroids in pixels]
[Frame 2 particle centroids in pixels]

where: pm.q01.p01.36.20.1.out – Name of output data file for iteration 1.
pm.q01.p01.36.20.1.log – Name of logos plot for vectors found in iteration 1 only.
pm.q01.p01.36.20 – Name of information file.
pm.q01.p01.36.20.01m2 – File name – see above.
pm.q01.p01.36.20.1.d – File name – see below.
C – Required correlation coefficient.

MINDISP – Minimum displacement criteria.

L – Length of edge of searching window in pixels, which is used only in iteration 1.

N1, N2 – Number of particles in frames 1 and 2.

COLOR – Pen color for iteration 1 logos plot.

pm.q01.p01.36.20.1.d – File containing number of particles in frame 1 which correlated with frame 2 but did not travel the minimum displacement criteria. Also contains the distance in pixels and angle in degrees that each particle travelled from frame 1 to 2.

pm.q01.p01.36.20.1.log – Logos plot of vectors found from iteration 1.

pm.q01.p01.36.20.1.out – Data file for iteration 1 which contains statistics for each particle in frame 1, including max. correlation, location, velocity, etc.

pm.q01.p01.36.20.2.comb – This is an input file for "pr2.go." It has the following format:

pm.q01.p01.36.20.2.out
pm.q01.p01.36.20.2.log
pm.q01.p01.36.20
pm.q01.p01.36.20.01m3
pm.q01.p01.36.20.2.d
pm.q01.p01.36.20.1.d
C
MINDISP
dT R S
Lunits Tunits
L N1 N2
NX NY
DIAMETER
COLOR
Mediafile
SPACING
LINT
[Frame 1 0s and 1s image matrix]
[Frame 3 0s and 1s image matrix]
[Frame 1 particle centroids in pixels]
[Frame 3 particle centroids in pixels]

where: pm.q01.p01.36.20.2.out – Name of output data file for iteration 2.

pm.q01.p01.36.20.2.log – Name of logos plot for vectors found in iteration 2 only.

pm.q01.p01.36.20 – Name of information file.

pm.q01.p01.36.20.01m3 – File name – see above.

pm.q01.p01.36.20.2.d – File name – see below.

pm.q01.p01.36.20.1.d – File name from previous iteration.

N1 – Number of remaining particles from frame 1 that have correlated but not travelled the minimum displacement criteria.

N2 – Number of particles in frame 3.

DIAMETER – Avg. diameter of particles in pixels, which is used for window size determination after iteration 1.

COLOR – Pen color for iteration 2 logos plot.

pm.q01.p01.36.20.2.d – same as pm.q01.p01.36.20.1.d, but for frame 1 and 3.

pm.q01.p01.36.20.2.log – Logos plot of vectors found from iteration 2.

pm.q01.p01.36.20.2.out – Data file for iteration 2 which contains statistics for each particle remaining from the first iteration which correlated but did not travel the minimum displacement criteria (includes the max. correlation, location, velocity, etc.)

pm.q01.p01.36.20.list – File which has the number of iterations performed and a list of the information file and the 2 frames which were analyzed for each iteration.

pm.q01.p01.36.20.log – This is a logos plot of the velocity vectors from all of the iterations combined.

COMMAND: Interpolate pm.q01.p01.36.20

or

interp4.go < pm.q01.p01.36.20 > pm.q01.p01.36.20.interp4.log

---------- Resulting Files ----------

pm.q01.p01.36.20.interp4.log – This is a logos plot of the interpolated velocity field for the experiment pm.q01.p01.36.20. However, this could also be done for a location at multiple instances in time by combining information files first with "Combine."

interp4.out – A debugging file.

interp4.vel.out – This file has the grid point X and Y velocities for the interpolated field. It is to be used by "Vavg2.go" to calculate average pore-water velocities.

COMMAND: Vavg2.go < interp4.vel.out > Vavg2.out

RESULT: Vavg2.out contains the average pore-water velocity for the field of view and the average Vx and Vy.

Appendix C - Manufacturers' Information

1. Video Equipment
   - Sony XC-75 Monochrome 1/2" CCD Camera
   - Fujinon 75 mm lens
   - Panasonic AG-1960 VCR
   - Frame grabber: Perceptics Corporation PixelBuffer (Model PTB425)

2. Laser
   - 300 mW multiline Argon ion laser: Ion Laser Technology Model 5500A
   - Fiber Optic and Cylindrical Lens: Dantec Measurement Technology, Inc.

3. Media
   - 3/8" PMMA spheres: Spex Industries, Inc. catalog no. 3112
   - 9 mm glass beads: Cataphote Inc.

4. Fluid
   - Laser Liquid: Cargille Laboratories 5610 Fluid

5. Tracers
   - 400 μm blue polystyrene spheres: Polysciences, Inc.
   - 8 μm Sphericel 110P8 hollow glass spheres: Potters Industries Inc.

6. Pump
   - Masterflex Peristaltic Pump: Cole-Parmer Instrument Company